



**Preparation and Characterization of Biomimetic Molecularly
Imprinted Polymer for Controlled Release Drug
Delivery System of Oral Insulin**

Pijush Kumar Paul

**A Thesis Submitted in Fulfillment of the Requirements for the
Degree of Doctor of Philosophy in Pharmaceutical Sciences
Prince of Songkla University**

2017

Copyright of Prince of Songkla University



**Preparation and Characterization of Biomimetic Molecularly
Imprinted Polymer for Controlled Release Drug
Delivery System of Oral Insulin**

Pijush Kumar Paul

**A Thesis Submitted in Fulfillment of the Requirements for the
Degree of Doctor of Philosophy in Pharmaceutical Sciences
Prince of Songkla University**

2017

Copyright of Prince of Songkla University

Thesis Title Preparation and Characterization of Biomimetic Molecularly Imprinted Polymer for Controlled Release Drug Delivery System of Oral Insulin

Author Mr. Pijush Kumar Paul

Major Program Pharmaceutical Sciences

Major Advisor

.....
(Assoc. Prof. Dr. Roongnapa Srichana)

Examining Committee :

.....Chairperson
(Assoc. Prof. Dr. Wantana Reanmongkol)

Co-advisor

.....
(Dr. Jongdee Nopparat)

.....Committee
(Assoc. Prof. Dr. Roongnapa Srichana)

.....Committee
(Assoc. Prof. Dr. Teerapol Srichana)

.....Committee
(Dr. Jongdee Nopparat)

.....Committee
(Dr. Apichart Atipairin)

The Graduate School, Prince of Songkla University, has approved this thesis as fulfillment of the requirements for the Doctor of Philosophy Degree in Pharmaceutical Sciences.

.....
(Assoc. Prof. Dr. Teerapol Srichana)

Dean of Graduate School

This is to certify that the work here submitted is the result of the candidate's own investigations. Due acknowledgement has been made of any assistance received.

.....Signature

(Assoc. Prof. Dr. Roongnapa Srichana)

Major Advisor

.....Signature

(Mr. Pijush Kumar Paul)

Candidate

I hereby certify that this work has not been accepted in substance for any degree, and is not being currently submitted in candidature for any degree.

.....Signature

(Mr. Pijush Kumar Paul)

Candidate

Thesis Title	Preparation and Characterization of Biomimetic Molecularly Imprinted Polymer for Controlled Release Drug Delivery System of Oral Insulin.
Author	Mr. Pijush Kumar Paul
Major Program	Pharmaceutical Sciences
Academic Year	2016

ABSTRACT

The synthesis and characterization of biomimetic molecularly imprinted nanoparticle polymers (MIPs) via chemical patterning was studied using two sources of insulin for determination of effective selectivity. Dynamic laser light scattering (DLS) measurements revealed that the zeta potentials of the nanoparticles were size-dependent and were between -20 to -33 mV with an average particle size in the range of 200 to 220 nm. This was confirmed by transmission electron microscopy (TEM) observations and atomic force microscopy (AFM) images which showed the template pattern-dependencies and confirmed that the accommodated bionanomaterial was inside the nanopores with a size of $2 \times 25 \times 25$ nm (height \times length \times width). This was also related to the geometry of the insulin. Analysis by the Brunauer-Emmett-Teller (BET) demonstrated the presence of mesopores of around 20 nm as well. AFM images showed the immobilization of isolated amino acids assembled on the insulin surface within the internal particle that tuned the scattering as determined by the Raman intensities and their expected involvement in the viability of the geometry. All the MIPs exhibited a much higher affinity towards the insulin and the bound islets with different adsorption kinetics due to two equilibria. There was a significantly higher partition behavior at a pH of 7.4 in a sustained-release manner for 12 h,

compared to the pH of 1.2. *In vitro-in vivo* correlations in diabetic Wistar rats showed that the measured rate limitation was the same within 2 h, as the result of the small-molecule ligands that were associated at the outer layer and presented a barrier for the diffusion of both types of oral insulin across the GI resulting in a significant hypoglycemic effect for up to 24 h. Thus, the MIPs biomimetic receptors were employed for analysis of functional and directional-molecular interactions in the nanoscale material for biocompatibility and showed a potential for designing switching formulations for the delivery of oral insulin. Further investigation in the effects of interaction of MIPs nanoparticles with insulin on intestinal transport was carried out in animal models. Fluorescence spectroscopic analysis and desorption test revealed the better interaction of MIP with insulin compared to the control polymer (NIPs). Immunohistochemistry study indicated that the insulin remained active after the oral administration. Immunofluorescence staining results showed the *in vivo* absorption of MIPs nanoparticles and insulin. The fluorescent intensity of rhodamine labeled insulin for MIPs was significantly greater ($P < 0.0001$) than that of NIPs. Ultrastructural examination of intestinal segments by electron microscope displayed the uptake of insulin loaded MIPs nanoparticles via transcellular pathway by enterocytes whereas; no insulin was observed in the paracellular space. Histopathological observation exhibited no obvious toxic effect after orally treated with MIPs loaded insulin (100 mg/kg) daily for 14 days compared to control group. The above results suggest that biomimetic-insulin MIPs nanoparticles could be an effective tool for oral insulin delivery. The approach of imprinting for oral delivery application has potential to enhance bioavailability.

ACKNOWLEDGEMENT

I would like to extend gratitude to the people who have contributed in some way during the completion of this thesis. First and foremost, I would like to express my sincere gratitude to my academic advisor Assoc. Prof. Dr. Roongnapa Srichana, for accepting me in her group. Her guidance, encouragement, continuous support and patience molded me into the scientist I am today. I am thankful to her for the inspiration, giving me intellectual freedom, forcing me to develop critical thinking throughout my Ph.D. study. I am grateful to Dr. Jongdee Nopparat, whose door was always open, and her guidance and motivation inspired me to do the histology part of my research. Besides, I would like to thank my committee members Assoc. Prof. Dr. Wantana Reanmongkol, Assoc. Prof. Dr. Teerapol Srichana and Dr. Apichart Atipairin for their insightful comments and valuable suggestions. A special thanks to Dr. Brian Hodgson for assistance with the English.

I am indebted to Mr. Maitri Nuanplub for the help with animal work and Ms. Piyakorn Boonyoung for assistance with the experiments related to rat tissue sections and Mr. Alongkot Treetong for cooperation in AFM study. I would like to thank all the scientist of the department of Pharmaceutical Chemistry and Drug Delivery System Excellent Centre and NANOTEC Centre of Excellence, Faculty of Pharmaceutical Sciences, Prince of Songkla University for their support and help.

I am thankful to my labmates and friends Ms. Sirirat Rakkit, Mrs. Ramana Jadda, Ms Supannika Klangphukhiew, Dr. Wanpen Naklua, Dr. Acharee Suksuwan, Dr. Chonlatid Sontimuang, Dr. Sreenu Madhumanchi, Dr. Lily Jaiswal, Ms. Kaewkarn Thaiprayoon who always had open ears and offered a helping hand.

Many thanks to special friends Ms. Suchipha Wannaphatchaiyong, Ms. Rungtiwa Waiprib, Dr. Kashif-ur-Rehman Khan and Mr. Amitav Paul for their moral support and encouragement during the study. I am thankful for YouTube and Wikipedia for providing answers to many questions.

I am grateful to the various funding agencies that allowed me to pursue my research: National Research University Project of Thailand, Office of the Higher Education Commission, Drug Delivery System Excellence Center at PSU; Nanotechnology Center (NANOTEC), Ministry of Science and Technology, Thailand, the Graduate School, Prince of Songkla University. I would like to acknowledge the department of Pharmaceutical Chemistry, Faculty of Pharmaceutical Sciences, Prince of Songkla University for providing me with the lab facilities and the high-quality seminars that the faculty organized.

Last but not least, I would like to extend my deepest gratitude to my parents, brother and sister for their endless love and unyielding support for completing this project.

Pijush Kumar Paul

CONTENTS

Approval page	ii
Certificate of original work	iii
Certificate of thesis for submit Ph.D. degree	iv
Abstract	v
Acknowledgement	vii
Contents	ix
List of tables	x
List of figures	xi
List of abbreviations and symbols	xiii
List of papers and proceedings	xvi
CHAPTER 1 General introduction and literature review	1
CHAPTER 2 Objectives	20
CHAPTER 3 Significant results and discussion	23
CHAPTER 4 Conclusion	33
References	36
Appendices	51
Paper 1	52
Paper 2	76
Animal ethic approval	115
Vitae	116

LIST OF TABLES

Table 1	Characteristics of prepared polymers.	24
Table 2	Raman data of the insulin and polymers.	26
Table 3	Binding parameters and Release kinetics data of the MIPs.	27
Table 4	Relative pharmacological bioavailability and parameters of plasma glucose levels (n=5).	28

LIST OF FIGURES

Figure 1	Illustration of the synthesis of molecularly imprinted polymer nanoparticles. (A) Mixture of template (protein), functional monomers and crosslinkers. (B) Complexation between template and functional monomers via non-covalent interaction. (C) Polymer network formation by free radical polymerization. (D) Removal of template allows remaining the complementary binding sites.	5
Figure 2	Amino acid sequence of human insulin (Drachev <i>et al.</i> , 2004).	10
Figure 3	Different types of light scattering after monochromatic radiation exposure on sample (Butler <i>et al.</i> , 2016).	14
Figure 4	A schematic diagram of AFM (Shan and Wang, 2015).	15
Figure 5	Schematic illustrations of different transport mechanisms of nanoparticles across the intestinal epithelium. The detailed mechanism of phagocytosis, macropinocytosis and endocytosis is shown in insets (Chen <i>et al.</i> , 2011).	18
Figure 6	Nitrogen adsorption /desorption isotherms of the MIPs and NIPs.	25
Figure 7	Fluorescent intensity of insulin-Rh for MIP and NIP. Values are mean \pm SEM (n=4) per group. ***P< 0.0001 compared to NIP.	30

LIST OF FIGURES (CONTINUED)

Figure 8 TEM micrographs of immunogold-stained intestinal segments after 3 h of orally administered insulin loaded with MIP (A, B) and NIP (C, D). Insulin was investigated by immunolabeling with guinea pig anti-insulin antibody followed by goat anti-guinea pig antibody conjugated with 60 nm biotin gold nanoparticles (black dots). The permeation of insulin occurs through the transcellular route (white arrows) and absence of insulin in the surface of paracellular space indicated by black arrows. Scale bar, 2 μ m. Insets designate the 12000 x magnified views of tissue region.

LIST OF ABBREVIATIONS AND SYMBOLS

AAC	area above the blood glucose level-time curve
AAm	acrylamide
AIBN	2,2'-Azobis-(isobutyronitrile)
AFM	atomic force microscopy
BET	Brunauer-Emmett-Teller
BJH	Barrett-Joyner-Halenda
B_{\max}	maximum number of the binding sites
BSA	bovine serum albumin
CA	cellulose acetate
DAB	diaminobenzidine
DAPI	4',6-Diamidino-2-phenylindole dihydrochloride
°C	degree Celsius
DSC	differential scanning calorimetry
DLS	dynamic light scattering
FITC	fluorescein isothiocyanate
GI	gastrointestinal
h	hour
H&E	hematoxylin and eosin
HEAA	<i>N</i> -hydroxyethyl acrylamide
HPLC	high performance liquid chromatography
ICP-OES	inductively coupled plasma optical emission spectrometer
IDF	International Diabetes Federation

LIST OF ABBREVIATIONS AND SYMBOLS (CONTINUED)

IHC	immunohistochemistry
IP	isoelectric point
IR	infrared spectroscopy
IU	international unit
K_d	dissociation constant
kg	kilogram
MAA	methacrylic acid
MBAA	<i>N,N</i> -methylene-bisacrylamide
$\mu\text{g/mL}$	microgram per milliliter
μM	micromolar
μm	micrometer
mg	milligram
mg/g	milligram per gram
mM	millimolar
mV	millivolts
min	minute
MIP	molecularly imprinted polymer
nm	nanometer
NIP	non-imprinted polymer
OCT	optimum cutting temperature
PBS	phosphate buffer saline
PBST	0.3% Triton x-100 in phosphate buffer saline

LIST OF ABBREVIATIONS AND SYMBOLS (CONTINUED)

PCL-T	polycaprolactone triol
PDI	polydispersity index
Phe	phenylalanine
p.o.	peroral
Rh	rhodamine
rpm	revolutions per minute
s.c.	subcutaneous
SEM	scanning electron microscopy
STZ	streptozotocin
TEM	transmission electron microscopy
T1D	type I diabetes
Tyr	tyrosine
UV-vis	ultraviolet-visible spectroscopy

LIST OF PAPERS AND PROCEEDINGS

This thesis is based on the following papers, referred to their order of experimental design in the text. The publications are attached as appendices at the end of the thesis. Reprinted are published with kind permission of the journals.

- Paper 1** Paul, P. K., Treetong, A., Suedee, R., 2017. Biomimetic insulin-imprinted polymer nanoparticles as a potential oral drug delivery system. *Acta Pharmaceutica* 67: 149-168.
- Paper 2** Paul, P. K., Nopparat, J., Nuanplub, M., Treetong, A., Suedee, R., 2017. Improvement in insulin absorption into gastrointestinal epithelial cells by using molecularly imprinted polymer nanoparticles: Microscopic evaluation and ultrastructure. accepted in *International Journal of Pharmaceutics*.
- Proceeding 1** Paul, P. K. and Suedee, R., 2014. Protein Imprinted Nanoparticles as Drug Delivery Vehicles. The 3rd Current Drug development (CDD 2014), Ao Nang Beach, Krabi, Thailand, May 1-3, 2014.
- Proceeding 2** Paul, P. K. and Suedee, R., 2016. P Molecularly imprinted polymer as a nanocarrier for protein drug delivery. Asian Graduate Congress on Pharmaceutical Technology, National University of Singapore, Singapore, July 10-13, 2016.

CHAPTER 1

GENERAL INTRODUCTION AND LITERATURE REVIEW

Rapid advancement in biotechnology and cell biology research has resulted in a variety of potent therapeutics including proteins and peptides. Several chronic diseases (i.e., hepatitis, rheumatoid arthritis, cancer and diabetes) have been treated with proteins and peptides drugs (Tan *et al.*, 2010; Patel *et al.*, 2014). Diabetes is a group of metabolic disorder associated with hyperglycemia which occurs due to lack of insulin production or ineffective action of insulin. The chronic hyperglycemic condition can cause long-term damage to body tissues which can lead to life-threatening diseases including risk of blindness, renal failure, nerve damage and heart diseases (Gavin *et al.*, 2003). The prevalence of diabetes is now considered as a global public health threat and 415 million people estimated to have diabetes according to information of the International Diabetes Federation (IDF) 7th edition, 2015. Currently 78.3 million people of South-East Asia are suffering from diabetes which will soar to 140.2 million by 2040, if the current demographic pattern continues. As a result the overwhelming burden of diabetes will continue to have an adverse impact on economy. Pancreatic beta cells produce insulin hormone that is essential for utilizing glucose from food to convert into energy as well as to maintain glucose homeostasis (Fu *et al.*, 2013). Insulin therapy has been used to combat the both type I (insulin-dependent) and type II (noninsulin-dependent) diabetes. Since the introduction of insulin as a therapeutic agent in 1922, the subcutaneous (s.c.) has been the main route of choice for insulin therapy. However, daily multiple injections of insulin have major drawbacks such as risk of pain, infection, hyper-insulinemia,

lipoatrophy, insulin neuropathy etc. lacking patient compliance (Owens *et al.*, 2003). Therefore, a number of alternative insulin formulations have been explored including oral, buccal, nasal, transdermal, pulmonary and other non-invasive systems but only with a little success (Owens, 2002; Cefalu, 2004; White *et al.*, 2005; Lelej-Bennis *et al.*, 2001; Bruce *et al.*, 1991; Heinemann, 2010). Intrapulmonary route gained lots of interest for administering insulin due to the large surface area of the respiratory tract that have potential for peptide drug and encouraged for the development of inhaled insulin (Owens *et al.*, 2003). However, the inhaled insulin was withdrawn from the market because of long term safety and patient compliance issues (Bailey and Barnett, 2007). In insulin dependent diabetes mellitus pancreatic transplantation could be the best intervention to control the blood glucose level avoiding insulin therapy. Nevertheless, the highest morbidity rate of pancreas transplantation limits its application to the patients (Afaneh *et al.*, 2011).

Among the alternative routes, the most compelling method for insulin administration is oral route due to the convenience and high patient compliance. In addition, orally administered insulin would imitate the physiologic insulin secretion pathway similar to non-diabetic individuals and could provide better glucose homeostasis (Kim *et al.*, 2010). However, insulin is a protein drug therefore it is susceptible to enzymatic degradation due to the digestive enzymes like proteases in the gastrointestinal (GI) tract and chemical degradation by the harsh chemical environment of the GI tract (Huining *et al.*, 2013). In recent years various approaches have been investigated to improve oral insulin including chemical alteration of peptides (Hinds and Kim, 2002), use of enzyme inhibitors (Marschütz and Bernkop-Schnürch, 2000; Su *et al.*, 2012), enteric coating with chitosan (Cui *et al.*, 2009; Fonte

et al., 2012) and microencapsulation of insulin (Kim *et al.*, 2009; Cárdenas-Bailón *et al.*, 2015). The other obstacle of oral insulin delivery is the limited permeability of insulin to the gastrointestinal mucosal epithelial layer results in poor bioavailability of the drug even after high dose of oral administration (Avadi *et al.*, 2010).

Hydrogel delivery system is another prominent contemporary effort to develop oral delivery using 'smart' carrier for achieving controlled release of insulin (Lowman *et al.*, 1999; Kumar *et al.*, 2006). The advantage of hydrogel delivery is their ability to slow the drug release due to the interaction of drug with the hydrogel networks. Therefore, they provided slower rate of insulin release than the conventional injection therapy and enabled the delivery of insulin in the GI tract (Morishita *et al.*, 2006). However, the drawbacks of this system still remained to solve owing to the lack of molecular recognition leads to difficulties such as significant insulin release in stomach resulted in inactivation of insulin by digestive enzymes or physiological conditions in stomach. Besides the reloading of insulin occurred mainly from non-specific adsorption which lacks an effective treatment (Byrne and Salian, 2008).

Recently, nanoparticle based approaches have gained interest for proteins/peptides drug delivery. Polymeric nanoparticles may be defined as the solid, colloidal carriers in the size range of 10 to 1000 nm (Rao and Geckeler, 2011). Polymeric nanoparticles have advantages over the other carrier system which is attributed to their high surface area to volume ratio that enables the surface of nanoparticles to interact with the GI epithelium and mucus result in the improvement of transmucosal transport. In addition, they are capable of protecting the encapsulated proteins/peptides from chemical degradation. Moreover, controlled-release properties

can be offered by nanoparticulate system for encapsulated drugs (Lowe and Temple, 1994; Janes *et al.*, 2001; Galindo-Rodriguez *et al.*, 2005).

Molecular recognition is an essential biological process ubiquitous in nature can be considered as the mainspring of life courses that mimics the natural counterparts (Bergmann and Peppas, 2008). Molecular imprinting is a promising technique to form a synthetic network with molecular recognition sites for a specific template molecule, with selectivity mimicking antigen-antibody interaction and enzymatic catalysis. The drawback of biological receptors is their physicochemical stability and limited shelf-life as well as isolation and purification is expensive and time consuming. Molecularly imprinted polymers (MIPs) are able to selectively recognize a specific biomolecule (template) because of the presence of complementary recognition sites within the polymer matrix. MIPs are usually prepared by the polymerization of the functional monomers and crosslinkers in the presence of the desired template in suitable porogenic solvent. Afterwards the template is removed and left behind the memory of the template inside the polymer structure which is complementary in terms of size, shape and positioning of the functional groups as shown in **Figure 1** (Kryscio and Peppas, 2012).

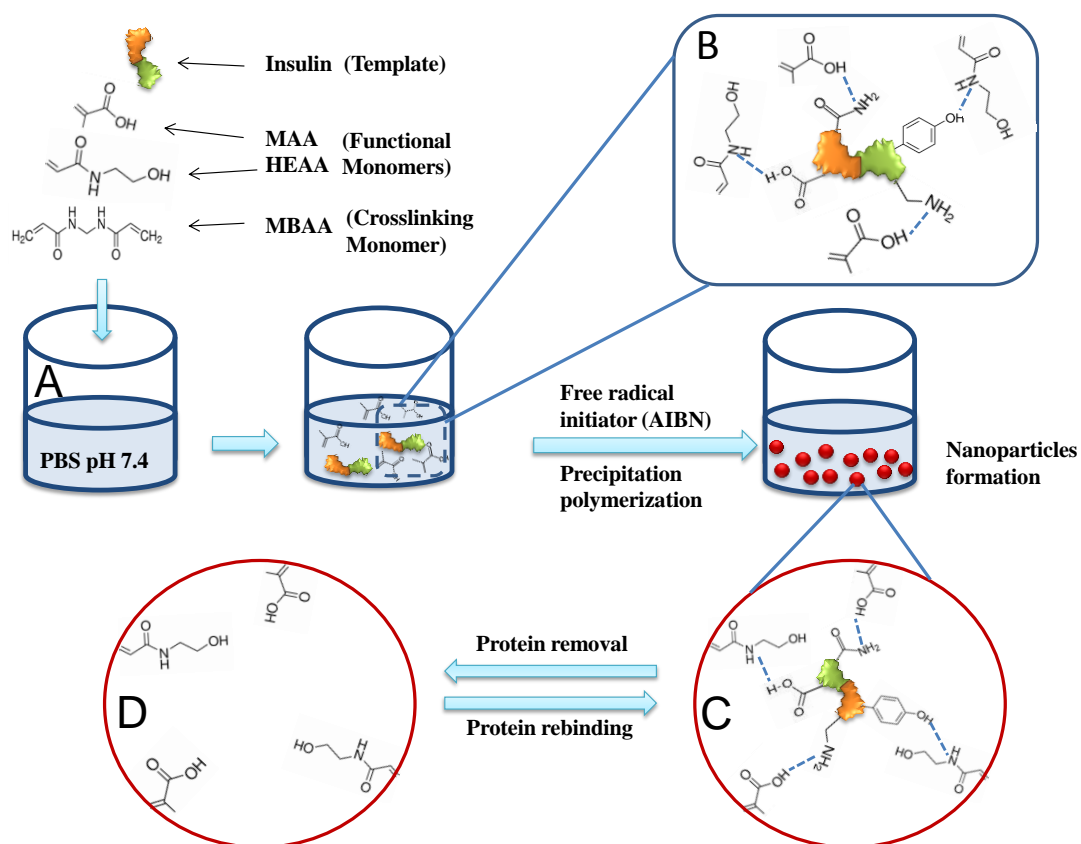


Figure 1 Illustration of the synthesis of molecularly imprinted polymer nanoparticles in this study. (A) Mixture of template (protein), functional monomers and crosslinkers. (B) Complexation between template and functional monomers via non-covalent interaction. (C) Polymer network formation by free radical polymerization. (D) Removal of template allows remaining the complementary binding sites.

The selective recognition of MIPs originates from the interaction of the template molecule with the functional monomers via non-covalent or covalent chemistry. Non-covalent approach involves self-assembly process which occurs from various interactions i.e., ionic, electrostatic, van der Waals, hydrophobic and hydrogen bonding. The non-covalent imprinting has been employed for the biomacromolecules because it is simple in operation, easy to remove the template and provides higher affinity binding sites (Vasapollo *et al.*, 2011; Yan and Row, 2006;

EL-Sharif *et al.*, 2014). Unlike small molecule the protein templates provide several binding sites from different cluster of peptide sequences which may participate in recognition characteristics via hydrogen bonding, hydrophobic or other electrostatic interactions. The hydrophobic residues are the target regions of molecular recognition for protein. Polar residues remaining on the protein surface are suitable for hydrophobic and electrostatic interactions which are responsible for maintaining the protein conformation and folding of proteins even though the amino acids composition and sequence is associated to structure and function cannot be effectively imprinted because of specific dynamic effects of some amino acids. Therefore, capitalizing non-covalent interaction to create the binding sites in different region of the polymer matrix that is corresponding to the suitable position of the protein surface would promote effective binding (Turner *et al.*, 2006). The functional material obtained by this approach may lead to the opportunities in the formation of synthetic biomimetic system that is able to detect and function in cell signaling pathway. The covalent imprinting comprises pre-organized approach by the formation of covalent linkage between template and functional monomers. The success of this technique relies on the maintenance of stable reversible covalent interaction during polymerization at the same time the covalent linkage should be easily removable without affecting the binding sites (Wulff *et al.*, 1977; Wulff, 1995).

The advantages of MIPs include the high stability, re-usability, resistance to harsh environment, ease of preparation and cost-effectiveness. These make MIPs suitable to use in several fields such as in chemical sensors (Kotova *et al.*, 2013; Latif *et al.*, 2014; Suksuwan *et al.*, 2015; Naklua *et al.*, 2016), separation (Balamurugan *et al.*, 2012; Yang *et al.*, 2016), catalysis (Czulak *et al.*, 2013; Orozco *et al.*, 2013),

artificial antibodies (Karimian *et al.*, 2014; Kunath *et al.*, 2015), and discovery of potential drugs (Yu *et al.*, 2002; Naklua *et al.*, 2015). Other applications of MIPs in pharmaceutical aspects include protein crystallization (Saridakis *et al.*, 2011; Saridakis and Chayen, 2013), cell culturing (DePorter *et al.*, 2012; Murray *et al.*, 2014), tissue regeneration (Rosellini *et al.*, 2010) and molecular probes (Naklua *et al.*, 2016a; Iwata *et al.*, 2016). Furthermore, the high loading capacity of MIPs and their ability to sustain the release of the drug which can be achieved from modification of the cross-linking type and amount that allow them to fulfill the requirements for modern drug delivery systems (Puoci *et al.*, 2011). Suedee *et al.* developed the enantioselective drug delivery system employing MIPs for selective release of the target β -blockers (Suedee *et al.*, 2000).

A biomimetic recognition system of MIPs relies on the synthesis of the polymerized materials surrounded by template protein structure regarding the monomeric mixture consisted of MIPs formulation. The resultant biomimetic imprinted materials play a massive role in mimicking as a surface layer barrier of solutes, chemical molecules and microorganisms (Hussain *et al.*, 2013). The ability of the MIPs of mimicking the nature of the enzymes by the formation of three dimensional cavities enabled them the biomimetic recognition of biomacromolecules (Parmpi and Kofinas, 2004). Rational design of biomimetic protein imprinted materials involves the selection of template, functional monomers, cross-linker and polymerization process plays an important role to get the desired imprinted polymers. The recognition properties of biomimetic MIPs are strongly dependent on the judicious choice of functional monomers and monomer-template ratio. Acrylic derivative such as methacrylic acid (MAA) is the most widely used functional

monomer for protein imprinting. It provides strong ionic interaction with basic functional group of protein and carboxyl group of this monomer act as an excellent H-bond donor and acceptor (Chen *et al.*, 2009). Acrylamide (AAm) is a common monomer which is usually exploited for imprinting macromolecules with affinity and selectivity as well as specific recognition to the target protein (Pan *et al.*, 2009). Cross-linker provides the mechanical properties to the polymer matrix which combined the ingredient to form a component assembly is important for maintaining the porous structure of the polymer and three-dimensional shape of the recognition sites after template removal. The choice of cross-linking monomer greatly affects the rigidity of the polymer, which is important for rebinding process especially for protein where the flexibility of the cross-linked polymer is required that play vital role on maintaining the resultant imprinted sites from collapsing after washing out the template (Yang *et al.*, 2012). In the typical formation of protein recognition water soluble cross-linker, *N,N*-methylene-bisacrylamide (MBAA) is suitable for template protein solubility and can provide the affinity in the polymer matrix. The imprinted polymer consisted of polyacrylamide hydrogel prepared by using MBAA as cross-liner has been investigated for protein crystallization that demonstrated selective affinity between MIPs and target protein (Saridakis and Chayen, 2013).

Preparation of highly selective protein imprinted polymers is extremely challenging in contrast to small molecules because there are few key issues need to be addressed such as protein solubility, size, conformational instability and nonselective binding (Verheyen *et al.*, 2011). Most of the proteins are water soluble therefore an aqueous system is usually used as porogenic solvent during polymerization. However, aqueous medium can interfere with the non-covalent interaction between functional

monomers and template protein that may lead to the formation of less recognition sites (Yang *et al.*, 2012). Due to the large size of the protein, cross-linked density of the imprinted polymer affect the mass transfer of the template that result in low rebinding kinetics (Valdebenito *et al.*, 2010). The presence of large number of potential binding sites at the protein surface can cause non-specific binding of the template and may give little imprint effect (Zahedi *et al.*, 2016). The complexation between functional monomers and protein template (**Figure 1 B**) during pre-polymerized process governs the nature of imprinted pattern and the protein imprinted binding sites. Therefore, this template-functional monomer assembly creates the imprint cavity which should keep intact during polymerization process and simultaneously assist in subsequent template removal without affecting the recognition sites in the polymer network (Kryscio and Peppas, 2012).

Human insulin which is the template of interest in this study is a globular protein composed of 51 amino acid residues with molecular mass of 5808 Da. It is consisted of two polypeptide chains named as A- and B- chains are connected by two disulphide bonds (**Figure 2**). The A-chain consists of 21 amino acids and has an extra disulphide bond between A6 and A11 residues while chain B has 30 residues (Gualandi-Signorini and Giorgi, 2001). At low concentration (about 1 ng/mL) and neutral pH insulin exists as monomer which is the active form of the hormone, zinc ions promotes the formation of hexamer state at higher concentration (Drachev *et al.*, 2004). The isoelectric point (IP) of human insulin is 5.3. The insulin exhibits a net negative charge above the pH than IP and it shows positive charge when the pH is below than isoelectric point. In this work, we used intermediate acting insulin as suspension formulation that acts as one template and another one is insulin-bound

islets that were isolated from rat pancreas. The insulin formulation is hexameric form of insulin containing glycerol as tonic stabilizer and meta-cresol or phenol as preservative. The pH of the vehicle is buffered at 6.9-7.5 (Gualandi-Signorini and Giorgi, 2001).

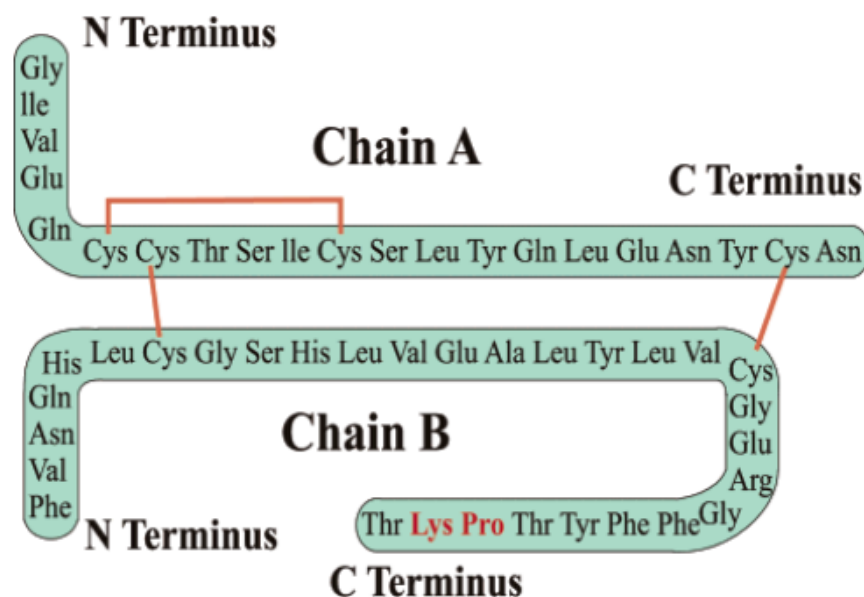


Figure 2 Amino acid sequence of human insulin (Drachev *et al.*, 2004).

Monodisperse MIPs nanoparticles have been reported to allow surface imprinting for small molecules in polymer and they can be prepared by various polymerization methods such as suspension polymerization (Alizadeh *et al.*, 2012), microemulsion polymerization (Belmont *et al.*, 2007), multi-step swelling polymerization (Haginaka and Sanbe, 2001), nonaqueous dispersion (Dvorakova *et al.*, 2010) and precipitation polymerization (Yoshimatsu *et al.*, 2007). Among these techniques, precipitation polymerization is a common method for synthesizing of monodispersed MIPs due to its ability to produce spherical particles with controlled size distribution (Wang *et al.*, 2007). The other advantages of this method are devoid of grinding and/or sieving that destroy the template binding sites (Pardeshi *et al.*,

2014) and ease of preparation without addition of surfactant or stabilizer (Chaitidou *et al.*, 2008). This technique provides the high affinity with greater accessible binding sites over the entire particle since it does not require any solid substrate. The size of particles can be controlled by sedimentation and filtration during purification and extraction of the template. The choice of functional monomers, solvent and amount of cross-linker is related to particle size of the resultant synthesized nanoparticles. Previous study showed that aqueous precipitation polymerization is a rapid and facile procedure with biocompatibility for the preparation of the protein imprinted nanoparticles (Pan *et al.*, 2013). In this study, we employed aqueous precipitation polymerization technique to generate recognition sites into MIP nanoparticles.

Biomimetic systems using recognition materials in nanotechnology exhibit long-term stability that has recognition mimics to natural system for the nanoparticle-protein association. Schirhagl *et al.* successfully prepared biomimetic materials for insulin sensing using molecular imprinting and showed that the approach can address the loss of mass transfer kinetics and the difficulty to remove large macromolecules. In addition, the design of MIPs enabled their prolonged usage (Schirhagl *et al.*, 2010; Schirhagl *et al.*, 2012). The mechanism of action of the increased protein/peptide uptake into cell for pharmacological effect is not precisely known. Recent evidence has shown that a number of protein translocation can penetrate into the epithelial cell (Nakayama *et al.*, 2011). It is well known that the chemical compounds and sensing molecules that provide the active transport of macromolecules passing across the GI epithelial layer in the electroporation interaction. However, the dynamic amino acids within protein structure that maintain the natural integrity for protein folding would affect the uptake on the lipid-protein bilayer in the cell membrane. The MIPs carrier is

associated to not only geometry effect of the protein but also diversity of cell activities. Their surface properties such as charge, chemical groups, and hydrophobic effect should be adjusted to make the complementary binding sites with the functional monomers within the surrounded cross-linking chain. In addition, the uses of the imprinted materials as a biomimetic information processing unit may gain insight into molecular mechanism of a particular protein passage into the body that despite the potential barrier to absorption via oral route could provide the systemic delivery of biopharmaceuticals.

Verspohl and Ammon reported that the insulin receptor present in the rat pancreatic islets interact with the exogenous insulin (Verspohl and Ammon, 1980). It is highly desirable to understand the nature of the specificity of the insulin's natural counterparts of the pancreatic receptors. In this study, adsorptions pattern of insulin molecule and cell attachment are imprinted in different regions on insulin formulation. For this the insulin as the pharmaceutical formulation containing the amino and carboxylic group or the islets bound insulin that was isolated from the rat pancreas formed the interaction with the functional monomer and polymerization into the polymer matrix. Furthermore, recent study identified the presence of several *N*-linked glycoproteins on mouse beta cell surface that could be used in targeting and promoting protein on the cell membrane for accessibility (Stützer *et al.*, 2012). The hydrophilic and hydrophobic property of functional monomer promotes stronger adsorption of protein-monomer assembly into the polymer matrix that may provide nanomaterial size features and an effective imprinting effect.

Raman spectroscopy has been widely used for the study of biological and nanomaterial characterization to get biological information. It provides the vibrational

fingerprint information that is very sensitive to composition, chemical structure, conformation, bonding and interactions and enables for the determination of biological molecules (Ortiz *et al.*, 2004). The proof-of-principle of vibration transitions involves the interaction between the monochromatic incident radiation and molecules of the sample that cause inelastic collision and give rise to the Raman spectrum. After striking the sample with the monochromatic radiation, when it scatters the same frequency with the incident light, it creates Rayleigh scattering. If the scattered radiation is lower than the incident light frequency then it is Stokes Raman Scattering. On the other hand, when the frequency of scattered radiation becomes higher than the incident radiation anti-Stokes line appears (**Figure 3**). Stokes bands are used in Raman spectroscopy (Bumrah and Sharma, 2016). The confocal Raman spectroscopy was used to investigate the structural information of insulin. This technique was well suited for examining the interaction between the functional monomers of the MIP nanoparticles and dynamic amino acids of template during the polymerization process and that transferred the chemical entities surrounded by the polymer nanoparticles.

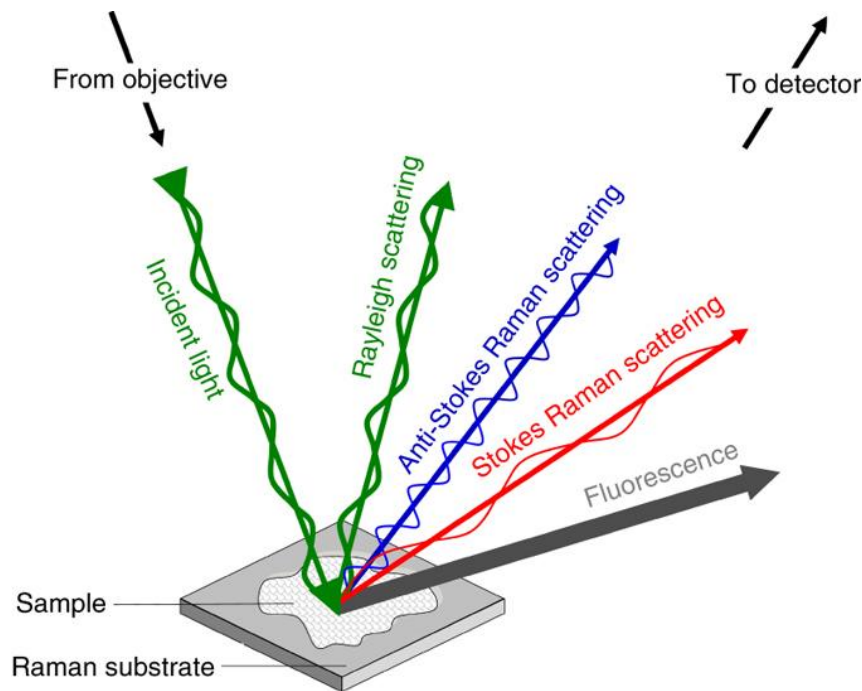


Figure 3 Different types of light scattering after monochromatic radiation exposure on sample (Butler *et al.*, 2016).

Atomic force microscopy (AFM) has been broadly used for the surface analysis at the atomic level to interpret topographic features. AFM system consists of a sharp tip attached to cantilever which is mounted on a piezoelectric scanner as shown in **Figure 4**. The AFM works by scanning the tip over the sample surface up and down, the laser beam deflected due to the tip movement give information to the photodetector. The deflection of the cantilever is used to determine the force between the tip and the surface of the sample (Maver *et al.*, 2016). The imprinting pattern of insulin crystal on the polyurethane surface showing the formation of receptor sites has been assessed by the AFM (Schirhagl *et al.*, 2012). Surface topography and imprinted cavity at nanoscale level after the template removal was evaluated by the AFM, which provided the nature of molecular structure within the three-dimensional space for the

imprinted cavity that remained or transferred the information of the protein during imprinting process.

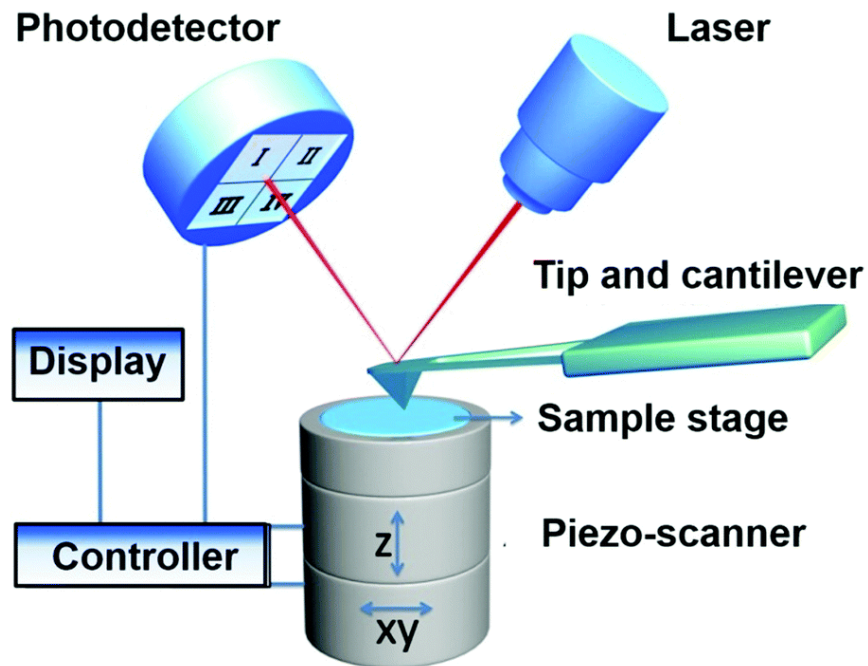


Figure 4 A schematic diagram of AFM (Shan and Wang, 2015).

The amount of insulin adsorbed by the polymers was determined by the following equation:

$$Q = (C_o - C) \times V / 1000 \times W \quad (1)$$

, where Q is the amount of adsorbed insulin (mg/g); C_o and C are the initial and final concentrations of insulin ($\mu\text{g/mL}$), respectively; V is the volume of the solution (mL); and W is the amount of polymer (g) (He *et al.*, 2014).

The physicochemical characterization of the prepared insulin-imprinted nanoparticles was carried out by Zetasizer analysis, pore size analysis, surface morphology by scanning electron microscopy (SEM) and transmission electron microscopy (TEM). The surface solid-state properties of the synthesized MIPs were

examined using AFM. Confocal Raman spectroscopy was used to examine the specific region of the insulin on the surface of the nanoparticles that is responsible for the interaction with the binding sites of the polymer. Protein adsorption and in vitro release were assessed. Oral administration of insulin-loaded MIPs on Wistar rats was also evaluated to investigate blood glucose level reduction.

The interaction of the nanoparticles with the intestinal epithelium plays the pivotal role in the systemic absorption and site-specific toxicity of nanoparticles. Hence, it is so important to understand the interaction which is the crucial area of drug delivery. Moreover, a better understanding of the physicochemical properties of nanomaterials and their influence in the interaction with biological systems at various levels such as systemic, organ, tissue, cell etc. are required for safe and effective clinical use (Bannunah *et al.*, 2014). The physicochemical properties (e.g., chemical composition, size, surface charge, and surface chemistry) of nanoparticles influence the interaction with biological system resulting in intestinal uptake (Albanese *et al.*, 2012; Sohaebuddin *et al.*, 2010). Safety and toxicity are the major concerns for the successful application of the nanotechnology in drug delivery (De Jong and Borm, 2008).

Fluorescence spectroscopy is a powerful technique to examine the interactions of protein with other element. The fluorescence of the insulin molecule originates from tyrosine residues are intrinsic fluorophores present in the protein. The previous study have reported about the using of fluorescence microscopy to determine the interaction and surface heterogeneity effect of MIP surface on the adsorption of the protein (Naklua *et al.*, 2016a). Tumor cell lines have been studied to investigate the study of the nanoparticle uptake into the cell in the recent years (Wang *et al.*, 2012;

He *et al.*, 2013). However, Tissue level study is needed to elucidate the detail mechanism of nanoparticle transport. It is more realistic approach to investigate the uptake of nanoparticles within intestinal tissues rather than the monitoring nanoparticle bulk transport through Caco-2 cells or everted intestinal sac of mouse models with inhibitors. The shortcomings of these approaches are firstly, because of their specific metabolic needs the cancer cells including Caco-2 cells exhibit over expression of nutritional ligands and uptake of nutrients from the extracellular space. Secondly, the possibility of nanoparticle retention due to the change of cellular structures by inhibitors leads to difficulty in elucidating the real mechanism (Simovic *et al.*, 2015).

Sonaje *et al.* used fluorescent nanoparticles to determine the *in vivo* absorption of the fluorescent labeled insulin after the treatment to the rat model with the nanoparticles and the confocal images of the rat intestinal segments showed that the nanoparticles were within the adsorptive intestinal villi (Sonaje *et al.*, 2012). Previous study reported that chitosan can act as an absorption enhancer for insulin via paracellular route by opening tight junction in lanthanum-stained intestinal segments upon the delivery of chitosan loaded with insulin (Chen *et al.*, 2013). Nevertheless, the paracellular space represents <0.5% of intestinal absorptive surface and restrict the passage of nanoparticles. Therefore, other routes of transport such as transcellular pathway have gained much attention which involves transcytosis of nanoparticles by enterocytes (Munishkina and Fink, 2007). Different mechanisms of nanoparticles uptake in the intestinal epithelium are shown in the **Figure 5**.

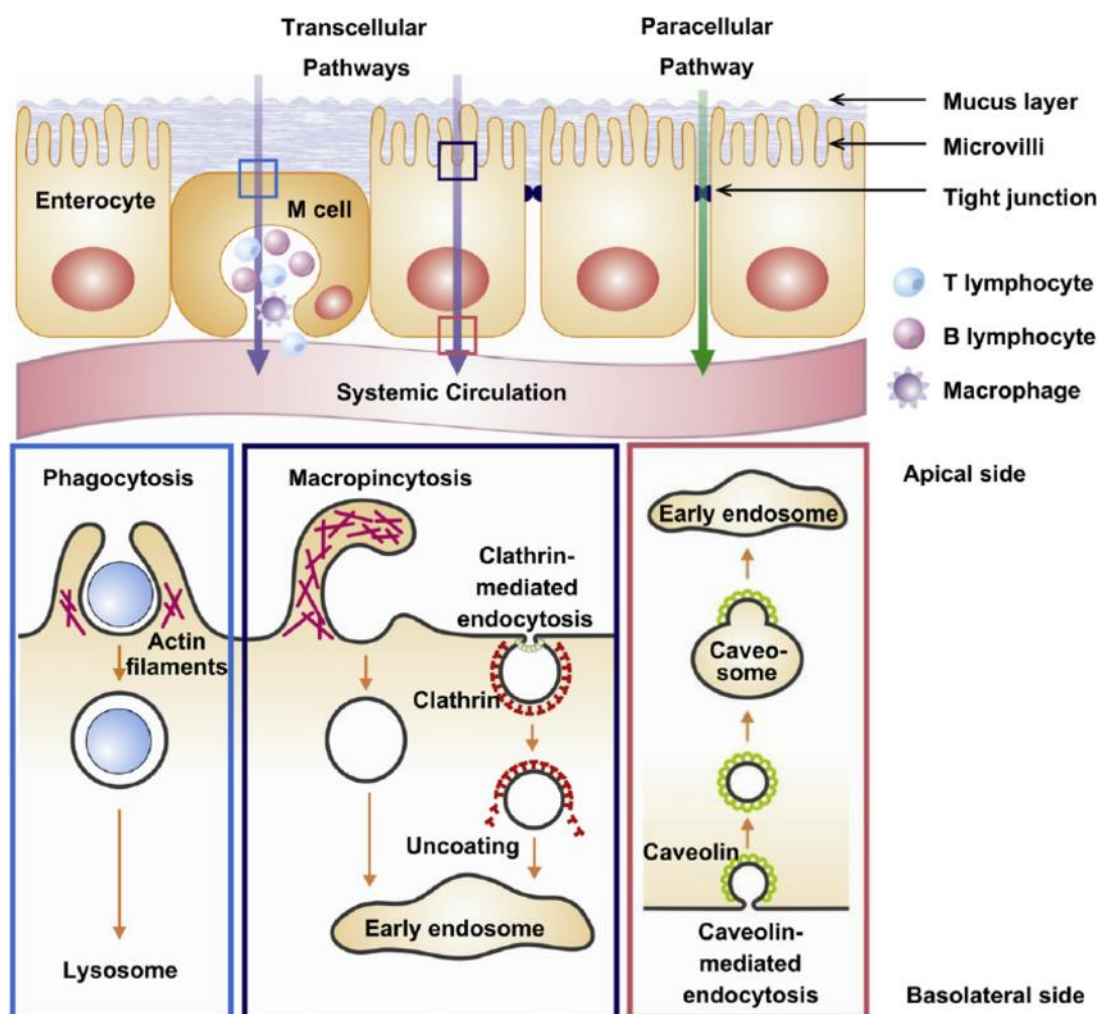


Figure 5 Schematic illustrations of different transport mechanisms of nanoparticles across the intestinal epithelium. The detailed mechanism of phagocytosis, macropinocytosis and endocytosis is shown in insets (Chen *et al.*, 2011).

Within this work, MIPs with insulin and the isolated islets from rat containing insulin binding sites were prepared which created both hydrophilic and hydrophobic surfaces on MIPs that could be obtained from the monomeric reaction in different polymerizing mixtures. The selectivity of the MIPs to the templates was related to the imprinted recognition sites formed from combination of MAA and *N*-hydroxyethyl acrylamide (HEAA) as functional monomers and MBAA as a cross-linking monomer in different ratios. The insulin and insulin in rat pancreatic islets

were used as the templates and aqueous precipitation polymerization technique was employed using pH 7.4 phosphate buffer saline (PBS) as porogen to synthesis the MIPs. According to previous study, MAA exhibits mucoadhesive properties at higher concentration (Achar and Peppas, 1994). HEAA acts as a hydrophilic nonionic monomer with adhesive characteristic to protein owing to better coordination effect of the binding block as hydrogen bond receptor (Li *et al.*, 2011). This could be advantageous for the chemical stability of the protein during polymerization process.

We investigated the intestinal uptake of insulin loaded MIP nanoparticles within intestinal tissues to elucidate the transport mechanism and intracellular localization of internalized nanoparticles. Evaluation of the activity of orally administered MIP nanoparticles, which may provide nature and the extent of their toxicity effect in rat model that were carried out by immunohistochemistry and immunofluorescence studies as well as ultrastructural examination using TEM. Within the second part of the thesis work, we attempted to develop the synthetic material in nanosized scale by molecular imprinting for studying on reactive toxicity into their appropriate component regarding to MIPs formulation. Toxicity study was conducted by repeated oral administration of MIPs nanoparticles to Wistar rats for 14 days.

CHAPTER 2

OBJECTIVES

The main objective was to develop a nanoparticulate carrier system for controlled release delivery of oral insulin by using molecular imprinting approach.

The aims of this work were:

1. To prepare molecularly imprinted polymers (MIPs) consisted of selective recognition of imprinted cavity for template by aqueous precipitation polymerization technique using insulin and islets bound insulin as templates. MAA and HEAA were used as functional monomers with different template/monomer ratio and MBAA as cross-linker with different degree of crosslinking. Non-imprinted polymers (NIPs) were synthesized by similar protocol except the addition of the template protein. The average particle size and the zeta potential of the nanoparticles were determined by the dynamic light scattering (DLS) measurements.
2. To characterize the surface morphology of the prepared MIPs and NIPs by SEM, TEM, AFM after template removal. Confocal Raman spectroscopy was used to examine the interaction between protein template and functional monomer during polymerization and imprinting process.
3. To measure the surface areas and porosity of the polymers by Brunauer-Emmett-Teller (BET) analysis with automated gas sorption system. Barrett-Joyner-Halenda (BJH) method was employed to determine the pore size distribution and pore volume of the nanoparticles. The thermal properties of

the obtained polymer nanoparticles both MIPs and NIPs were evaluated by the differential scanning calorimetry (DSC) analysis.

4. To determine the recognition ability of all the MIPs by protein adsorption study using batch binding experiments. Binding isotherm was obtained by incubating nanoparticles with different concentrations of insulin in parallel experiment with the corresponding NIPs.
5. To investigate the interaction between MIPs and insulin by fluorescence spectroscopic analysis was using fluorescence spectroscopy. To study the *in vitro* protein release from the MIPs and NIPs nanoparticles buffer solution pH 1.2 and pH 7.4 were used to examine the effect of protein structure in the solution media mimicking the environment of GI tract.
6. To assess the *in vivo* hypoglycemic effect the pharmacological activity insulin loaded MIPs were determined by administering orally to streptozotocin induced diabetic Wistar rat and blood glucose level was measured by using a glucose meter.
7. To investigate the effect of rat intestinal tissue lysate on insulin transfer from MIPs, desorption and partitioning of insulin was carried out. To investigate the development of pancreatic tissue response after the oral administration to the diabetic animals, bioactivity of the insulin loaded in MIPs was examined via immunohistochemistry (IHC) using anti-insulin antibody.
8. To study *in vivo* absorption of MIPs loaded insulin by immunofluorescence study. The transport of the MIPs and insulin across the intestinal epithelium was investigated by ultrastructural examination of intestinal segments using immunogold staining technique and visualization with TEM.

9. To study the toxicological effect of the resultant MIPs nanoparticles, the insulin loaded MIPs were administered orally to male Wistar rats for 14 days daily and examined the intestine, liver and kidney tissues to detect morphological changes.

CHAPTER 3

SIGNIFICANT RESULTS AND DISCUSSION

Preparation and characterization of MIPs

In this work, we used molecular imprinting to generate the recognition sites for pharmaceutically active insulin and the evaluation of the synthesized materials for selective delivery of the insulin via oral route of administration. The MIPs were prepared by aqueous precipitation polymerization technique. The present method led to the MIPs nanoparticles that specifically targeted the insulin for function and activity in the body that possessed the amine and carboxylic groups in the polymer, which endowed a high expression level of biomimetic sites to the template molecules. The varying amounts of MBAA as well as the concentrations of the MAA functional monomer and addition of HEAA eventually formed the polymeric region which was responsible for the protein affinity to its rebinding sites. The average particle size and the zeta potential of the synthesized MIPs obtained by dynamic light scattering measurements are shown in **Table 1**.

The average hydrodynamic sizes of MIPs were in the range of 200-220 nm with negative surface charge around -32 mV. Surface charges played an important role in the uptake of nanoparticles by the intestinal epithelium. Positively charged nanoparticles interacted with the negatively charged mucin and enhanced the duration of the retention of the particles on the mucosa. Nonetheless, the absorption of the nanoparticles that led to intestinal uptake decreased due to the high interaction between the positively charged nanoparticles and the mucin (Andreani *et al.*, 2014). Previous studies reported a better transport capacity of the negatively charged

nanoparticles across the intestinal epithelial layer as well as a better penetration through the mucus layer passage inside the epithelial cells. In addition, the negatively charged nanoparticles could mimic the virus like characteristics that allowed them to diffuse into the mucus as a result of the lower interaction between the mucin (de Sousa *et al.*, 2016). The results obtained in this study supported that the imprinted nanoparticles might enhance the permeation across the mucus barrier and therefore increased the absorption of the insulin higher than the control polymer NIPs. The research findings indicated that the NIPs had a slightly higher PDI and larger particle size than that of MIPs where penetration through the adsorptive epithelial layer is increased, the blood glucose level was significantly reduced and the ultrastructural examination was clearly noticeable.

Table 1 Characteristics of prepared polymers.

Polymer	Particle size analysis			Pore analysis		
	Mean diameter (nm)	Polydispersity index	Zeta potential (mV)	Surface area (m ² /g)	Pore volume (ml/g)	Pore diameter (nm)
MIP1	221.86 ± 23.55	0.39 ± 0.03	-32.2 ± 5.1	21.83	0.089	14.82
MIP2	198.73 ± 3.05	0.33 ± 0.02	-32.3 ± 4.23	149.1	0.462	12.40
NIP1	302.46 ± 10.5	0.46 ± 0.08	-28.9 ± 3.7	27.39	0.263	38.02
NIP2	236.56 ± 31.33	0.43 ± 0.05	-33.6 ± 2.3	86.85	1.031	47.50

The pore diameter of the MIPs was around 14 nm which was 3 times smaller than the corresponding NIPs (**Table 1**). **Figure 6** shows the nitrogen adsorption-desorption isotherms of MIPs nanoparticles displayed similar characteristics of type-IV isotherm indicating the mesoporous construction of the polymers. The pore diameter of the NIPs was larger than the MIPs in which no template was used during polymerization and the isotherm exhibited type-III curve characteristics demonstrating nonporous structure with low interaction.

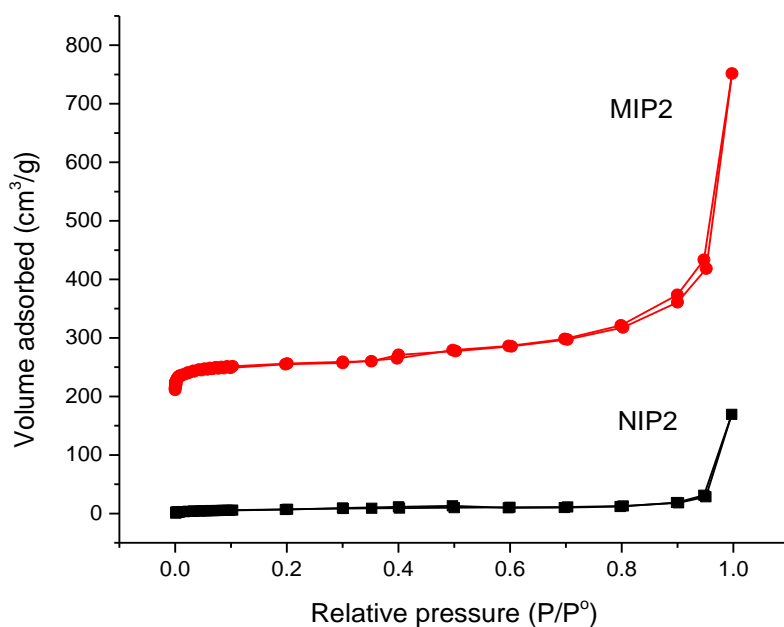


Figure 6 Nitrogen adsorption /desorption isotherms of the MIPs and NIPs.

Confocal Raman spectroscopy was used to assess the interaction of the insulin-MIPs nanoparticles during the polymerization process after template removal, the functionalities of the protein that transferred into the polymer networks. The Raman shift and the peak intensities of insulin and the polymers are presented in **Table 2**. The Raman fingerprint of insulin is found in different wavenumbers such as tyrosine (Tyr) at 832 cm^{-1} , phenylalanine (Phe) at 1010 cm^{-1} and the 1215 cm^{-1} band for Tyr and Phe. These are characteristics peaks for R_6 conformation of hexameric

human insulin. We took the advantage of the detection of the peak intensities of MIPs derived from changed orientation of the insulin molecule upon polymerization process which led to a self-assembly component of a polymer in the presence of insulin predicting the spatial motifs and functional modification. Further information of the insulin-bound islet in the imprint was not discernable from the Raman spectra.

Table 2 Raman data of the insulin and polymers after template removal.

Raman peak	Raman shift (cm ⁻¹)	Peak intensity				
		Insulin	MIP1	MIP2	NIP1	NIP2
Tyrosine (Tyr)	832.53	464.38	330.25	45.56	306.33	250.92
C-C	940.24	307.84	279.05	66.66	175.59	162.64
Phenylalanine (Phe)	1010.98	369.50	332.96	85.14	133.21	164.16
Tyr and Phe	1215.25	1005.62	743.97	154.27	470.31	421.45

Rebinding capacity of MIPs and *in vitro* insulin release

The adsorption capacity of the MIP1 and MIP2 were 2.65 and 3.26 mg/g, respectively which were 2.5 times greater than that of the corresponding NIPs. The binding parameters determined by Scatchard equation are summarized in **Table 3**. The equilibrium dissociation constant (K_d) value of MIP2 (3.049 μ M) is slightly higher than MIP1 (1.914 μ M). However, the apparent maximum number of the binding sites (B_{max}) for both MIP1 and MIP2 were the same (4 μ M/g) indicating the construction of uniform binding sites. MIP2 consisted of two functional monomers (MAA and HEAA) with lower amount of cross-linker showed a much faster *in vitro* release ($k = 7.35 \pm 0.89$) than the MIP1 ($k = 4.73 \pm 2.57$) which comprises with single monomer, MAA only with high degree of cross-linkage at pH 7.4. The greater insulin

release from MIP2 was further corroborated by a higher K_d value of MIP2 (3.049 μM) compared to MIP1 (1.914 μM).

Table 3 Binding parameters and Release kinetics data of the MIPs.

Polymer	Binding parameters			Release kinetics data at pH 7.4		
	K_d (μM)	B_{max} ($\mu\text{M/g}$)	R^2	n^*	k^*	r^2
MIP1	1.91 ± 0.18	4.05 ± 0.15	0.997	0.536 ± 0.122	4.74 ± 2.57	0.977
MIP2	3.05 ± 0.43	4.34 ± 0.29	0.995	0.451 ± 0.028	7.36 ± 0.90	0.998

* For mean \pm SD (n=3).

The drug release data at pH 7.4 were analyzed by the Korsmeyer-Peppas equation as follows:

$$Mt / M_{\infty} = kt^n \quad (2)$$

, where Mt / M_{∞} is the fraction of insulin released at time t and k is the release rate constant. The diffusion exponent n characterizes the release mechanism of the drug depending on the geometry of the material tested. For the radial geometry, $n = 0.45$ corresponds to the Fickian transport, $0.45 < n < 0.89$ corresponds to the non-Fickian (anomalous) transport, and $n = 0.89$ is related to the case II transport (36). The diffusion exponent (n) values of MIP1 and MIP2 were found to be between 0.45 and 0.89 (**Table 3**), which imply a non-Fickian transport. The results suggested that the release of insulin occurred from diffusion and dissolution in the aqueous medium that may change the hydrodynamic properties of the particles, corroborated to effective adsorption data and hence, the reduced mass transfer resistance of protein in the imprinted matrix.

***In vivo* evaluation of insulin loaded MIPs on diabetic rats**

After the oral administration of the insulin-loaded MIPs (50 IU/kg) to the diabetic rats, the blood glucose level was reduced markedly compared to the NIPs. Using MIP2, the initial blood glucose level was reduced significantly ($p < 0.05$) by (44% within 4 h) and was maintained at this level for up to 12 h. On the other hand, no hypoglycemic effect was found for the insulin loaded with NIPs nanoparticles. The results indicated that the insulin bound to these MIPs rather than onto a non-specific site to pass from an aqueous phase to the membrane of the GI lumen. **Table 4** shows the parameters of the plasma glucose levels at a dose of 50 IU/kg. The relative pharmacological bioavailability in the percentage reduction of glucose of the MIP1 and MIP2 were 1.73% and 1.55%, respectively. The results suggested that the insulin absorption was markedly increased by the action of the MIPs delivery system after oral administration.

Table 4 Relative pharmacological bioavailability and parameters of plasma glucose levels (n=5).

Parameters	INS-MIP1	INS-MIP2	INS-SC
Insulin dose (IU/kg)	50	50	1
C_{\min}^* (mg/dL)	61.58 ± 10.57	54.65 ± 9.43	40.76 ± 11.65
t_{\min}^{**} (h)	4	4	2
AAC	1577.71 ± 208.29	1422.887 ± 254.90	1816.2 ± 188.96
PA%	1.74	1.55	100

* C_{\min} , minimum plasma glucose concentration (% of initial)

** t_{\min} , time at which C_{\min} is attained; AAC, area above the blood glucose level-time curves; PA%, relative pharmacological bioavailability.

The observation in significant difference of surface morphology between MIP nanoparticles and NIP with fluorescein isothiocyanate (FITC) and rhodamine (Rh) conjugated MIP-FITC were higher than that for corresponding NIP-FITC loaded with insulin-Rh when the polymers were exposed to the Wistar rats intestinal segments. The MIP-FITC was observed on the mucus layer as well as a greater amount was present in the lacteal side of the villi for the tissue sections. The insulin-Rh with MIP-FITC was found mostly inside the enterocytes and lacteal side of the villi. An oral administration of the MIP loaded with insulin produced a significantly elevated ($P < 0.0001$) fluorescent intensity of insulin-Rh which is almost 10 times greater than that of NIP (**Figure 7**). We found that the insulin imprint promoted the absorption rate and extent of Rh-insulin probably via diffusion of protein concentrations through lipid bilayer across the surface of epithelial cell of intestine, while the fluorescence of insulin-Rh was diminished for NIP in every section under the same condition. The similar fluorescence intensity of insulin-Rh for MIP in all the segments of the intestinal epithelial cells indicated that has dissipated after 3 h of oral administration.

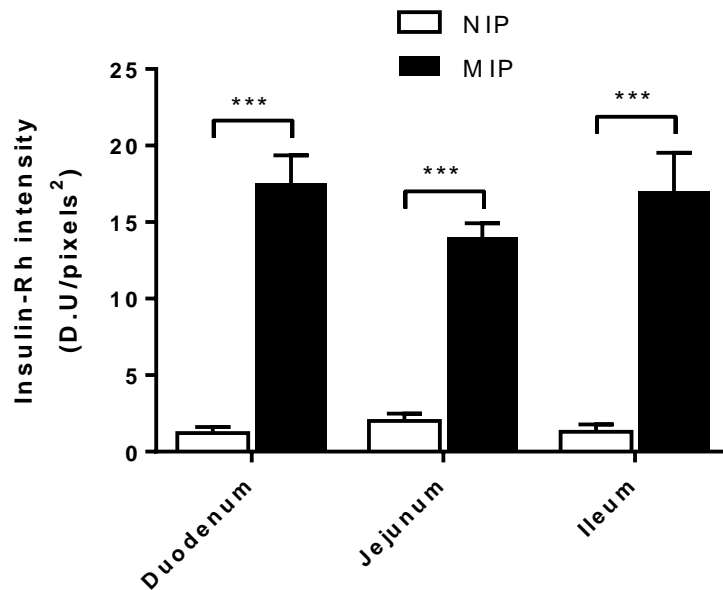


Figure 7 Fluorescent intensity of insulin-Rh for MIP and NIP. Values are mean \pm SEM (n=4) per group. ***P< 0.0001 compared to NIP.

The extent of insulin transport along with the polymer nanoparticles across the intestinal epithelium as determined by immunoreactivity using anti-insulin antibody followed by anti-guinea pig antibody and detection by immunogold staining using TEM appeared to be strongly affected in different segments of rat intestine. The consequence of the transport of insulin in the MIP delivery across the intestinal epithelial cells is that the amount of insulin increased as immunoreactivity of the anti-insulin antibody followed by the detection of the biotin gold nanoparticles at the same time has been shown to be correlated to the barrier function of the GI tract (**Figure 8**).

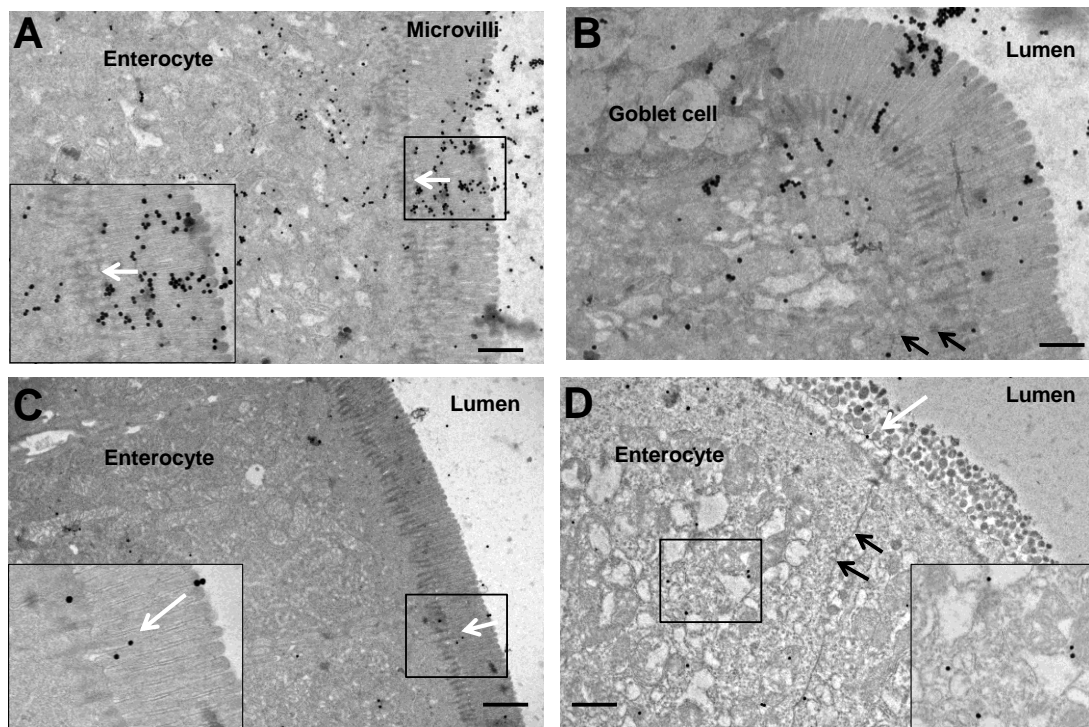


Figure 8 TEM micrographs of immunogold-stained intestinal segments after 3 h of orally administered insulin loaded with MIP (A, B) and NIP (C, D). Insulin was investigated by immunolabeling with guinea pig anti-insulin antibody followed by goat anti-guinea pig antibody conjugated with 60 nm biotin gold nanoparticles (black dots). The permeation of insulin occurs through the transcellular route (white arrows) and the absence of insulin in the surface of paracellular space indicated by black arrows. Scale bar, 2 μ m. Insets designate the 12000 x magnified views of tissue region.

We found that the amount of insulin molecules was greater when administered orally with MIP than that of NIP. The nanoparticle-biotin absorption for MIP ($P < 0.0001$) was statistically significant while the amount of insulin for NIP was diminished. However, intestinal absorption of insulin from NIP was examined and it has less effect which confirmed that the recognition of insulin into MIP nanoparticles

leading to the distinctive response in the insulin activity which is in conformity with the immunofluorescence results. Interestingly, the penetration of insulin to enterocytes was observed via transcellular pathway (white arrows) as they were absent in the surface of paracellular space (black arrows). These findings suggested that there was a difference in the underlying interaction of dynamic molecular mechanisms of the transport for insulin contained in the nanoparticles for MIP preserving the small entities or amino acid sequence could translocate the insulin into specific cellular organelles as a result of insulin imprint in nanoparticles upon polymerization process for biomolecular system in the polymer matrix. We found that the transcellular pathway so as to deliver insulin effectively in the cell organelles by MIP.

The results indicated that after orally administered insulin loaded MIP for 14 days using hematoxylin and eosin (H&E) staining the examination of the intestine, liver and kidney tissues were morphologically not changed that affected by the STZ-induced diabetes. No toxicity was found concerning body weight change, histopathological characteristics, and clinical symptoms like diarrhea or fever for 14 days of the experiment. When considering the varying of functional monomer and cross-linker content in the monomeric mixture resulted in different mean diameter of nanoparticles and pore volume for NIPs compared to the respective MIPs. In addition, the use of mixed functional monomers (MAA and HEAA) and lower amount of cross-linker the mean diameter and pore volume were reduced. We conclude that the introduction of MIPs is advantageous in oral insulin delivery with potential benefit as nanocarrier system.

CHAPTER 4

CONCLUSION

The current study results suggested that the insulin-rebinding with respect to the different functional chemistries and changed charges in the hysteresis pore, engaged the dynamic reactivities of the protein and appeared to maintain high selectivity. These studies proved considerable drug delivery system and selectivity towards optimal release of the insulin regardless of the environment in the GI tract that confirmed the absorption of insulin into blood circulation. By adjusting the functionalized chemistry in a nanosized particulate drug adsorption capacity of the biomimetic recognition enhanced loading and accessibility for the template protein to recognition sites when placed into the GI cavity that represented a preventative barrier for the oral delivery. The findings may have important functional implementations for transport of protein and peptide therapeutics in the body. It is possible to use MIPs to overcome biological barrier for the biopharmaceuticals which could indicate the response of cell signaling and the insulin uptake across the intestinal epithelial cells into the blood circulation. Quite interestingly, the transport across the microporous plate impregnated with the MIPs which was incubated within the intestinal tissue lysate appears to be markedly reduced insulin release *in vitro* as compared to the NIPs. The *in vitro* and *in vivo* correlation for oral administration with the insulin-Rh loaded MIPs is substantial that resulted in the observation of insulin crosses the cell membrane into the rat intestine. This is likely due to the insulin-MIP interaction by self-assembly that greatly increased the ability to transport across intestinal epithelial

cells via transcellular pathway. On the other hand, the complementary functional monomers and template functionality within three-dimensional structure of the protein imprint was modified by the highly cross-linked MBAA-polymer which could indicate the adaptation of binding sites for spatial conformation and chemical structure of insulin with physical properties as they could provide chemical interactions more closely with the biological membrane of the different parts of Wistar rat intestine. This can be explained by the significant difference in protein absorption, relatively protein uptake and the distribution within the intestinal tissues. The driving force of this phenomenon could be the surface free energies of the polymer carrier and the biomacromolecule that were influenced by hydration energy of the protein was different for NIPs. This allowed for faster protein viability by the entropy and hence the lower free energy than that of the natural protein while the movement of nanoparticles present in outermost of the blood vessel within the GI tissue led to effective transport. No inflammatory or immunogenic effect was detected in the subjects tested. Thus, these MIPs nanomaterial obtained by imprinting technique are capable of improving the treatment of diabetes. In future, further investigation on endocytic trafficking pathway of MIPs loaded with insulin uptake into intracellular matrix and organelles would be interesting to gain a better insight into the detailed mechanism of localization and internalization of nanomaterial. Our study showed that the MIPs nanoparticles on delivery of insulin via oral route improved the pancreatic β -cells produced insulin and the normal function of the organs was observed which influenced the lower blood glucose level. These studies clearly support that the added insulin in MIPs is important for the functional activity of insulin through the intestinal epithelial layer into the blood circulation and the

development of pancreatic tissue in the STZ-induced diabetic rats by increasing the absorption in the intestinal cell layer and the systemic delivery of the insulin.

REFERENCES

- Achar, L. and Peppas, N. 1994. Preparation, characterization and mucoadhesive interactions of poly (methacrylic acid) copolymers with rat mucosa. *Journal of Controlled Release* 31: 271-276.
- Afaneh, C., Rich, B. S., Aull, M. J., Hartono, C., Leaser, D. B. and Kapur, S. 2011. Pancreas transplantation: does age increase morbidity? *Journal of Transplantation* 2011.
- Albanese, A., Tang, P. S. and Chan, W. C. 2012. The effect of nanoparticle size, shape, and surface chemistry on biological systems. *Annual Review of Biomedical Engineering* 14: 1-16.
- Alizadeh, T., Ganjali, M. R. and Akhoundian, M. 2012. Synthesis and application of different nano-sized imprinted polymers for the preparation of promethazine membrane electrodes and comparison of their efficiencies. *International Journal of Electrochemical Science* 7: 7655.
- Andreani, T., de Souza, A. L. R., Kiill, C. P., Lorenzón, E. N., Fangueiro, J. F., Calpena, A. C., Chaud, M. V., Garcia, M. L., Gremião, M. P. D. and Silva, A. M. 2014. Preparation and characterization of PEG-coated silica nanoparticles for oral insulin delivery. *International Journal of Pharmaceutics* 473: 627-635.
- Avadi, M. R., Sadeghi, A. M. M., Mohammadpour, N., Abedin, S., Atyabi, F., Dinarvand, R. and Rafiee-Tehrani, M. 2010. Preparation and characterization of insulin nanoparticles using chitosan and Arabic gum with ionic gelation method. *Nanomedicine: Nanotechnology, Biology and Medicine* 6: 58-63.

- Bailey, C. J. and Barnett, A. H. 2007. Personal Views: Why is Exubera being withdrawn? *BMJ: British Medical Journal* 335: 1156.
- Balamurugan, K., Gokulakrishnan, K. and Prakasam, T. 2012. Preparation and evaluation of molecularly imprinted polymer liquid chromatography column for the separation of Cathine enantiomers. *Saudi Pharmaceutical Journal* 20: 53-61.
- Bannunah, A. M., Vllasaliu, D., Lord, J. and Stolnik, S. 2014. Mechanisms of nanoparticle internalization and transport across an intestinal epithelial cell model: effect of size and surface charge. *Molecular Pharmaceutics* 11: 4363-4373.
- Belmont, A.-S., Jaeger, S., Knopp, D., Niessner, R., Gauglitz, G. and Haupt, K. 2007. Molecularly imprinted polymer films for reflectometric interference spectroscopic sensors. *Biosensors and Bioelectronics* 22: 3267-3272.
- Bergmann, N. M. and Peppas, N. A. 2008. Molecularly imprinted polymers with specific recognition for macromolecules and proteins. *Progress in Polymer Science* 33: 271-288.
- Bruce, D., Chisholm, D., Storlien, L., Borkman, M. and Kraegen, E. 1991. Meal-time Intranasal Insulin Delivery in Type 2 Diabetes. *Diabetic Medicine* 8: 366-370.
- Bumrah, G. S. and Sharma, R. M. 2016. Raman spectroscopy–Basic principle, instrumentation and selected applications for the characterization of drugs of abuse. *Egyptian Journal of Forensic Sciences* 6: 209-215.
- Butler, H. J., Ashton, L., Bird, B., Cinque, G., Curtis, K., Dorney, J., Esmonde-White, K., Fullwood, N. J., Gardner, B. and Martin-Hirsch, P. L. 2016. Using Raman

- spectroscopy to characterize biological materials. *Nature Protocols* 11: 664-687.
- Byrne, M. E. and Salian, V. 2008. Molecular imprinting within hydrogels II: Progress and analysis of the field. *International Journal of Pharmaceutics* 364: 188-212.
- Cárdenas-Bailón, F., Osorio-Revilla, G. and Gallardo-Velázquez, T. 2015. Microencapsulation of insulin using a W/O/W double emulsion followed by complex coacervation to provide protection in the gastrointestinal tract. *Journal of Microencapsulation* 32: 308-316.
- Cefalu, W. T. 2004. Concept, strategies, and feasibility of noninvasive insulin delivery. *Diabetes Care* 27: 239-246.
- Chaitidou, S., Kotrotsiou, O., Kotti, K., Kammona, O., Bukhari, M. and Kiparissides, C. 2008. Precipitation polymerization for the synthesis of nanostructured particles. *Materials Science and Engineering: B* 152: 55-59.
- Chen, M.-C., Mi, F.-L., Liao, Z.-X., Hsiao, C.-W., Sonaje, K., Chung, M.-F., Hsu, L.-W. and Sung, H.-W. 2013. Recent advances in chitosan-based nanoparticles for oral delivery of macromolecules. *Advanced Drug Delivery Reviews* 65: 865-879.
- Chen, M.-C., Sonaje, K., Chen, K.-J. and Sung, H.-W. 2011. A review of the prospects for polymeric nanoparticle platforms in oral insulin delivery. *Biomaterials* 32: 9826-9838.
- Chen, Y.-W., Rick, J. and Chou, T. C. 2009. A systematic approach to forming micro-contact imprints of creatine kinase. *Organic & Biomolecular Chemistry* 7: 488-494.

- Cui, F., He, C., He, M., Tang, C., Yin, L., Qian, F. and Yin, C. 2009. Preparation and evaluation of chitosan-ethylenediaminetetraacetic acid hydrogel films for the mucoadhesive transbuccal delivery of insulin. *Journal of Biomedical Materials Research Part A* 89: 1063-1071.
- Czulak, J., Jakubiak-Marcinkowska, A. and Trochimczuk, A. 2013. Polymer catalysts imprinted with metal ions as biomimics of metalloenzymes. *Advances in Materials Science and Engineering* 2013.
- De Jong, W. H. and Borm, P. J. 2008. Drug delivery and nanoparticles: applications and hazards. *International Journal of Nanomedicine* 3: 133.
- de Sousa, I. P., Moser, T., Steiner, C., Fichtl, B. and Bernkop-Schnürch, A. 2016. Insulin loaded mucus permeating nanoparticles: Addressing the surface characteristics as feature to improve mucus permeation. *International Journal of Pharmaceutics* 500: 236-244.
- DePorter, S. M., Lui, I. and McNaughton, B. R. 2012. Programmed cell adhesion and growth on cell-imprinted polyacrylamide hydrogels. *Soft Matter* 8: 10403-10408.
- Drachev, V. P., Thoreson, M. D., Khaliullin, E. N., Davisson, V. J. and Shalaev, V. M. 2004. Surface-enhanced Raman difference between human insulin and insulin lispro detected with adaptive nanostructures. *The Journal of Physical Chemistry B* 108: 18046-18052.
- Dvorakova, G., Haschick, R., Chiad, K., Klapper, M., Müllen, K. and Biffis, A. 2010. Molecularly imprinted nanospheres by nonaqueous emulsion polymerization. *Macromolecular Rapid Communications* 31: 2035-2040.

- EL-Sharif, H. F., Hawkins, D. M., Stevenson, D. and Reddy, S. M. 2014. Determination of protein binding affinities within hydrogel-based molecularly imprinted polymers (HydroMIPs). *Physical Chemistry Chemical Physics* 16: 15483-15489.
- Fonte, P., Andrade, F., Araujo, F., Andrade, C., Neves, J. and Sarmiento, B. 2012. Chitosan-coated solid lipid nanoparticles for insulin delivery. *Methods in Enzymology* 508: 295-314.
- Fu, Z., R Gilbert, E. and Liu, D. 2013. Regulation of insulin synthesis and secretion and pancreatic Beta-cell dysfunction in diabetes. *Current Diabetes Reviews* 9: 25-53.
- Galindo-Rodriguez, S. A., Allemann, E., Fessi, H. and Doelker, E. 2005. Polymeric nanoparticles for oral delivery of drugs and vaccines: a critical evaluation of in vivo studies. *Critical ReviewsTM in Therapeutic Drug Carrier Systems* 22.
- Gavin, J. R., Alberti, K. G., Davidson, M. B., DeFronzo, R. A., Drash, A., Gabbe, S. G., Genuth, S., Harris, M. I., Kahn, R. and Keen, H. 2003. Report of the expert committee on the diagnosis and classification of diabetes mellitus. *Diabetes Care* 26.
- Gualandi-Signorini, A. and Giorgi, G. 2001. Insulin formulations-a review. *European Review for Medical and Pharmacological Sciences* 5: 73-84.
- Haginaka, J. and Sanbe, H. 2001. Uniformly sized molecularly imprinted polymer for (S)-naproxen: Retention and molecular recognition properties in aqueous mobile phase. *Journal of Chromatography A* 913: 141-146.

- He, B., Lin, P., Jia, Z., Du, W., Qu, W., Yuan, L., Dai, W., Zhang, H., Wang, X. and Wang, J. 2013. The transport mechanisms of polymer nanoparticles in Caco-2 epithelial cells. *Biomaterials* 34: 6082-6098.
- He, H., Xiao, D., He, J., Li, H., He, H., Dai, H. and Peng, J. 2014. Preparation of a core-shell magnetic ion-imprinted polymer via a sol-gel process for selective extraction of Cu (ii) from herbal medicines. *Analyst* 139: 2459-2466.
- Heinemann, L. 2010. New ways of insulin delivery. *International Journal of Clinical Practice* 64: 29-40.
- Hinds, K. D. and Kim, S. W. 2002. Effects of PEG conjugation on insulin properties. *Advanced Drug Delivery Reviews* 54: 505-530.
- Huining, H., Junxiao, Y., Jianyong, S., Jianxin, W., Yongzhuo, H., Guanyi, C., Jingkang, W. and Victor, C. Y. 2013. Overcoming oral insulin delivery barriers: application of cell penetrating peptide and silica-based nanoporous composites. *Frontiers of Chemical Science and Engineering* 7: 9-19.
- Hussain, M., Wackerlig, J. and Lieberzeit, P. A. 2013. Biomimetic strategies for sensing biological species. *Biosensors* 3: 89-107.
- Iwata, K., Yamashita, S., Yoshioka, H.-T., Liu, C. and Hayashi, K. 2016. Preparation of Fluorescent Molecularly Imprinted Polymer Micropowder for Odorant Visualization. *Sensors and Materials* 28: 173-179.
- Janes, K., Calvo, P. and Alonso, M. 2001. Polysaccharide colloidal particles as delivery systems for macromolecules. *Advanced Drug Delivery Reviews* 47: 83-97.

- Karimian, N., Turner, A. P. and Tiwari, A. 2014. Electrochemical evaluation of troponin T imprinted polymer receptor. *Biosensors and Bioelectronics* 59: 160-165.
- Kim, B. S., Oh, J. M., Hyun, H., Kim, K. S., Lee, S. H., Kim, Y. H., Park, K., Lee, H. B. and Kim, M. S. 2009. Insulin-loaded microcapsules for in vivo delivery. *Molecular Pharmaceutics* 6: 353-365.
- Kim, S. K., Lee, S., Jin, S., Moon, H. T., Jeon, O. C., Lee, D. Y. and Byun, Y. 2010. Diabetes Correction in Pancreatectomized Canines by Orally Absorbable Insulin–Deoxycholate Complex. *Molecular Pharmaceutics* 7: 708-717.
- Kotova, K., Hussain, M., Mustafa, G. and Lieberzeit, P. A. 2013. MIP sensors on the way to biotech applications: Targeting selectivity. *Sensors and Actuators B: Chemical* 189: 199-202.
- Kryscio, D. R. and Peppas, N. A. 2012. Critical review and perspective of macromolecularly imprinted polymers. *Acta Biomaterialia* 8: 461-473.
- Kumar, A., Lahiri, S. S. and Singh, H. 2006. Development of PEGDMA: MAA based hydrogel microparticles for oral insulin delivery. *International Journal of Pharmaceutics* 323: 117-124.
- Kunath, S., Panagiotopoulou, M., Maximilien, J., Marchyk, N., Sanger, J. and Haupt, K. 2015. Cell and tissue imaging with molecularly imprinted polymers as plastic antibody mimics. *Advanced Healthcare Materials* 4: 1322-1326.
- Latif, U., Qian, J., Can, S. and Dickert, F. L. 2014. Biomimetic receptors for bioanalyte detection by quartz crystal microbalances—From molecules to cells. *Sensors* 14: 23419-23438.

- Lelej-Bennis, D., Boillot, J., Bardin, C., Zirinis, P., Coste, A., Escudier, E., Chast, F., Peynegre, R., Slama, G. and Selam, J. 2001. Six month administration of gelified intranasal insulin in type 1 diabetic patients under multiple injections: efficacy versus subcutaneous injections and local tolerance. *Diabetes & Metabolism* 27: 372-377.
- Li, S., Davis, E. N., Huang, X., Song, B., Peltzman, R., Sims, D. M., Lin, Q. and Wang, Q. 2011. Synthesis and development of poly (n-hydroxyethyl acrylamide)-ran-3-acrylamidophenylboronic acid polymer fluid for potential application in affinity sensing of glucose. *Journal of Diabetes Science and Technology* 5: 1060-1067.
- Lowe, P. J. and Temple, C. S. 1994. Calcitonin and insulin in isobutylcyanoacrylate nanocapsules: protection against proteases and effect on intestinal absorption in rats. *Journal of Pharmacy and Pharmacology* 46: 547-552.
- Lowman, A., Morishita, M., Kajita, M., Nagai, T. and Peppas, N. 1999. Oral delivery of insulin using pH-responsive complexation gels. *Journal of Pharmaceutical Sciences* 88: 933-937.
- Marschütz, M. K. and Bernkop-Schnürch, A. 2000. Oral peptide drug delivery: polymer-inhibitor conjugates protecting insulin from enzymatic degradation in vitro. *Biomaterials* 21: 1499-1507.
- Maver, U., Velnar, T., Gaberšček, M., Planinšek, O. and Finšgar, M. 2016. Recent progressive use of atomic force microscopy in biomedical applications. *TrAC Trends in Analytical Chemistry* 80: 96-111.
- Morishita, M., Goto, T., Nakamura, K., Lowman, A. M., Takayama, K. and Peppas, N. A. 2006. Novel oral insulin delivery systems based on complexation

- polymer hydrogels: single and multiple administration studies in type 1 and 2 diabetic rats. *Journal of Controlled Release* 110: 587-594.
- Munishkina, L. A. and Fink, A. L. 2007. Fluorescence as a method to reveal structures and membrane-interactions of amyloidogenic proteins. *Biochimica et Biophysica Acta (BBA)-Biomembranes* 1768: 1862-1885.
- Murray, L. M., Nock, V., Evans, J. J. and Alkaisi, M. M. 2014. Bioimprinted polymer platforms for cell culture using soft lithography. *Journal of Nanobiotechnology* 12: 60.
- Nakayama, F., Yasuda, T., Umeda, S., Asada, M., Imamura, T., Meineke, V. and Akashi, M. 2011. Fibroblast growth factor-12 (FGF12) translocation into intestinal epithelial cells is dependent on a novel cell-penetrating peptide domain involvement of internalization in the in vivo role of exogenous FGF12. *Journal of Biological Chemistry* 286: 25823-25834.
- Naklua, W., Mahesh, K., Aundorn, P., Tanmanee, N., Aenukulpong, K., Sutto, S., Chen, Y. Z., Chen, S. and Suedee, R. 2015. An imprinted dopamine receptor for discovery of highly potent and selective D₃ analogues with neuroprotective effects. *Process Biochemistry* 50: 1537-1556.
- Naklua, W., Mahesh, K., Chen, Y. Z., Chen, S. and Roongnapa, S. 2016a. Molecularly imprinted polymer microprobes for manipulating neurological function by regulating temperature-dependent molecular interactions. *Process Biochemistry* 51: 142-157.
- Naklua, W., Suedee, R. and Lieberzeit, P. A. 2016b. Dopaminergic receptor–ligand binding assays based on molecularly imprinted polymers on quartz crystal microbalance sensors. *Biosensors and Bioelectronics* 81: 117-124.

- Orozco, J., Cortés, A., Cheng, G., Sattayasamitsathit, S., Gao, W., Feng, X., Shen, Y. and Wang, J. 2013. Molecularly imprinted polymer-based catalytic micromotors for selective protein transport. *Journal of the American Chemical Society* 135: 5336-5339.
- Ortiz, C., Zhang, D., Xie, Y., Davisson, V. J. and Ben-Amotz, D. 2004. Identification of insulin variants using Raman spectroscopy. *Analytical Biochemistry* 332: 245-252.
- Owens, D. R. 2002. New horizons—alternative routes for insulin therapy. *Nature Reviews Drug Discovery* 1: 529-540.
- Owens, D. R., Zinman, B. and Bolli, G. 2003. Alternative routes of insulin delivery. *Diabetic Medicine* 20: 886-898.
- Pan, G., Guo, Q., Cao, C., Yang, H. and Li, B. 2013. Thermo-responsive molecularly imprinted nanogels for specific recognition and controlled release of proteins. *Soft Matter* 9: 3840-3850.
- Pan, J., Xue, X., Wang, J., Xie, H. and Wu, Z. 2009. Recognition property and preparation of Staphylococcus aureus protein A-imprinted polyacrylamide polymers by inverse-phase suspension and bulk polymerization. *Polymer* 50: 2365-2372.
- Pardeshi, S., Dhodapkar, R. and Kumar, A. 2014. Molecularly imprinted microspheres and nanoparticles prepared using precipitation polymerisation method for selective extraction of gallic acid from Emblica officinalis. *Food Chemistry* 146: 385-393.
- Parmpi, P. and Kofinas, P. 2004. Biomimetic glucose recognition using molecularly imprinted polymer hydrogels. *Biomaterials* 25: 1969-1973.

- Patel, A., Patel, M., Yang, X. and K Mitra, A. 2014. Recent advances in protein and peptide drug delivery: a special emphasis on polymeric nanoparticles. *Protein and Peptide Letters* 21: 1102-1120.
- Puoci, F., Cirillo, G., Curcio, M., Parisi, O. I., Iemma, F. and Picci, N. 2011. Molecularly imprinted polymers in drug delivery: state of art and future perspectives. *Expert Opinion on Drug Delivery* 8: 1379-1393.
- Rao, J. P. and Geckeler, K. E. 2011. Polymer nanoparticles: preparation techniques and size-control parameters. *Progress in Polymer Science* 36: 887-913.
- Rosellini, E., Barbani, N., Giusti, P., Ciardelli, G. and Cristallini, C. 2010. Novel bioactive scaffolds with fibronectin recognition nanosites based on molecular imprinting technology. *Journal of Applied Polymer Science* 118: 3236-3244.
- Saridakis, E. and Chayen, N. E. 2013. Imprinted polymers assisting protein crystallization. *Trends in Biotechnology* 31: 515-520.
- Saridakis, E., Khurshid, S., Govada, L., Phan, Q., Hawkins, D., Crichlow, G. V., Lolis, E., Reddy, S. M. and Chayen, N. E. 2011. Protein crystallization facilitated by molecularly imprinted polymers. *Proceedings of the National Academy of Sciences* 108: 11081-11086.
- Schirhagl, R., Latif, U., Podlipna, D., Blumenstock, H. and Dickert, F. L. 2012. Natural and biomimetic materials for the detection of insulin. *Analytical Chemistry* 84: 3908-3913.
- Schirhagl, R., Podlipna, D., Lieberzeit, P. A. and Dickert, F. L. 2010. Comparing biomimetic and biological receptors for insulin sensing. *Chemical Communications* 46: 3128-3130.

- Shan, Y. and Wang, H. 2015. The structure and function of cell membranes examined by atomic force microscopy and single-molecule force spectroscopy. *Chemical Society Reviews* 44: 3617-3638.
- Simovic, S., Song, Y., Nann, T. and Desai, T. A. 2015. Intestinal absorption of fluorescently labeled nanoparticles. *Nanomedicine: Nanotechnology, Biology and Medicine* 11: 1169-1178.
- Sohaebuddin, S. K., Thevenot, P. T., Baker, D., Eaton, J. W. and Tang, L. 2010. Nanomaterial cytotoxicity is composition, size, and cell type dependent. *Particle and Fibre Toxicology* 7: 1.
- Sonaje, K., Chuang, E.-Y., Lin, K.-J., Yen, T.-C., Su, F.-Y., Tseng, M. T. and Sung, H.-W. 2012. Opening of epithelial tight junctions and enhancement of paracellular permeation by chitosan: microscopic, ultrastructural, and computed-tomographic observations. *Molecular Pharmaceutics* 9: 1271-1279.
- Stützer, I., Esterházy, D. and Stoffel, M. 2012. The pancreatic beta cell surface proteome. *Diabetologia* 55: 1877-1889.
- Su, F.-Y., Lin, K.-J., Sonaje, K., Wey, S.-P., Yen, T.-C., Ho, Y.-C., Panda, N., Chuang, E.-Y., Maiti, B. and Sung, H.-W. 2012. Protease inhibition and absorption enhancement by functional nanoparticles for effective oral insulin delivery. *Biomaterials* 33: 2801-2811.
- Suedee, R., Srichana, T. and Martin, G. P. 2000. Evaluation of matrices containing molecularly imprinted polymers in the enantioselective-controlled delivery of β -blockers. *Journal of Controlled Release* 66: 135-147.
- Suksuwan, A., Lomlim, L., Dickert, F. L. and Suedee, R. 2015. Tracking the chemical surface properties of racemic thalidomide and its enantiomers using a

- biomimetic functional surface on a quartz crystal microbalance. *Journal of Applied Polymer Science* 132.
- Tan, M. L., Choong, P. F. and Dass, C. R. 2010. Recent developments in liposomes, microparticles and nanoparticles for protein and peptide drug delivery. *Peptides* 31: 184-193.
- Turner, N. W., Jeans, C. W., Brain, K. R., Allender, C. J., Hlady, V. and Britt, D. W. 2006. From 3D to 2D: a review of the molecular imprinting of proteins. *Biotechnology Progress* 22: 1474-1489.
- Valdebenito, A., Espinoza, P., Lissi, E. and Encinas, M. 2010. Bovine serum albumin as chain transfer agent in the acrylamide polymerization. Protein-polymer conjugates. *Polymer* 51: 2503-2507.
- Vasapollo, G., Sole, R. D., Mergola, L., Lazzoi, M. R., Scardino, A., Scorrano, S. and Mele, G. 2011. Molecularly imprinted polymers: present and future prospective. *International Journal of Molecular Sciences* 12: 5908-5945.
- Verheyen, E., Schillemans, J. P., van Wijk, M., Demeniex, M.-A., Hennink, W. E. and van Nostrum, C. F. 2011. Challenges for the effective molecular imprinting of proteins. *Biomaterials* 32: 3008-3020.
- Verspohl, E. and Ammon, H. 1980. Evidence for presence of insulin receptors in rat islets of Langerhans. *Journal of Clinical Investigation* 65: 1230.
- Wang, J., Cormack, P. A., Sherrington, D. C. and Khoshdel, E. 2007. Synthesis and characterization of micrometer-sized molecularly imprinted spherical polymer particulates prepared via precipitation polymerization. *Pure and Applied Chemistry* 79: 1505-1519.

- Wang, Z., Li, N., Zhao, J., White, J. C., Qu, P. and Xing, B. 2012. CuO nanoparticle interaction with human epithelial cells: cellular uptake, location, export, and genotoxicity. *Chemical Research in Toxicology* 25: 1512-1521.
- White, S., Bennett, D. B., Cheu, S., Conley, P. W., Guzek, D. B., Gray, S., Howard, J., Malcolmson, R., Parker, J. M. and Roberts, P. 2005. EXUBERA®: pharmaceutical development of a novel product for pulmonary delivery of insulin. *Diabetes Technology & Therapeutics* 7: 896-906.
- Wulff, G. 1995. Molecular imprinting in cross-linked materials with the aid of molecular templates—a way towards artificial antibodies. *Angewandte Chemie International Edition in English* 34: 1812-1832.
- Wulff, G., Vesper, W., Grobe-Einsler, R. and Sarhan, A. 1977. Enzyme-analogue built polymers, 4. On the synthesis of polymers containing chiral cavities and their use for the resolution of racemates. *Macromolecular Chemistry and Physics* 178: 2799-2816.
- Yan, H. and Row, K. H. 2006. Characteristic and synthetic approach of molecularly imprinted polymer. *International Journal of Molecular Sciences* 7: 155-178.
- Yang, K., Zhang, L., Liang, Z. and Zhang, Y. 2012. Protein-imprinted materials: rational design, application and challenges. *Analytical and Bioanalytical Chemistry* 403: 2173-2183.
- Yang, S., Wang, Y., Jiang, Y., Li, S. and Liu, W. 2016. Molecularly Imprinted Polymers for the Identification and Separation of Chiral Drugs and Biomolecules. *Polymers* 8: 216.
- Yoshimatsu, K., Reimhult, K., Krozer, A., Mosbach, K., Sode, K. and Ye, L. 2007. Uniform molecularly imprinted microspheres and nanoparticles prepared by

precipitation polymerization: The control of particle size suitable for different analytical applications. *Analytica Chimica Acta* 584: 112-121.

Yu, Y., Ye, L., Haupt, K. and Mosbach, K. 2002. Formation of a Class of Enzyme Inhibitors (Drugs), Including a Chiral Compound, by Using Imprinted Polymers or Biomolecules as Molecular-Scale Reaction Vessels. *Angewandte Chemie International Edition* 41: 4459-4463.

Zahedi, P., Ziaee, M., Abdouss, M., Farazin, A. and Mizaikoff, B. 2016. Biomacromolecule template-based molecularly imprinted polymers with an emphasis on their synthesis strategies: a review. *Polymers for Advanced Technologies* 27: 1124-1142.

APPENDICES

Appendix 1 Paper

Appendix 2 Animal ethic approval

Appendix 3 Vitae

PAPER 1

Biomimetic insulin-imprinted polymer nanoparticles as a potential oral drug delivery
system

(Published in *Acta Pharmaceutica*)

ACTA PHARMACEUTICA**Croatian Pharmaceutical Society**

10000 Zagreb, Masarykova 2/II, Croatia

Phone: +385 1 48 72 849

Phone/fax: +385 1 48 72 853

Editor: Prof. Dr. SVJETLANA LUTEROTTI

Zagreb, March 2, 2017

E-mail: svjetlana.luterotti@gmail.com
svjetlana.luterotti@pharma.hr**Dear Authors,****Re: AP 3095/16/JL/SL****Title: Biomimetic insulin-imprinted polymer nanoparticles as a potential oral drug delivery system****Authors: Pijush Kumar Paul, Alongkot Treetong, Roongnapa Suedee**

I am pleased to inform you that your paper referred to above has been accepted for publication and will be published in 2/2017 issue of *Acta Pharmaceutica*. Proofs for correction will be sent to you in a due course.

Publication charge is 450 € per manuscript (excl. VAT). Price is subject to change without notice.

Authors will receive an invoice right after acceptance of their paper which will not be published before the fee has been paid. The invoice will be sent to the corresponding author by e-mail. Payments should be made to the invoice of the publisher, Croatian Pharmaceutical Society, Masarykova 2, HR-10000 Zagreb, Croatia, through ZAGREBACKA BANKA ZAGREB, Savska 60, Zagreb, Croatia, account no. 70300-840-3206386 SWIFT ZABA HR 2X (for foreign currency payments). The copy of the bank draft should be sent by fax or by e-mail as a scanned document, within 72 h of receipt of the invoice, to the Publisher (fax No.: +385 1 48 72 853).

The uncorrected version of the article appears instantly on our web site (<http://acta.pharmaceutica.farmaceut.org/>). This „early bird“ version of the article is posted in order to provide the fastest access to the article. This first version will be replaced by the final version of the article as soon as the latter becomes available.

Yours sincerely

Prof. Dr. Svjetlana Luterotti
Editor-in-Chief, *Acta Pharmaceutica*

Biomimetic insulin-imprinted polymer nanoparticles as a potential oral drug delivery system*

PIJUSH KUMAR PAUL¹
ALONGKOT TREETONG²
ROONGNAPA SUEDEE^{1,*}

¹ *Molecular Recognition Materials
Research Unit, Nanotec-PSU Center
of Excellence on Drug Delivery System
Department of Pharmaceutical
Chemistry, Faculty of Pharmaceutical
Sciences, Prince of Songkla University
Hatyai, Songkhla 90112, Thailand*

² *National Nanotechnology Center
(NANOTEC), National Science
and Technology Development Agency
(NSTDA), Thailand Science Park
Phahonyothin Road
Pathum Thani 12120, Thailand*

Accepted March 2, 2017
Published online April 6, 2017

In this study, we investigate molecularly imprinted polymers (MIPs), which form a three-dimensional image of the region at and around the active binding sites of pharmaceutically active insulin or are analogous to β cells bound to insulin. This approach was employed to create a well-defined structure within the nanospace cavities that make up functional monomers by cross-linking. The obtained MIPs exhibited a high adsorption capacity for the target insulin, which showed a significantly higher release of insulin in solution at pH 7.4 than at pH 1.2. *In vivo* studies on diabetic Wistar rats showed that the fast onset within 2 h is similar to subcutaneous injection with a maximum at 4 h, giving an engaged function responsible for the duration of glucose reduction for up to 24 h. These MIPs, prepared as nanosized material, may open a new horizon for oral insulin delivery.

Keywords: molecularly imprinted polymers, insulin, nanoparticles, islet cells, oral drug delivery

Biomimetic materials are attractive agents that demonstrate the importance of inherent properties of efficiently delivering drugs to desired sites in the biological system (1). Recent evidence has shown that nanoparticles have a potential for delivering proteins, since they can offer protection from the digestive proteins in the gastrointestinal (GI) environment and provide biomacromolecule passage at the desired adsorption sites within the GI tract for systemic drug delivery (2). Molecularly imprinted polymers (MIPs) can serve as good drug delivery agents especially for peptides/proteins due to their high stability, drug loading capabilities and ease of preparation (3). Biomimetic systems using MIPs involve the nanoparticle-biomolecule association that can produce actual interactions between the initial templates and simulate biological recognition just as it does in replication (4). Furthermore, the use of nanoparticles in molecular imprinting on polymerization materials can be achieved with biomimetic carriers, including core-shell nanoparticles, microgels, cross-linked chains, chitosan, and quantum dots (5, 6). In mo-

* This work is dedicated to Professor Wolfgang Lindner on the occasion of his 75th birthday.

** Corresponding author; e-mail: roongnapa.s@psu.ac.th

lecular imprinting, self-association of polymer nanoparticles with the template has produced multiple binding site points for the recognition of biologically important macromolecules within three dimensions of the polymer chains surrounding them (7). The MIPs designed with the coordinative effect of functional groups in the polymeric chain can bind a short peptide with high affinity (8). It has the preponderance of the uptake of protein structure on the lipid-protein bilayer, which is not only the binding affinity under the conditions but also the diversity of cell activities, reflecting the surface properties such as charge, chemical groups, and hydrophobic effect. A major advantage of molecular imprinting by precipitation polymerization is that it creates a selective nanoscale environment with increased affinity of specific functional groups at recognition sites that mimic the structure of the cell membrane surface layer. The possibility of differently targeted delivery by the imprinting approach, not just an alternative in enhancing selective drug delivery but the opportunity of being used as the key of biomolecule recognition, impacted the uptake of the drug or biomolecule into the cells (9). Nevertheless, good design of MIPs suitable for protein delivery still remains a challenge.

Insulin administered into the body can cause hypoglycemia or affect the elevated glucose level during transport *via* the route of administration into muscle cells and tissues. Insulin is typically administered through a subcutaneous route involving the risk of pain, infection, hyperinsulinemia, and deposition of fat around the injection site, which often leads to poor patient compliance (10). Therefore, oral delivery of insulin is of great interest owing to the benefit of an appropriate release rate of the payload in the GI tract over an extended period of time. In addition, insulin transport from the site of action needs to be investigated with the specific target of the lipid-protein or membrane assembly at the site. A previous report described the interaction of the exogenous insulin with the insulin receptor contained in rat pancreatic islets (11). In this work, we exploited molecular imprinting for generation of recognition sites of insulin binding to cell membranes of the islets. It is interesting to study the molecules and receptors present in the islets as imprinting templates for insulin binding. To our knowledge, no isolated/digested islets have been explored as an imprinting template in the literature. Exploiting the cross-linked *N,N*-methylene-bisacrylamide (MBAA) nanoparticles prepared from a single and mixed functional monomer of methacrylic acid (MAA) and *N*-hydroxyethyl acrylamide (HEAA) copolymer allows reversible complexation on MIP binding sites that emerged from the intrinsic property of a protein drug. Furthermore, the property of template imprinting on the polymer nanoparticle can affect the cellular uptake into blood circulation (12). The varying of ratios of the functional monomer and cross-linker can improve the selectivity and allow for specific adsorption of the insulin at the imprint site of the polymer. MIP nanoparticle-based carriers may enable the protection of the protein from degradation and its passage through the absorption barrier.

The goal of this work is to synthesize MBAA cross-linked nanoparticles consisting of different functional groups that will interact with the template. MAA exhibits mucoadhesive properties at higher concentrations (13) and the added HEAA functional monomer is a hydrophilic nonionic monomer with adhesive characteristics during the polymerization procedure (14) and thus can be anchored on the cross-linked chains of insulin-MIPs. Precipitation polymerization is a common technique for producing spherical particles with controlled size distribution (15). Pan *et al.* used precipitation polymerization for the preparation of protein-imprinted nanoparticles (16). The other advantages of this method are easy preparation, without addition of surfactants or stabilizers. This polymerization will

form individual molecules *via* non-covalent interactions from a very specific functionality through the nanoparticle-protein association so that it can help improve the protein loading and delivery efficiency. The paper describes the preparation of a biomimetic insulin MIP-based nanocarrier for drug delivery.

EXPERIMENTAL

Materials

Methacrylic acid (MAA), *N*-hydroxyethyl acrylamide (HEAA), *N,N*-methylene-bisacrylamide (MBAA), polycaprolactone triol (PCL-T), collagenase, streptozotocin, and recombinant human insulin expressed in yeasts (proprietary host) were purchased from Sigma-Aldrich (USA). 2,2'-Azobis-(isobutyronitrile) (AIBN) was supplied by Wako Pure Chemical Industries Ltd. (Japan). MAA was distilled before use. Human insulin (recombinant DNA origin; 100 IU/mL) was from Eli Lilly Asia, Inc., (Humulin® *N*) and Novo Nordisk Pharma, Thailand (Insulatard® HM). All other reagents were of analytical grade and were used as received.

Preparation of molecularly imprinted nanoparticles

Insulin-imprinted nanoparticles were prepared by the precipitation polymerization method (17) using MBAA as a cross-linker in the presence of insulin or islet-bound insulin as the template in aqueous medium. The template and functional monomer mole ratio varied from 1:4 to 1:12 (Table I). Typically, MAA (1.6 mmol), HEAA (2.0 mmol), MBAA (8.5 mmol), insulin (35 mg), PCL-T (0.05 mmol), and phosphate-buffered saline (PBS; 10 mL) as a porogenic solvent were added into a 30 mL vial. After 30 min of stirring, a clear solution was obtained, to which AIBN (0.04 mmol) was added. The vial was then purged with nitrogen and polymerized under a UV lamp at 254 nm wavelength for 12 h at room temperature (25 °C). At low temperature, the decomposition of AIBN was lower and produced low efficacy of free radicals, which affected the double-bond conversion of the formed product. Nonetheless, the appropriate duration of polymerization that provided the formed polymer product was determined by infrared (IR) spectroscopy. Monomers are water soluble; however, the solubility decreases due to the formation of oligomers during polymerization and the monomers are finally precipitated. The resultant insulin-imprinted polymers were collected by centrifugation at 10,000 rpm for 5 min. After that, the adsorbed oligomers and unreacted monomers were removed from the MIP by washing with Milli-Q water. To remove the embedded insulin molecules from the polymer matrix, MIP nanoparticles were subsequently washed several times at room temperature with 0.5 mol L⁻¹ NaCl solution and Milli-Q water, and insulin removal from the prepared MIPs was tested using a UV-Vis spectrophotometer and analyzing the supernatant at the maximum wavelength (272 nm). Likewise, the non-imprinted polymer (NIP) nanoparticles were synthesized and washed, except for the omission of the template protein during the polymerization process.

Isolation of rat pancreatic islets

Wistar rats (200–250 g average body mass) were obtained from the Southern Laboratory Animal Facilities of the Prince of Songkla University. Experimental animals were maintained

on a dry pellet diet and water *ad libitum*. Rats were fed in standard propylene cages and acclimatized for 7 days to animal house conditions in an air-conditioned room, (temperature 22 ± 3 °C), relative humidity 46–70 %, 12:12 h light/dark cycle, adequate cross-ventilation), in accordance with the Ethical Committee (Ref. 36/2014). Fasting animals were deprived of food for at least 16 h but had free access to drinking water. Rats were sacrificed by cervical dislocation to obtain the pancreatic islets. Collagenase (0.8 mg mL^{-1}) dissolved in Hank's buffered salt solution (HBSS) was injected into numerous lobes of the pancreas; the pancreas was then removed and digested for 15 to 20 min at 37 °C. Islets of Langerhans within the pancreas were collected by centrifugation three times with cooled HBSS at 5 °C, at 1000 rpm for 1 min (18). A previous study has reported that insulin receptors on rat pancreatic islets bind to human insulin in a similar fashion as pork insulin (11). Immediately after the collection of islets, another batch of MIPs was prepared. The freshly isolated islets (about 100 islets) were incubated in 10 mL of PBS (pH 7.4) containing insulin (35 mg) at room temperature for 20 min, followed by the addition of MAA, HEAA, MBAA, and PCL-T under continuous stirring. Upon addition of AIBN, polymerization occurred and the islet-bound insulin-imprinted polymers (MIPs) were collected in a similar way to that described previously.

Particle size and z potentials

Average particle sizes and the z potential of MIP/NIP nanoparticles were determined using a Nanoparticle Analyzer (Zetasizer Nano ZS; Malvern Instruments Ltd., UK). Particle size was measured using the dynamic light scattering (DLS) technique. The samples were dispersed in PBS (pH 7.4; 0.2 mg mL^{-1}), followed by filtration through a $0.45 \mu\text{m}$ filter and were then ultrasonicated for 10 min at room temperature. Measurements were carried out at an angle of 90° at 25 °C. For z potential measurements, the samples were diluted in Milli-Q water. Each sample was analyzed in triplicate.

Morphological observations

Surface morphology of MIP nanoparticles was examined by scanning electron microscopy (SEM Quanta 400; FEI, Brno, Czech Republic). The sample was placed on an aluminum stub and coated with gold using a sputter coater in an argon atmosphere for 120 s. TEM was used to observe MIPs after removal of the template applying an established washing protocol in the preparation process. For TEM measurements, the particles in PBS were dropped onto a carbon-coated copper grid and then observed with a JEM 2100F (Japan).

Pore size distribution and surface area analysis

Pore size distribution and surface areas of washed polymers were determined using the Brunauer-Emmett-Teller (BET) analysis with an automated gas sorption system (Quantachrome Autosorb-1, USA). Relevant information was obtained as follows: the pore size and porosity data were obtained from a plot of pore size *versus* incremental pore volume to give the pore size distribution using the Barrett-Joyner-Halenda (BJH) method. A plot of pore size *versus* pore volume gave the total pore volume with an indication of the surface areas and total pore volumes of the polymers. In addition, the incremental volume that was depleted with changes of each pressure was determined by the change in capacitance of the stem. The intrusion volume was recorded for the respective pressure or pore size.

AFM and AFM-confocal Raman spectroscopy

In this study, the topography and surface geometry of the particles were examined by the combined method of AFM and Raman spectroscopy, because the environmental conditions can affect the interaction of particles and biological entities in different ways of drug release. Non-contact mode AFM (SPA-400-SPI4000; Seiko Instrument, Inc., Japan) was used to test the assembly and morphology of the nanostructure. A silicone cantilever with a spring constant of 12 N m^{-1} was employed. Topographic and phase images were collected at a scan rate of 1 Hz under ambient laboratory conditions. The images were further analyzed by the Nano Navi SPA400 (DFM) software. Raman spectra were collected with an AFM-confocal Raman spectrometer (NT-MDT model, Moscow, Russia) and NTEGRA Spectra equipped with hybrid mode (HD-AFM). The 632.8 nm excitation wavelength of a diode laser was focused onto the sample with a dry objective lens of 100× of 0.95 numerical aperture number (NA). The Stokes-shifted Raman scattering was recorded with 1200 groove mm^{-1} grating using a Peltier-cooled charged-coupled device (CCD; Andor Technology PLC, CA, USA).

Protein adsorption experiments

Protein adsorption experiments on MIPs and NIPs were performed in PBS (pH 7.4). The respective polymers (5 mg) were suspended in 5 mL of different insulin solutions in concentrations that ranged from 5 to $30 \mu\text{g mL}^{-1}$ at room temperature. After filtration with cellulose acetate (CA) membrane filters (25 mm, $0.45 \mu\text{m}$; Vertical Chromatography Co., Ltd., Bangkok, Thailand), the supernatant was analyzed using a Carry 60 UV-Vis spectrophotometer (Agilent Technologies) at a wavelength of 272 nm, since this would not interfere with the solvent and the excess of the matrix upon incubation with the polymer. The amount of the specifically and/or non-specifically adsorbed insulin in the polymers and the polymer matrix was calculated using the formula:

$$Q = (C_0 - C) \times V / 1000 \times W \quad (1)$$

where Q is the amount of adsorbed insulin (mg g^{-1}); C_0 and C are the initial and final concentrations of insulin ($\mu\text{g mL}^{-1}$), respectively; V is the volume of the solution (mL); and W is the polymer mass (g) (19). Each experiment was repeated three times. The binding parameters were determined from the Scatchard equation:

$$B / F = (B_{\text{max}} - B) / K_d \quad (2)$$

where K_d and B_{max} are the equilibrium dissociation constant and the apparent maximum number of the binding sites, respectively. The amounts of insulin adsorbed (B) were obtained from absorbance determination. F represents the amount of insulin remaining in the supernatants. Adsorption kinetic experiments were carried out by adding 10 mg polymer to 50 mL of a $10 \mu\text{g mL}^{-1}$ insulin solution in PBS solution at room temperature. The amounts of adsorbed protein on MIP/NIP nanoparticles were then evaluated with a UV-Vis spectrophotometer, as mentioned earlier. Bomb calorimetry using Isoperibol bomb calorimetry (IKA® Calorimeter System C5000 Control, Germany) was used to determine the gross heating value of the polymer incubated with insulin.

Protein release studies

The *in vitro* release of the protein was studied by carrying out the adsorption of insulin onto the MIP and NIP nanoparticles with an initial insulin concentration of 100 µg mL⁻¹ at 37 °C in PBS (pH 7.4). After incubation, the nanoparticles were collected by centrifugation at 10,000 rpm for 20 min. The samples (centrifuged) were then dispersed in buffer solutions of pH 1.2 and pH 7.4 at 37 °C. At specific time intervals, the amounts of insulin released in the supernatant were assayed by UV-Vis analysis following centrifugation (16). Experiments were performed in triplicate.

In vivo evaluation

Male Wistar rats (200–250 g) were obtained from the Southern Laboratory Animal facilities of the Prince of Songkla University, Thailand (Ethical No. 36/2014). Diabetes was induced in rats by an intraperitoneal injection of streptozotocin (35 mg kg⁻¹) dissolved in citrate buffer (pH 4.5) (20). After 3 days of injection, rats were considered to be diabetic when the glycaemia was above 250 mg dL⁻¹. The animals were fasted overnight (water *ad libitum*) and remained fasted during the whole experiment. There were seven groups of animals, each group containing five diabetic rats. The first two groups of rats were given orally MIP1 (170 mg kg⁻¹, single monomer MAA) and MIP2 (150 mg kg⁻¹, mixed functional monomer MAA and HEAA) loaded with insulin (50 IU kg⁻¹). The rats of the next two groups were administered orally the respective NIP nanoparticles loaded with insulin (50 IU kg⁻¹). The fifth group received an insulin solution orally (50 IU kg⁻¹). The rats of the placebo control group were orally administered MIP nanoparticles (without insulin). Insulin formulation alone was given subcutaneously (1 IU kg⁻¹) to the last group of rats. Blood samples were collected from the tail vein and the blood glucose level was measured using a glucose meter (Accu-Chek® Performa; Roche Diagnostics GmbH, Germany) at pre-determined time points. Pharmacological bioavailability (PA %) of insulin-loaded nanoparticles after oral administration was calculated according to the following formula (21):

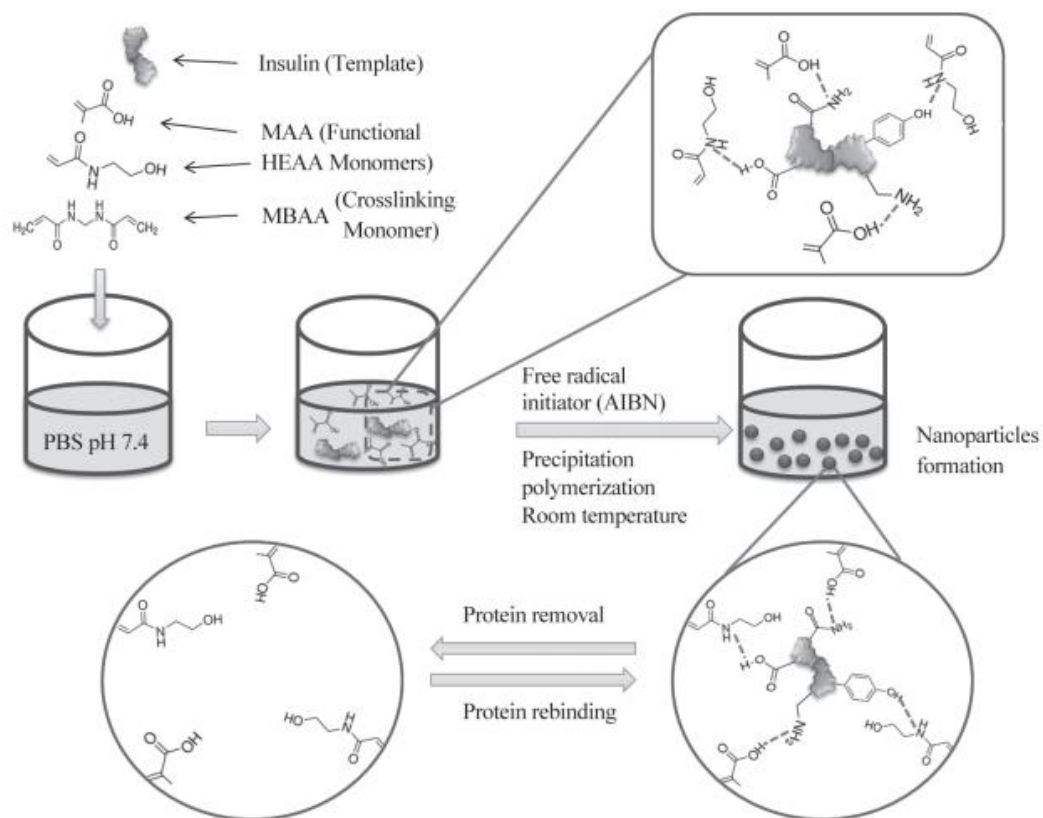
$$PA (\%) = ([AAC]_{p.o.} / [AAC]_{s.c.}) \times (Dose_{s.c.} / Dose_{p.o.}) \times 100 \quad (3)$$

where $[AAC]_{p.o.}$ and $[AAC]_{s.c.}$ represent the area above the blood glucose level-time curve of oral and subcutaneous insulin formulation, respectively, and $Dose_{p.o.}$ and $Dose_{s.c.}$ are the oral and subcutaneous doses given. AAC were calculated by applying the trapezoidal rule (22). One-way analysis of variance (ANOVA), followed by Tukey's test, was used for statistical analysis; $p < 0.05$ was considered to be statistically significant.

RESULTS AND DISCUSSION

Synthesis and characterization of MIPs

In this report, we chose molecular imprinting to investigate the recognition of pharmaceutically active insulin (F1) and rat islet-bound insulin (F2) as templates. Scheme 1 gives a schematic representation of the recognition of the insulin molecule at a binding pocket site prepared by aqueous precipitation polymerization. Varying the amount of



Scheme 1.

Table I. Polymeric composition of MIPs and NIPs nanoparticles

Compd. (mmol)	MIP1	MIP2	MIP3	MIP4	NIP1	NIP2
Template	Humulin® N	Humulin® N	Insulatard® HM	Insulatard® HM	–	–
	0.6	0.6	0.6	0.6	–	–
MAA	1.6	5.0	1.6	5.0	1.6	5.0
HEAA	–	2.0	–	2.0	–	2.0
MBAA	8.5	3.2	8.5	3.2	8.5	3.2
PCL-T	0.05	0.05	0.05	0.05	0.05	0.05
AIBN	0.04	0.04	0.04	0.04	0.04	0.04

MBAA as well as the concentrations of MAA and HEAA (Table I) led to the formation of MIPs, resulting in insulin affinity to the binding sites within the polymer matrix. MIP1 contains a single functional monomer (MAA) with high cross-linking whereas MIP2 com-

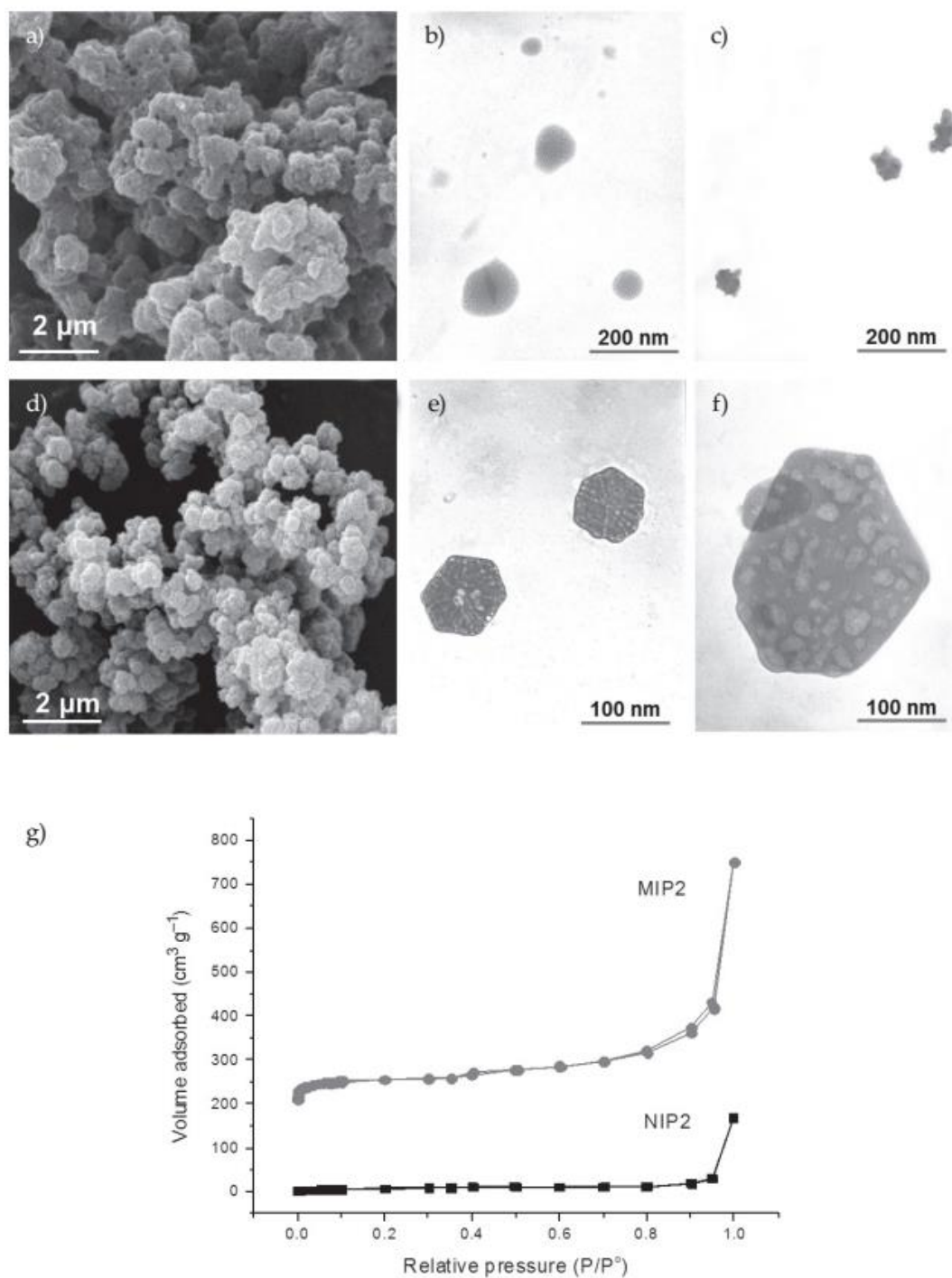


Fig. 1. a) and d) SEM, b), c), e) and f) TEM images of insulin and insulin imprinted polymers. e) the surface morphology of insulin. b) and f) TEM images showing the more porous structure of MIP than that of NIP (c). Micrograph A represents the rough surface of MIP compared to NIP (d). g) Nitrogen adsorption/desorption isotherms of MIPs compared to NIPs.

Table II. Characteristics of the insulin imprinted nanoparticles

Polymer	Without islets (F1)			With islets (F2)		
	Mean diameter (nm)	PDI ^a	Zeta potential (mV)	Mean diameter (nm)	PDI	Zeta potential (mV)
MIP1	221.86 ± 23.55	0.39 ± 0.03	−32.2 ± 5.1	200.46 ± 7.8	0.37 ± 0.01	−28.1 ± 3
MIP2	198.73 ± 3.05	0.33 ± 0.02	−32.3 ± 4.23	195.03 ± 3.11	0.34 ± 0.05	−24.8 ± 2.48
MIP3	214.56 ± 24.54	0.38 ± 0.05	−19.7 ± 3.21	199.13 ± 9.36	0.33 ± 0.02	−29 ± 3.26
MIP4	199.73 ± 5.9	0.34 ± 0.01	−30.4 ± 4.1	194.6 ± 8.17	0.35 ± 0.01	−31 ± 4.1
NIP1	302.46 ± 10.5	0.46 ± 0.08	−28.9 ± 3.7	204.13 ± 5.09	0.37 ± 0.02	−29.1 ± 3.4
NIP2	236.56 ± 31.33	0.43 ± 0.05	−33.6 ± 2.3	201.1 ± 16.21	0.35 ± 0.02	−29.8 ± 2.77

^aPDI = polydispersity index; mean ± SD (*n* = 3).

prises two functional monomers (MAA and HEAA) with lower cross-linking. MIP3 and MIP4 are similar to MIP1 and MIP2, except for the different insulin source (pharmaceutical company). Sizes obtained from the light scattering measurements are shown in Table II. Clearly, a slight decrease in particle size was observed, which was associated with an increase in the functional monomer concentration and the addition of a second monomer (HEAA) resulting from the interaction between the protein template and the surrounding monomers during polymerization.

SEM and TEM were used to examine the surface morphology and nanoparticle size of the formed MIP nanoparticles (Fig. 1a–e). In both SEM (Fig. 1a) and TEM (Fig. 1b), MIPs exhibited greater roughness and porous morphology than NIPs (Fig. 1d and c) due to the interaction of insulin with the functional monomer, which was finally washed out after polymerization. Further, the light scattering data of MIP nanoparticles revealed particle size ranges from 200 to 220 nm. This was confirmed by TEM observations, as shown in Fig. 1b–f. The optimum size ranged from 50 to 500 nm for the interaction between nanoparticles and epithelial cells (23). Therefore, MIPs could be suitable candidates for the transport of insulin across the cell membrane.

It is noteworthy that the PDI values of approximately 0.3 were found in all cases of MIPs. In contrast, NIP nanoparticles showed a higher PDI value of about 0.4 with higher particle size ranges from 230 to 300 nm. The results indicated the effect of template protein on the formation of MIP nanoparticles with homogeneous dispersion during the polymerization process. Although no template was added for NIP during polymerization, this resulted in a slightly broader size distribution compared to MIP. The z potentials of all imprinted nanoparticles were negative, as shown in Table II. As can be seen, MIPs produced with a mixed functional monomer had a lower surface charge than their corresponding NIPs, whereas the single functional monomer in F1 and the control polymer showed no differences in particle surface charges. The z potential of F1 was found slightly increased, whilst there was a relatively higher z potential value of MIP3 of F2 than of F1. This led to an increase in accessibility of the biotherapeutic molecule to the binding site

within the MIP; hence higher adsorption for MIP3 (2.69 mg g^{-1}). This result could be explained by the presence of zwitterionic molecules on the nanoparticles, caused by the bound insulin and N-linked glycoproteins on the rat β cells that self-assembled some structural motifs into polymer F2 (24, 25). The negative surface charge of MIPs varied between -20 and -33 mV and contained the hydrophilic functionalities on the MIP binding sites and the negatively charged side chains. The generation of insulin MIP nanoparticles in this study involved two point interactions of the insulin with the MAA and HEAA as a mixed functional monomer, forming an interaction with each of the amine and carbonyl moieties of the islets that would cause a strong interaction with the complementary template, hence expected the MIP show the intrinsic β cells-bound insulin template. Furthermore, this negative surface charge could allow them to diffuse into the mucus as a result of less interaction with the mucin (26, 27).

Surface area and pore size distribution of insulin MIPs

Macroscopic characteristics of MIPs and NIPs were examined by pore analysis such as the surface area, pore volume, and pore diameter of all of the synthesized materials. In supplemental data (Table S1), the mixture of a larger amount of the two monomers in MIP2 (MAA and HEAA) showed a larger surface area ($149.1 \text{ m}^2 \text{ g}^{-1}$), whereas a bigger quantity of the cross-linker (MBAA) generated a smaller surface area ($21.83 \text{ m}^2 \text{ g}^{-1}$) for MIP1. A similar trend was observed for MIP3 and MIP4. A large surface area of particles would lead to smaller particle sizes. BET analysis also demonstrated the presence of mesopores of about 20 nm for the polymer, leading to similar characteristics to those of a type IV isotherm, so their nanopore pores can be distinguished from NIPs. In the case of NIPs, the pore diameter was larger and the isotherm exhibited a type III curve characteristic due to the non-porous structure with low interaction (28). That insulin recognition sites formed within the nanopore pores was further corroborated by a bomb calorimeter. After incubation with insulin (suspension formulation, Novo Nordisk Pharma, Thailand), the gross heating value was almost similar for both MIP and NIP (see Table S2). Evidently, with insulin (crystalline powder form, Sigma-Aldrich, USA), the gross heating value was $16,844 \text{ J g}^{-1}$ for MIP2 and $13,518 \text{ J g}^{-1}$ for NIP2. This differential energy proved self-organization of the polymer in the medium that formed the biomimetic system. This result indicates the absence of surface adaptations of peptides after the template removal.

AFM studies

Fig. 2 shows the AFM image of the fine structure of insulin over the surface near the closely packed barrier of the nanoparticles for MIP1. It can be seen that there was a cloud-like blanket for MIP1, F1 (see Fig. 2f), and the distance between the interval of the neighboring nanoparticles and the individual pores was much smaller compared to that of the NIP1. The AFM image of the imprint with islets (MIP2) showed particle floccules, a worm-like cavity due to elastic interaction, and a larger overlap of surface coverage that resulted from adhesion of the induced association of the protein on the polymer to extend more, so that it was difficult to distinguish in the AFM image, as shown in Fig. 2f. The nanoscale contact geometry of the cavities was measured and found to be $2 \times 25 \times 25 \text{ nm}$ (height \times length \times width) for MIPs, as shown in Fig. 3a–e. According to the protein database, the size of the insulin hexamer is $3.5 \times 5 \text{ nm}$ and contains Zn as a coordinating atom (29). The three-dimensional

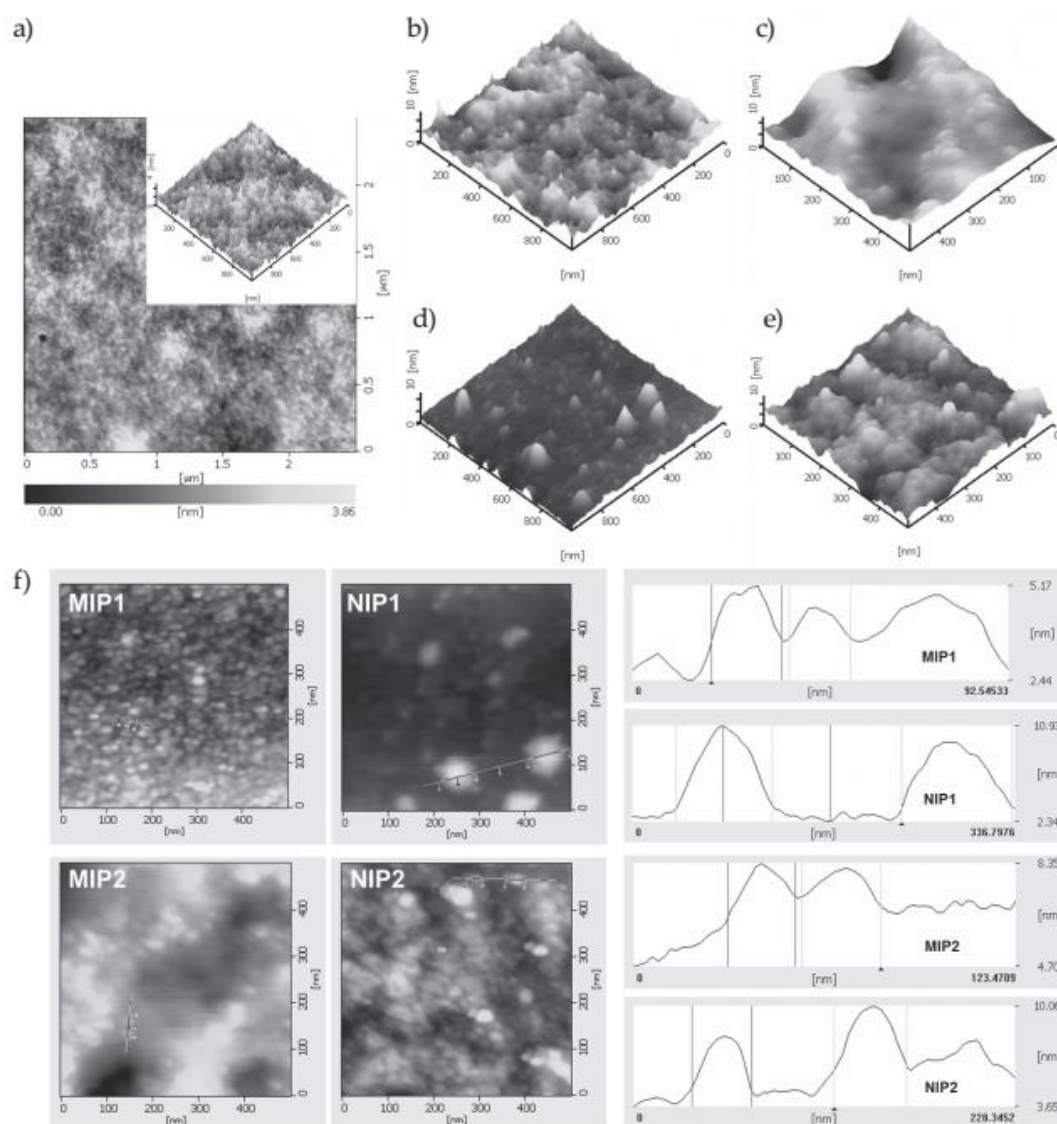


Fig. 2. a) Non-contact mode AFM of insulin, b) and c) surface topography of MIPs, d) and e) NIPs. This indicates the functionality of protein imprint after removal of the template. b) and d) represent F1 and c) and e) F2. f) AFM images of the colloidal patterns and 2D topography of the polymer surface with individual internal structures.

structure of both MIP1 (Fig. 3b) and MIP2 (Fig. 3c) indicates that they can accommodate the template protein with a size of the remaining cavity similar to the surface and possibly the geometrical change of the imprinted materials. Larger size of the cavity was observed for either the NIP1 (Fig. 3d) or NIP2 (Fig. 3e), each showing a shallow pore on the surface. Evidently, the AFM images confirmed successful generation of synthesized MIP nanoparticles after removal of the protein that formed the accommodated bionanomaterial inside the nanopore on the resultant synthetic materials. This was also related to insulin geometry.

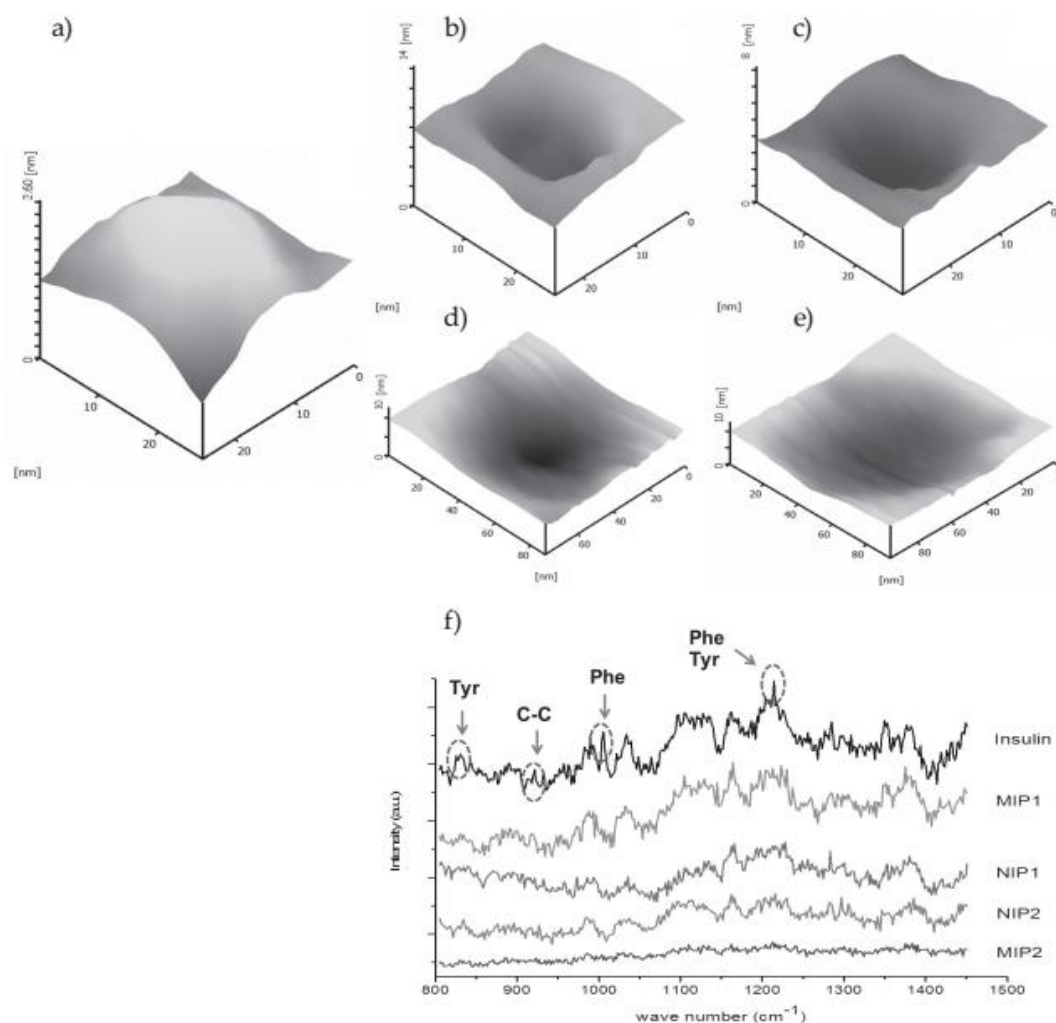


Fig. 3. AFM images of the imprinted cavity remaining after template removal. a) the nanoscale contact geometry of insulin molecule, b) and c) the imprinted cavities for MIP1 and MIP2, d) and e) the imprinted cavities for NIP1 and NIP2. b) and d) F1, c) and e) F2. Below: The difference between the imprint pattern and internal structure of insulin on the surface of nanoparticles. f) Raman spectra of insulin and MIPs with their corresponding NIP.

Raman-AFM study

We used confocal Raman spectroscopy to evaluate the structural information of biological entities in the protein template that remained in the synthesized nanoparticles. Fig. 3f illustrates the surface-enhanced Raman-AFM of the insulin and MIPs, showing different functional groups of interaction with the template that had an insulin imprint. The MIPs show the cluster of ridges and the grooves in the AFM image, which isolated a diameter of ~5 nm of an active trench attached to the structure of the nanoparticle surface. Table III shows Raman data obtained from the AFM-Raman studies for insulin and polymers.

Table III. Raman data of the insulin and polymers

Raman peak	Raman shift (cm ⁻¹)	Peak intensity				
		Insulin	MIP1	MIP2	NIP1	NIP2
Tyrosine (Tyr)	832.53	464.38	330.25	45.56	306.33	250.92
C-C	940.24	307.84	279.05	66.66	175.59	162.64
Phenylalanine (Phe)	1010.98	369.50	332.96	85.14	133.21	164.16
Tyr and Phe	1215.25	1005.62	743.97	154.27	470.31	421.45

The selected insulin in the Raman spectra was found at a different wave number, for example, tyrosine (Tyr) at 832 cm⁻¹, phenylalanine (Phe) at 1010 cm⁻¹, and the 1215 cm⁻¹ band for Tyr and Phe residues outside the polymer cross-linked chains, which is well known to be characteristic for R₆ conformation of hexameric human insulin (29). The Raman shift at 1010 cm⁻¹ can be used to confirm the intrinsic property of insulin formulation in the nanoscale environment of MIP1 (Fig. 3f). In contrast, the present method of generating the nanotopography for MIP2 was made to inhibit the Tyr and Phe residues in Raman spectra, allowing for the gap size of the captured surface to be probed. However, the oriented insulin indicated the structure and direction of peptide changes upon the template binding for MIPs. Dynamically, there was a far better interaction of the bulk layer of insulin than that of insulin in the pancreas islets with the MIP layer, which clearly showed the absence of a Raman peak shift for the islet imprint. For both NIPs, the spatial motifs of the insulin template were not fully distinguishable from the Raman shift.

Recognition ability of insulin MIPs

The recognition ability of the template for both the insulin-imprinted polymers and the corresponding NIPs was examined by batch binding experiments. Figs. 4a and b show the adsorption kinetic process of the protein to MIP and NIP nanoparticles. It can be seen that the MIPs of all formulations exhibited much higher adsorption capacities. Almost 80 % of equilibrium adsorption was achieved within 30 min and reached a steady-state for adsorption at around 2 h for both the F1 and F2 formulations. This was attributed to the high recognition efficiency of the template protein for the imprinting sites because of the nanoscale sizes of the imprinted cavity fitting to template structure through better diffusion properties (17). In contrast to NIPs, the adsorption of insulin was lower than that for MIPs due to the imprinting process. In addition, MIP2 showed a comparatively higher adsorption capacity than MIP1 for insulin, which was apparently different from that of MIP2, so a smaller amount of cross-linker contributed more than in the single monomer, as reported by previous studies (30). From the protein adsorption data, it is clear that MIPs adsorbed insulin more efficiently than NIPs. Between the two different mole ratios – a low mole ratio of MBAA containing the HEAA copolymer produced a relatively high density of binding sites, whereas a high mole ratio of cross-linkers and MAA lowered the imprinting efficiency of MIPs (31). This can be attributed to the different ratio of the amino acid-surface insulin on the imprinted cavities allowed for recognition sites, emphasizing the importance of the initial flexible conformation of protein (32).

Binding isotherms

The recognition behavior, which was dependent on the concentration of insulin in solution, was investigated to obtain the binding isotherm using insulin in a pH 7.4 buffer solution. The binding isotherm curves (Fig. 4c and d) show that the adsorption capacity of MIP nanoparticles was increased with an increase in the initial concentration of insulin in comparison with NIPs. Maximum adsorption capacity was obtained by MIP2 for both F1 and F2 formulations (3.26 and 3.34 mg g⁻¹, respectively). The Scatchard plots of insulin binding to MIP1 and MIP2 nanoparticles are shown in the insets (Fig. 4c and d) and the binding parameters are given in Table S3. This revealed a single straight line and implied the presence of homogeneous binding sites in the polymers (33). The equilibrium dissociation constant of insulin (K_d) of insulin binding to MIP2 (3.049 $\mu\text{mol L}^{-1}$) was somewhat higher than MIP1 (1.914 $\mu\text{mol L}^{-1}$), whereas the number of binding sites (B_{max}) was almost the same (4 $\mu\text{mol g}^{-1}$) and clearly indicated the formation of uniform recognition sites (34).

In vitro release studies

To understand how the fluid environment affected the attached surface of the polymers, insulin release was performed under gastric and intestinal conditions (pH 1.2 and

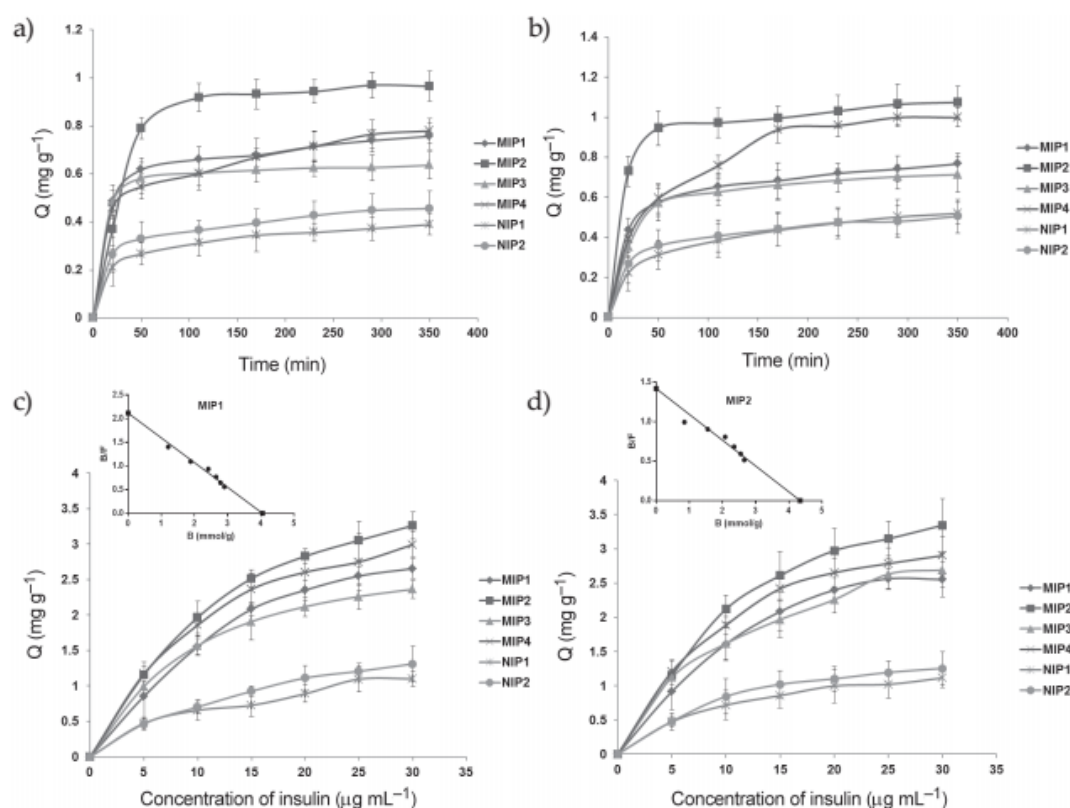


Fig. 4. a) Adsorption kinetic curves of MIPs and NIPs of F1 and b) F2 formulation at 25 °C (pH = 7.4); c) Binding isotherm curves of MIPs and NIPs of F1 and d) F2 formulation at 25 °C (pH = 7.4). Insets: Scatchard plot of insulin binding to MIP1 and MIP2 nanoparticles in PBS (pH = 7.4).

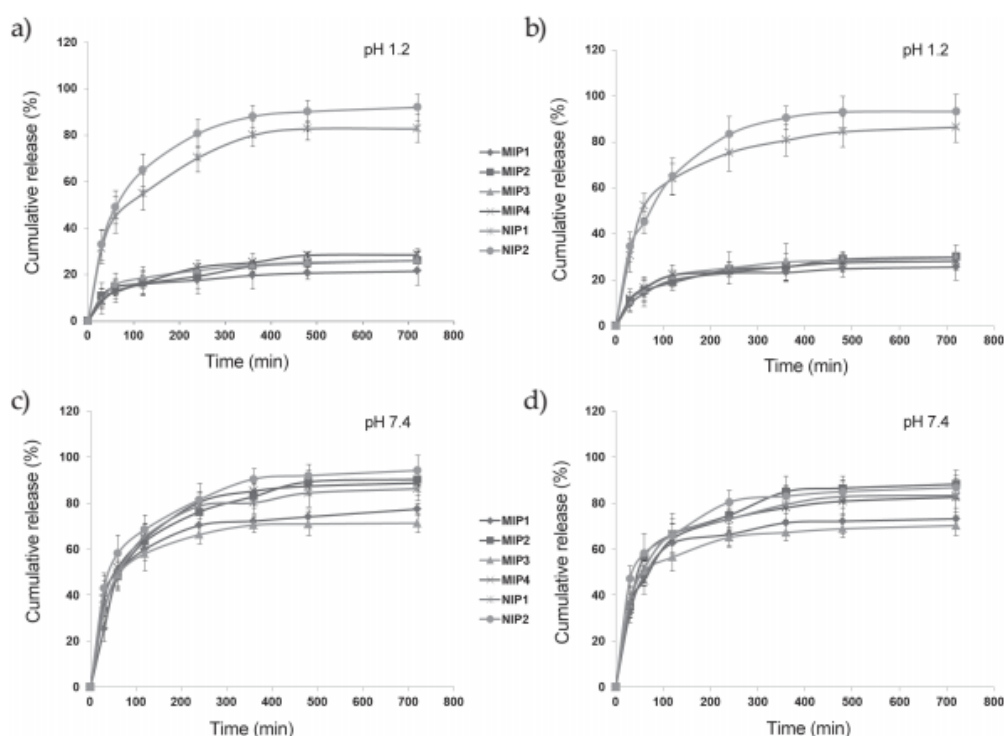


Fig. 5. Release profiles of insulin from MIPs and NIPs at pH 1.2: a) of formulation F1 and b) of F2; Release profiles of insulin from MIPs and NIPs at pH 7.4: c) of formulation F1 and d) F2.

7.4). At different pH values, the insulin release rate from MIPs for both F1 and F2 varied greatly compared to their corresponding NIPs. For MIPs at pH 1.2 (Fig. 5a), insulin release was retarded and less than 30 % of insulin was released, whereas, at pH 7.4, almost 90 % of insulin was released from MIPs (Fig. 5c). In contrast, the release profiles of insulin from NIPs at both pH values were almost the same, about 90 %. This could be attributed to the absence of recognition sites in NIPs, which resulted in low interaction with the insulin and its subsequent release to the external medium (35). In basic medium (pH 7.4), a gradual release of insulin from MIPs (30–40 % in the first 30 min) was observed, followed by sustained release (Fig. 5c and d). MIP2, which was produced by mixed functional monomers (MAA and HEAA) with a lower degree of cross-linkage, provided a considerably faster *in vitro* release ($k = 7.35 \pm 0.89$) than MIP1 ($k = 4.73 \pm 2.57$). MIP2 has a larger amount of MAA than MIP1 and offers a higher magnitude of solvated matrix, resulting in higher insulin release at basic pH. In addition, better insulin release from MIP2 nanoparticles was further supported by a greater K_d value of MIP2 ($3.049 \mu\text{mol L}^{-1}$) than that of MIP1 ($1.914 \mu\text{mol L}^{-1}$). Drug release data at pH 7.4 were analyzed by the Korsmeyer-Peppas equation as follows:

$$M_t / M_\infty = k t^n \quad (4)$$

where M_t/M_∞ is the fraction of insulin released at time t and k is the release rate constant. The diffusion exponent n characterizes the release mechanism of the drug depending on the geometry of the material tested. For radial geometry, $n = 0.45$ corresponds to the Fick-

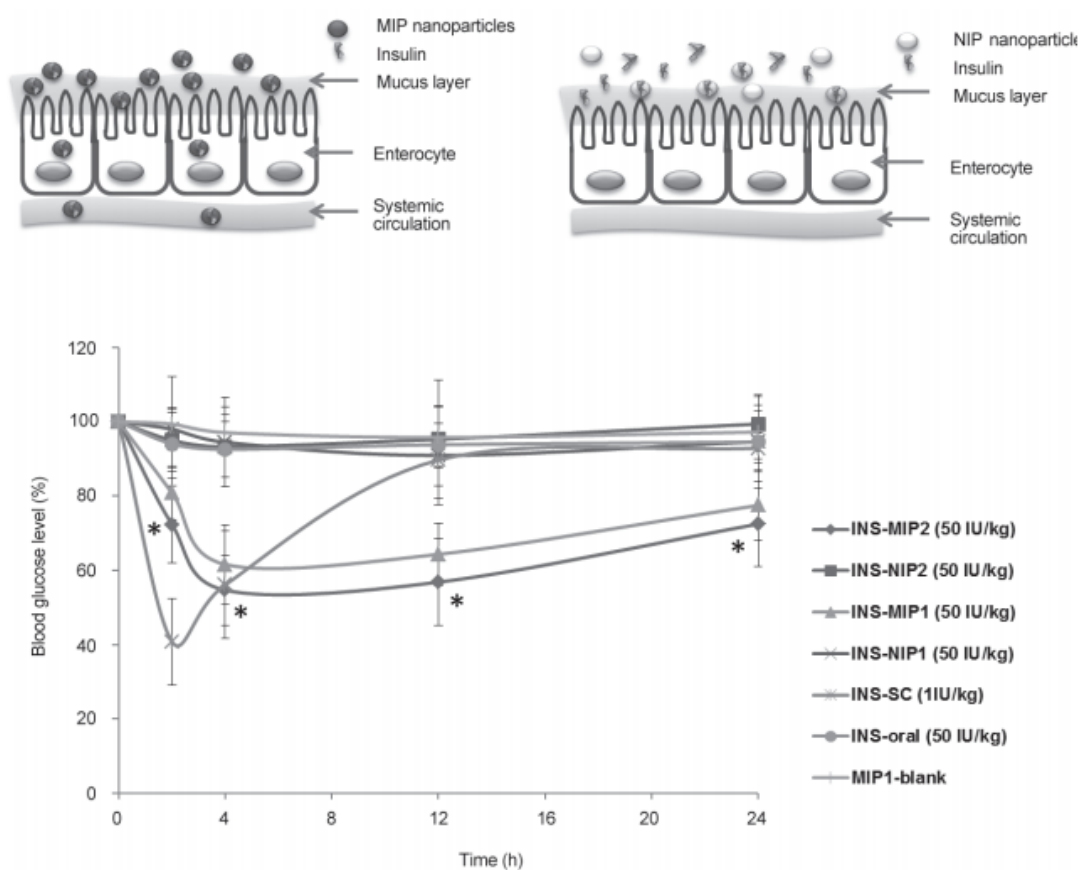


Fig. 6. Percentage reduction in blood glucose levels of diabetic rats after oral administration of insulin loaded MIPs and NIPs at a dose of (50 IU kg⁻¹), or after subcutaneous injection of insulin solution at 1 IU/kg ($n = 5$). *Statistically significant difference from the corresponding NIPs. Top: The proposed mechanism of delivery of insulin with biomimetic insulin-MIP by the transcellular nanoparticle transport mechanism

ian transport, $0.45 < n < 0.89$ corresponds to the non-Fickian (anomalous) transport, and $n = 0.89$ is related to the case II transport (36). The diffusion exponent (n) values of MIP1 and MIP2 were found to be between 0.45 and 0.89 (see Table S4), implying non-Fickian transport. The results indicated a higher mode of insulin release in aqueous medium owing to the reduced mass transfer resistance of the protein in the imprinted matrix. The effect of the polymer mixture in this work was in agreement with the previous study of MAA and in the polyethylene glycol-based hydrogel (37, 38) enabling the interaction with the receptor on the membrane subsequent to insulin release to the medium. Nonetheless, the proximity of the protein receptor or the dense packing of the amino acid groups affected the insulin structure within imprints, as determined by confocal Raman spectroscopy, favoring the interaction of the insulin at its binding site surrounded by the cross-linked chains. Thus, they have different affinities for a significant proportion of dormant molecules upon exposure to the environment, and the underlying porous network maintaining the structural stability resulted in significant effects on protein release.

In vivo studies of insulin-loaded nanoparticles on diabetic rats

Fig. 6 shows the blood glucose level-time profiles after oral administration of the insulin-loaded MIPs to diabetic rats. As can be seen, there was a sharp reduction in the blood glucose level (60 % within 2–3 h) after the subcutaneous injection of the free form of insulin (INS-SC) at a dose of 1 IU kg⁻¹; subsequently, the blood glucose level returned to its basal level with time. No obvious hypoglycemic effect was observed for the insulin solution (INS-oral) and the placebo control group (MIP1-blank) or either of the control polymers. After administration of both NIP nanoparticles loaded with insulin (INS-NIP1 and INS-NIP2) orally (50 IU kg⁻¹), there was no change in the blood glucose level, which showed superimposable reductions of blood glucose level in all cases. In contrast, the blood glucose level was reduced markedly after oral administration of the insulin-loaded MIPs (50 IU kg⁻¹). In comparison with both MIPs (INS-MIP1 and INS-MIP2), MIP1 showed the highest blood glucose level (39 % in 4 h) before gradual reduction, which lasted up to 12 h, whereas MIP2 reduced the initial blood glucose level significantly ($p < 0.05$; by 44 % within 4 h) and the blood glucose level was maintained at this level for up to 12 h. These results indicated that the distribution of insulin-MIP was unaffected by the GI environment due to the stabilization of insulin by MIPs after oral administration.

The parameters of plasma glucose levels are given in Table IV, and at a dose of 50 IU kg⁻¹, the relative pharmacological bioavailability in the percentage reduction of glucose of MIP1 and MIP2 was 1.73 and 1.55 %, respectively. In addition, the difference in the loading capacity between MIP2 and NIP2 was found to be 55.75 and 20.87 mg insulin/g nanoparticles, respectively (Table S5). The loading capacity of MIPs was almost threefold higher than that for NIPs. As opposed to the nanoparticulate MIPs loaded with insulin, NIP failed to reduce the blood glucose level, due to the lack of specific binding sites within the polymer, resulting in no protein affinity. There was further improvement in insulin absorption in the case of MIP2 over MIP1, which was clearly observed because of the effect of insulin on the lipid-protein layer. The results showed that it increased the interactions of the biomolecule at the spatial motifs of the insulin template into the biological milieu in rat, that mimicked the insulin-cell surface interaction (39). This could be ascribed to the surface of MIP2 enabling surface adhesion of insulin-MIPs with a dense set of nanoscale pores. Oral administration of the insulin loaded MIPs to diabetic rats displayed a more significant

Table IV. Relative pharmacological bioavailability and parameters of plasma glucose levels (n = 5)

Parameter	INS-MIP1	INS-MIP2	INS-SC
Insulin dose (IU kg ⁻¹)	50	50	1
C _{min} ^a (mg dL ⁻¹)	61.58 ± 10.57	54.65 ± 9.43	40.76 ± 11.65
t _{min} ^b (h)	4	4	2
AAC	1577.71 ± 208.29	1422.88 ± 254.90	1816.2 ± 188.96
PA%	1.74	1.55	100

^a C_{min}, minimum plasma glucose concentration (% of initial)

^b t_{min}, time at which C_{min} is attained; AAC, area above the blood glucose level-time curves; PA%, relative pharmacological bioavailability.

hypoglycemic effect than that of NIPs. Based on these important findings, we proposed insulin transport through the transcellular pathway (Fig. 6, top), related to the particle size, surface charge, and mucous adhesion in the GI tract, which would facilitate oral protein delivery. However, further investigations are required to make conclusions about the transport mechanisms.

CONCLUSIONS

We have successfully produced selective particles incorporating insulin and insulin-bound islets by the molecular imprinting of protein on nanoparticles using the precipitation polymerization method. Biomimetic MIPs nanoparticles can serve as potential insulin oral delivery systems and represent a new way for an alternative platform, especially because of their robust physical structures, biocompatibility and loading capabilities. The MIPs exhibited much higher affinity toward the insulin with rapid adsorption kinetics, which enabled them to selectively deliver the therapeutic agent. The application of MIPs showed a different response of the blood glucose level, depending on the variation in the ratio of the functional monomer and cross-linkers. Targeted delivery of biomolecule recognition-based therapies such as insulin using the molecular imprinting approach could be effective for improvement of its therapeutic efficiency.

Acknowledgements. – We greatly appreciate financial support from the National Research University Project of Thailand, Office of the Higher Education Commission (Code no. PHA 540545c). Drug Delivery System Excellence Center at PSU; Nanotechnology Center (NANOTEC), Ministry of Science and Technology, Thailand, through its Center of Excellence Network program. The authors also thank the Department of Pharmaceutical Chemistry, Faculty of Pharmaceutical Sciences, for lab facilities, Mr. Maitri Nuanplub for his assistance in animal work and Dr. Brian Hodgson for helping us with the English. Supplementary material is available upon request.

REFERENCES

1. F. Nakayama, T. Yasuda, S. Umeda, M. Asada, T. Imamura, V. Meineke and M. Akashi, Fibroblast growth factor-12 (FGF12) translocation into intestinal epithelial cells is dependent on a novel cell-penetrating peptide domain involvement of internalization in the in vivo role of exogenous FGF12, *J. Biol. Chem.* **286** (2011) 25823–25834; DOI: 10.1074/jbc.M110.198267.
2. L. M. Ensign, R. Cone and J. Hanes, Oral drug delivery with polymeric nanoparticles: the gastrointestinal mucus barriers, *Adv. Drug Deliv. Rev.* **64** (2012) 557–570; DOI: 10.1016/j.addr.2011.12.009.
3. S. A. Zaidi, Latest trends in molecular imprinted polymer based drug delivery systems, *RSC Adv.* **6** (2016) 88807–88819; DOI: 10.1039/c6ra18911c.
4. R. Schirhagl, D. Podlipna, P. A. Lieberzeit and F. L. Dickert, Comparing biomimetic and biological receptors for insulin sensing, *Chem. Commun.* **46** (2010) 3128–3130.
5. R. Suedee, W. Naklua, S. Laengchokshoi, K. Thepkau, P. Pathaburee and M. Nuanplub, Investigation of a self-assembling microgel containing an (S)-propranolol molecularly imprinted polymer in a native tissue microenvironment: Part I preparation and characterization. Part II biological application and testing, *Process Biochem.* **50** (2015) 517–544.
6. K. Eunkyung and C. Seung-Woo, Biomimetic polymer scaffolds to promote stem cell-mediated osteogenesis, *Int. J. Stem Cells* **6** (2013) 87–91.
7. R. Schirhagl, U. Latif, D. Podlipna, H. Blumenstock and F. L. Dickert, Natural and biomimetic materials for the detection of insulin, *Anal. Chem.* **84** (2012) 3908–3913.

8. E. M. Kolonko, J. K. Pontrello, S. L. Mangold and L. L. Kiessling, General synthetic route to cell-permeable block copolymers via ROMP, *J. Am. Chem. Soc.* **131** (2009) 7327–7333.
9. F. Puoci, G. Cirillo, M. Curcio, O. I. Parisi, F. Iemma and N. Picci, Molecularly imprinted polymers in drug delivery: state of art and future perspectives, *Expert Opin. Drug Deliv.* **8** (2011) 1379–1393; DOI: 10.1517/17425247.2011.609166.
10. A. Viehof, L. Javot, A. Béduneau, Y. Pellequer and A. Lamprecht, Oral insulin delivery in rats by nanoparticles prepared with non-toxic solvents, *Int. J. Pharm.* **443** (2013) 169–174; DOI: 10.1016/j.ijpharm.2013.01.017.
11. E. Verspohl and H. Ammon, Evidence for the presence of insulin receptors in rat islets of Langerhans, *J. Clin. Invest.* **65** (1980) 1230; DOI: 10.1172/JCI109778.
12. D. R. Kryscio and N. A. Peppas, Critical review and perspective of macromolecularly imprinted polymers, *Acta Biomater.* **8** (2012) 461–473; DOI: 10.1016/j.actbio.2011.11.005.
13. L. Achar and N. Peppas, Preparation, characterization and mucoadhesive interactions of poly (methacrylic acid) copolymers with rat mucosa, *J. Control. Release* **31** (1994) 271–276; DOI: 10.1016/0168-3659(94)90009-4.
14. S. Li, E. N. Davis, X. Huang, B. Song, R. Peltzman, D. M. Sims, Q. Lin and Q. Wang, Synthesis and development of poly (*n*-hydroxyethyl acrylamide)-ran- 3-acrylamidophenylboronic acid polymer fluid for potential application in affinity sensing of glucose, *J. Diabetes Sci. Technol.* **5** (2011) 1060–1067.
15. J. Wang, P. A. Cormack, D. C. Sherrington and E. Khoshdel, Synthesis and characterization of micrometer-sized molecularly imprinted spherical polymer particulates prepared via precipitation polymerization, *Pure Appl. Chem.* **79** (2007) 1505–1519; DOI: 10.1351/pac200779091505.
16. G. Pan, Q. Guo, C. Cao, H. Yang and B. Li, Thermo-responsive molecularly imprinted nanogels for specific recognition and controlled release of proteins, *Soft Matter* **9** (2013) 3840–3850; DOI: 10.1039/C3SM27505A.
17. S. Chaitidou, O. Kotrotsiou, K. Kotti, O. Kammona, M. Bukhari and C. Kiparissides, Precipitation polymerization for the synthesis of nanostructured particles, *Mater. Sci. Eng. B* **152** (2008) 55–59; DOI: 10.1016/j.mseb.2008.06.024.
18. J. D. Carter, S. B. Dula, K. L. Corbin, R. Wu and C. S. Nunemaker, A practical guide to rodent islet isolation and assessment, *Biol. Proced. Online* **11** (2009) 3–31; DOI: 10.1007/s12575-009-9021-0.
19. H. He, D. Xiao, J. He, H. Li, H. He, H. Dai and J. Peng, Preparation of a core-shell magnetic ion-imprinted polymer via a sol–gel process for selective extraction of Cu (ii) from herbal medicines, *Analyst* **139** (2014) 2459–2466; DOI: 10.1039/c3an02096g.
20. S. Sajeesh, K. Bouchemal, V. Marsaud, C. Vauthier and C. P. Sharma, Cyclodextrin complexed insulin encapsulated hydrogel microparticles: An oral delivery system for insulin, *J. Control. Release* **147** (2010) 377–384; DOI: 10.1016/j.jconrel.2010.08.007.
21. A. Cilek, N. Celebi, F. Tirnaksız and A. Tay, A lecithin-based microemulsion of rh-insulin with aprotinin for oral administration: Investigation of hypoglycemic effects in non-diabetic and STZ-induced diabetic rats, *Int. J. Pharm.* **298** (2005) 176–185; DOI: 10.1016/j.ijpharm.2005.04.016.
22. W. Ritschel, G. Ritschel, B. Ritschel and P. Lückner, Rectal delivery system for insulin, *Methods Find. Exp. Clin. Pharmacol.* **10** (1988) 645–656.
23. M. P. Desai, V. Labhasetwar, G. L. Amidon and R. J. Levy, Gastrointestinal uptake of biodegradable microparticles: effect of particle size, *Pharm. Res.* **13** (1996) 1838–1845.
24. I. Stützer, D. Esterházy and M. Stoffel, The pancreatic beta cell surface proteome, *Diabetologia* **55** (2012) 1877–1889; DOI: 10.1007/s00125-012-2531-3.
25. M. García-Díaz, C. Foged and H. M. Nielsen, Improved insulin loading in poly (lactic-co-glycolic) acid (PLGA) nanoparticles upon self-assembly with lipids, *Int. J. Pharm.* **482** (2015) 84–91; DOI: 10.1016/j.ijpharm.2014.11.047.

26. T. Andreani, A. L. R. de Souza, C. P. Kiill, E. N. Lorenzon, J. F. Fangueiro, A. C. Calpena, M. V. Chaud, M. L. Garcia, M. P. D. Gremião and A. M. Silva, Preparation and characterization of PEG-coated silica nanoparticles for oral insulin delivery, *Int. J. Pharm.* **473** (2014) 627–635; DOI: 10.1016/j.ijpharm.2014.07.049.
27. B. C. Tang, M. Dawson, S. K. Lai, Y.-Y. Wang, J. S. Suk, M. Yang, P. Zeitlin, M. P. Boyle, J. Fu and J. Hanes, Biodegradable polymer nanoparticles that rapidly penetrate the human mucus barrier, *Proc. Natl. Acad. Sci. U.S.A.* **106** (2009) 19268–19273; DOI: 10.1073/pnas.0905998106.
28. P. de Sousa Irene, M. Thomas, S. Corinna, F. Barbara and B.-S. Andreas, Insulin loaded mucus permeating nanoparticles: Addressing the surface characteristics as feature to improve mucus permeation, *Int. J. Pharm.* (2016); DOI: 10.1016/j.ijpharm.2016.01.022.
29. K. Rostamizadeh, H. Abdollahi and C. Parsajoo, Synthesis, optimization, and characterization of molecularly imprinted nanoparticles, *Int. Nano Lett.* **3** (2013) 1–9; DOI: 10.1186/2228-5326-3-20.
30. V. P. Drachev, M. D. Thoreson, E. N. Khaliullin, V. J. Davisson and V. M. Shalaev, Surface-enhanced Raman difference between human insulin and insulin lispro detected with adaptive nanostructures, *J. Phys. Chem. B* **108** (2004) 18046–18052; DOI: 10.1021/jp047254h.
31. H. Zeng, Y. Wang, X. Liu, J. Kong and C. Nie, Preparation of molecular imprinted polymers using bi-functional monomer and bi-crosslinker for solid-phase extraction of rutin, *Talanta* **93** (2012) 172–181; DOI: 10.1016/j.talanta.2012.02.008.
32. L. Xu, Y.-A. Huang, Q.-J. Zhu and C. Ye, Chitosan in molecularly-imprinted polymers: Current and Future Prospects, *Int. J. Mol. Sci.* **16** (2015) 18328–18347; DOI: 10.3390/ijms160818328.
33. M. Odabaşı, R. Say and A. Denizli, Molecular imprinted particles for lysozyme purification, *Mater. Sci. Eng. C* **27** (2007) 90–99; DOI: 10.1016/j.msec.2006.03.002.
34. S. Scorrano, L. Mergola, R. Del Sole and G. Vasapollo, Synthesis of molecularly imprinted polymers for amino acid derivatives by using different functional monomers, *Int. J. Mol. Sci.* **12** (2011) 1735–1743; DOI: 10.3390/ijms12031735.
35. M. R. Avadi, A. M. M. Sadeghi, N. Mohammadpour, S. Abedin, F. Atyabi, R. Dinarvand and M. Rafiee-Tehrani, Preparation and characterization of insulin nanoparticles using chitosan and arabic gum with ionic gelation method, *Nanomedicine* **6** (2010) 58–63; DOI: 10.1016/j.nano.2009.04.007.
36. C. Ferrero, D. Massuelle and E. Doelker, Towards elucidation of the drug release mechanism from compressed hydrophilic matrices made of cellulose ethers. II. Evaluation of a possible swelling-controlled drug release mechanism using dimensionless analysis, *J. Control. Release* **141** (2010) 223–233; DOI: 10.1016/j.jconrel.2009.09.011.
37. S. Li, A. Tiwari, Y. Ge and D. Fei, A pH-responsive, low crosslinked, molecularly imprinted insulin delivery system, *Adv. Mater. Lett.* **1** (2010) 4–10; DOI: 10.5185/amlett.2010.4110.
38. E. Lee, K. Kim, M. Choi, Y. Lee, J.-W. Park and B. Kim, Development of smart delivery system for ascorbic acid using pH-responsive P (MAA-co-EGMA) hydrogel microparticles, *Drug Deliv.* **17** (2010) 573–580; DOI: 10.3109/10717544.2010.500636.
39. Y. Hoshino, T. Urakami, H. Koido and K. J. Shea, Recognition, neutralization, and clearance of target peptides in the bloodstream of living mice by molecularly imprinted polymer nanoparticles: A plastic antibody, *J. Am. Chem. Soc.* **132** (2010) 6644–6645; DOI: 10.1021/ja102148f.

SUPPLEMENTARY MATERIALS

Table S1

Polymer	F1			F2		
	Surface area (m ² g ⁻¹)	Pore volume (mL g ⁻¹)	Pore diameter (nm)	Surface area (m ² g ⁻¹)	Pore volume (mL g ⁻¹)	Pore diameter (nm)
MIP1	21.83	0.089	14.82	134.50	0.340	10.12
MIP2	149.1	0.462	12.40	212.60	0.581	10.94
NIP1	27.39	0.263	38.02	39.81	0.257	25.85
MIP3	90.77	1.415	22.36	111.60	0.634	22.74
MIP4	189.7	0.845	17.72	252.50	0.772	12.24
NIP2	86.85	1.031	47.50	47.44	0.276	23.24

Table S2

Polymer	Gross heating value (J g ⁻¹)	
	Insulin (crystalline)	Insulin (suspension)
MIP1	14,409	14,171
NIP1	16,265	14,796
MIP2	16,844	15,344
NIP2	13,518	15,869

Table S3

Formulation	K_d (μM)	B_{max} (μmol g ⁻¹)	R ²
MIP1	1.91 ± 0.18	4.05 ± 0.15	0.997
MIP2	3.05 ± 0.43	4.34 ± 0.29	0.995

P. Kumar Paul *et al.*: Biomimetic insulin-imprinted polymer nanoparticles as a potential oral drug delivery system, *Acta Pharm.* **67** (2017) Supplementary materials

Table S4

Formulation	n^*	k^*	r^2
MIP1	0.536 ± 0.122	4.74 ± 2.57	0.977
MIP2	0.451 ± 0.028	7.36 ± 0.90	0.998

* For mean \pm SD ($n = 3$).

Table S5

	MIP1	MIP2	NIP1	NIP2
Loading capacity (mg g ⁻¹)	42.51	55.75	18.53	20.87
Loading efficiency (%)	78.94	82.13	47.01	50.81

PAPER 2

Improvement in insulin absorption into gastrointestinal epithelial cells by using
molecularly imprinted polymer nanoparticles: Microscopic evaluation and
ultrastructure

(Accepted in *International Journal of Pharmaceutics*)

Date: Jul 24, 2017
To: "Roongnapa Suedee" roongnapa.s@psu.ac.th
From: "International Journal of Pharmaceutics" eesserver@eesmail.elsevier.com
Reply To: "International Journal of Pharmaceutics" ijp@elsevier.com
Subject: Your Submission

Ms. Ref. No.: IJP-D-17-01021R2

Title: Improvement in insulin absorption into gastrointestinal epithelial cells by using molecularly imprinted polymer nanoparticles: Microscopic evaluation and ultrastructure
International Journal of Pharmaceutics

Dear Dr. Suedee,

I am pleased to confirm that your paper "Improvement in insulin absorption into gastrointestinal epithelial cells by using molecularly imprinted polymer nanoparticles: Microscopic evaluation and ultrastructure" has been accepted for publication in International Journal of Pharmaceutics.

Your accepted manuscript will now be transferred to our production department and work will begin on creation of the proof. If we need any additional information to create the proof, we will let you know. If not, you will be contacted again in the next few days with a request to approve the proof and to complete a number of online forms that are required for publication.

When your paper is published on ScienceDirect, you want to make sure it gets the attention it deserves. To help you get your message across, Elsevier has developed a new, free service called AudioSlides: brief, webcast-style presentations that are shown (publicly available) next to your published article. This format gives you the opportunity to explain your research in your own words and attract interest. You will receive an invitation email to create an AudioSlides presentation shortly. For more information and examples, please visit <http://www.elsevier.com/audioslides>.

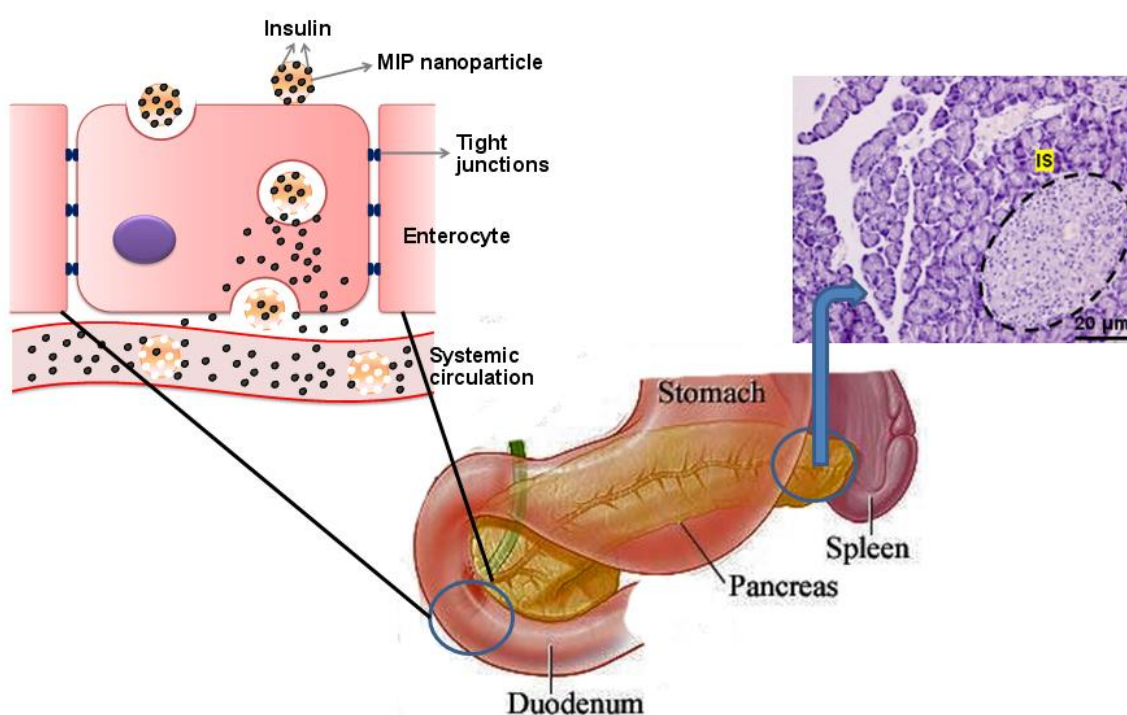
Thank you for submitting your work to this journal.

With kind regards,

Fumiyoshi Yamashita
Editor-in-Chief
International Journal of Pharmaceutics

Graphical Abstract

An innovative mimicking of the structure of therapeutic protein for GI transport in vivo was achieved in this work. When it incubated within the extracellular mucous gel seemed to have a markedly reduced insulin release, leading to the lipophilic domains within affected areas across the epithelial cells.



Improvement in insulin absorption into gastrointestinal epithelial cells by using molecularly imprinted polymer nanoparticles: Microscopic evaluation and ultrastructure

Pijush Kumar Paul¹, Jongdee Nopparat², Mitree Nuanplub³, Alongkot Treetong⁴, and Roongnapa Suedee^{1,*}

¹Molecular Recognition Materials Research Unit, Nanotec-PSU Center of Excellence on Drug Delivery System, Department of Pharmaceutical Chemistry, Faculty of Pharmaceutical Sciences, ²Department of Anatomy, ³Animal House Division, Faculty of Science, Prince of Songkla University, Hatyai, Songkhla 90112, Thailand

⁴National Nanotechnology Center (NANOTEC), National Science and Technology Development Agency (NSTDA), Thailand Science Park, Phahonyothin Road, Pathum Thani 12120, Thailand

This work is dedicated to the memory of Dr. Brian Hodgson.

*Corresponding author: Roongnapa Suedee, Tel.: +66-74-288862; fax: +66-74-428239; e-mail: roongnapa.s@psu.ac.th

Abstract

A molecularly imprinted polymer nanoparticle (MIP) was prepared by integrating a mixed functional monomer into a highly cross-linked polymer. The nanosized insulin as a template transferred into the binding cavities, anchored functional monomer(s) that the insulin structure formed within free space of the molecular size region by MIP nanoparticles. The oral administration with the insulin-loaded MIP resulted in higher fluorescence intensity of rhodamine-labeled insulin into the epithelial cells. We observed the correlation between the lipophilic domains of dye over the affected areas of sites with the interplay of the intestinal epithelial layer on the different intestinal sections. And, the detection with guinea pig anti-insulin antibody followed by goat anti-guinea pig antibody clearly elicited the efficient insulin function in the necessary biological milieu. The root mean square roughness of the MIP indicated difference of the surface density, significantly lower compared with the polymer attributed to the protein-mucin uptake that efficiently promoted the insulin penetration. Eventually electron microscopy data of the conjugated biotin-gold nanoparticles showed the transport of insulin across the intestinal epithelium via transcellular pathway, and the development of the pancreatic β cell in the streptozocin-induced diabetic rats. Histopathological observation exhibited no obvious toxic effect after orally treated with MIP loaded insulin (100 mg/kg) daily for 14 days compared to control group. The use of an insulin-loaded MIP was proven to be an effective therapeutic protein delivery through transmucosal oral route.

Keywords: Molecularly imprinted polymers, biomimetic system, extracellular mucus gel, insulin, nanotechnology, diabetes.

1. Introduction

Many diabetic patients currently receive subcutaneous injections, which have the drawbacks of insulin leakage due to dose measurement error and pain at the injection area leading to poor patient compliance [1]. The use of insulin pens (e.g., Novo fill with NovoFine needles or insulin discs) limited the number of administration and expensive. If its shortcoming of low stability in the gastrointestinal (GI) environment [2] is addressed, alternative administration of insulin through the oral route can solve to the problem. Since most biomacromolecules have poor absorption through the cell membrane into the blood circulation. Using of an innovative approach that was produced with a highly selective material capable of adjusting of the small dynamic part of protein structure for the diversity of bioactivity and translational function and penetration in vivo. By this means, the molecular imprinting related to nanotechnology drawn much attention for biomacromolecular uptake and advanced drug delivery [3]. A molecularly imprinted polymer (MIP) has all the attributes to be a candidate for efficient delivery due to its predetermined selectivity of robust artificial material and the biocompatibility suitable for the development into the blood circulation [4]. The small entities of inhibitor or amino acid sequences for specific recognition bind to the target receptor, where structurally driven groups of natural peptide transport into the cell membrane [5]. A polymer matrix anchored functional groups e.g. deoxycholic acid was found to act on the integral membrane bilayer for enhanced of the cellular absorption [6]. Within this study the systemic absorption of biopharmaceutical compounds can be accomplished by the approach related to the physicochemical properties (e.g., composition, surface charge, and surface chemistry).

The imprinting of the insulin template is important in diabetic treatment, which is one of the fatal diseases in the world. The strategic method of MIP in nanotechnology is selection of an appropriate monomer that emerged from the naturally occurring compound derived template is of interesting and great advantageous for the therapeutic protein delivery [7]. The surface properties of a peptide, protein drug is largely dependent on the viscoelastic nature of the extracellular mucus gel. The effective adhesive interaction of mucous and mucins allowed for their protective and lubricating properties within the GI lumen that made

the feasibility in bio-interactions between the nanoparticles and the intestinal mucus. MIP can facilitate to produce the nanoparticle-protein association besides; previous studies have successfully prepared biomimetic materials for insulin sensing using molecular imprinting [8].

However, very little is known so far about the transport mechanism of MIP across the intestinal epithelium into the deeper cell layers. In addition, the toxicity of the polymer nanoparticles has to be understood in greater depth and this usually induces specific molecular interaction. The reason for this is that the systemic levels, organs, tissues, and cells are needed to corroborate the various systems into a biological process reflects the functions and signaling pathways of the body [9]. MIP under physiological medium mimics a molecular interaction would affect the biological activity of the protein that can exploit a biomimetic system [10]. MIP nanoparticles with desired affinity have been used for in vivo application that can effectively capture the cytotoxic peptide in bloodstream [11]. A molecular imprinting, which is one aspect of nanotechnology, is applied and discussed in biomimetic approach with respect to the pharmaceutically active insulin as a template. Though, a new method for determination of reaction or transformation in diabetes treatment [12], that the outermost epithelial cells and the enterocyte spaces of tight junctions restrict the passage of nanoparticles, which determine directly that, cannot be characterized by sequencing or structural similarity [13]. Mounting evidence in molecular imprinting techniques has emerged the use of a single monomer seemed to control flexible complex in water and produce the recognition sites with weak interaction [14]. Our recent report demonstrated the MIP helped to facilitate transport of insulin delivery. The key functional material was the hydrophobicity of the methacrylic acid (MAA) based material with the particle size, which allowed for a prolonged transit time. A series of tests previously supported that controlled size of the polymer nanoparticles can be achieved by a mixed functional monomer, methacrylic acid (MAA) and *N*-hydroxyethyl acrylamide (HEAA) in different ratios and PCL-T in the presence of insulin as the template, using an aqueous precipitation polymerization technique. The size of the insulin-imprinted polymers was influenced by the amount of the cross-linking monomer and variations of the concentrations of the functional monomers.

Lower degree of crosslinking by *N,N*-methylene-bisacrylamide (MBAA) which allowed high binding efficiency with minimum non-specific binding for the re-bound protein target of MIP nanoparticles during the polymerization process [15]. However, only adjusting of the polymer composition in MIP formulation enabled higher strength and selectivity of MIP which was important for determining the efficiency for template recognition and to stabilize interaction between the functionality of the monomers and the insulin crossed the intestinal cell membrane. As a consequence of the change in the environment and enzyme catalysis the fate of the essential protein was dependent on its accessibility to the imprint sites. To the best of our knowledge presently, this molecular imprinting created the opportunities for interactions triggered resulted in effects on the stability of protein into the environment that led to a detectable protein when administered orally to the diabetic rats which was supported by the immunohistochemistry. By repertoire of functional significance of such template-MIP assemblies in the polymer matrix, we could investigate of the insulin uptake into the gastrointestinal cell layers [16]. Recently, the studies of the nanoparticle uptake into cells have drawn interest, mostly in tumor cell lines [17] involving either a paracellular or a transcellular route [18]. Previous reports in the literature have indicated that chitosan acts as an enhancer of insulin absorption, by opening tight junctions reversibly [19], which accounts for <0.5% of the intestinal absorptive surface in the Caco-2 cell monolayer [20].

In this study, we synthesized and characterized an insulin-imprinted polymer prior to the investigations in the orally-administered insulin. Then by immunohistochemical and immunofluorescence analyses based on transmission electron microscopy (TEM), we studied the intracellular localization of internalized nanoparticles in order to investigate the biomacromolecular absorption mechanism of the insulin-loaded MIP. The non-imprinted polymer (NIP) was also used to assess the selectivity of the imprinted material. An ultrastructural examination was carried out, and the nanotoxicity within diabetes-induced Wistar rats after treatment for 14 days was discussed.

2. Materials and Methods

2.1. Chemicals and reagents

Human insulin (recombinant DNA origin; 100 IU/mL) was obtained from Eli Lilly Asia, Inc. (Bangkok, Thailand). Methacrylic acid (MAA), *N*-hydroxyethyl acrylamide (HEAA), *N,N*-methylene-bisacrylamide (MBAA), polycaprolactone triol (PCL-T), fluorescein isothiocyanate (FITC), rhodamine 6G (Rh), streptozotocin, protease inhibitor cocktail, goat anti-guinea pig IgG, and gold nanoparticles conjugated with biotin (60 nm) were purchased from Sigma-Aldrich (St. Louis, MO, USA). 2,2'-Azobis-(isobutyronitrile) (AIBN) was obtained from Wako Pure Chemical Industries Ltd (Osaka, Japan), 4',6-diamidino-2-phenylindole dihydrochloride (DAPI) from Thermo Fisher Scientific (Waltham, MA, USA), and guinea pig anti-insulin antibody from Abcam (Cambridge, UK). The Vectastain[®] Elite ABC kit and diaminobenzidine (DAB) were from Vector Laboratories (Burlingame, USA). All the other reagents were either analytical or HPLC grade and were used as received.

2.2. *Synthesis of insulin imprinted nanoparticles*

The MIP nanoparticles were prepared by aqueous precipitation polymerization with insulin as template. MAA and HEAA were used as mixed functional monomers, MBAA as the cross-linker, and phosphate-buffered saline (PBS; pH 7.4) as the porogenic solvent. Initially, 35 mg (0.6 mM) of insulin was added to 10 ml of PBS (pH 7.4), followed by the addition of 430.3 mg (1.6 mM) MAA, 230.26 mg (2.0 mM) HEAA, 493.34 mg (8.5 mM) MBAA, and 15 mg (0.05 mM) PCL-T. The reaction mixture was transferred into a 30-ml vial and 6.56 mg (0.04 mmol) AIBN was added. The resulting mixture was purged with nitrogen gas for 5 min and then polymerized overnight at room temperature, with UV exposure at 254-nm wavelength. After polymerization, the synthesized MIP was washed with Milli-Q water to remove unreacted monomers and then was collected by centrifugation at 10,000 rpm for 5 min. The insulin was removed from the polymers by washing with 0.5-M NaCl solution and Milli-Q water several times. The complete extraction of insulin was confirmed by testing the supernatant at 272 nm with the use of a UV-Vis spectrophotometer. Similarly, the control polymers (NIP) were prepared by using the same protocol applied for the MIP, except for the addition of insulin during polymerization.

2.3. Characterization of MIP

The average hydrodynamic diameter of the MIP was determined by dynamic light scattering (DLS) with the use of a Zetasizer Nano ZS system (Malvern Instruments Ltd, Malvern, UK) at a detection angle of 90° and temperature of 25°C. The zeta potential was determined with the same instrument by diluting the samples in Milli-Q water. The surface morphology of the insulin-imprinted nanoparticles was observed by scanning electron microscopy (SEM; Quanta 400; FEI, Czech Republic) and transmission electron microscopy (TEM; JEM-2100F; JEOL Inc., Tokyo, Japan). The topography and surface geometry of the polymers were examined by atomic force microscopy (AFM; SPA400-SPI4000; Seiko Instruments Inc., Chiba, Japan).

2.4. Fluorescence study and recognition ability of the MIPs for insulin

The interaction between the MIP and insulin was studied by fluorescence spectroscopic analysis with the use of a spectrofluorometer (FP-6200; JASCO International Co., Ltd, Tokyo, Japan). Five milliliters of insulin solution (0.5 mg/ml, 0.08 mM) in phosphate buffer (pH 7.4) was used for the assay. The fluorescence emission spectra from 290–320 nm were recorded at an excitation wavelength of 280 nm. MIP/NIP nanoparticles concentrations of 1, 3, 5, and 10 mg were added to the insulin solution, and the fluorescence emission intensity of insulin was determined [21]. The fluorescence emission spectra of six different concentrations of insulin, ranging from 0.5 to 3 µM, were recorded at 300 nm. The solutions were incubated with 10 mg of the MIP/NIP for 2 h. The emission spectra were then measured by excitation of the sample at 280 nm to obtain the relative intensity (I/I_0), where I and I_0 denoted the fluorescence intensity of the insulin solution in the absence and the presence of the MIP/NIP polymer, respectively. A gradient plot was drawn for the concentration of insulin, in which the correlation coefficients of linear regression were determined.

2.5. Differential scanning calorimetry

The thermal properties of the MIP and NIP nanoparticles were examined by differential scanning calorimetry (DSC 8000; Perkin–Elmer, Norwalk, CT, USA). A

Pyris Manager Software system (version 11.0.0) was used for data acquisition. Polymer samples (3 mg) were crimped into an aluminum pan and heated from 20 to 350°C at a rate of 10°C/min under a stream flow of nitrogen.

2.6. Evaluation of the desorption and partitioning of insulin

Wistar rats weighing 200 to 250 g were used in this study, which was approved by the Animal Ethical Committee of the Prince of Songkla University (Ref. 36/2014). The rat small intestines were collected and homogenized in Tris-EDTA (10 mM Tris-HCl and 1 mM EDTA; pH 7.4) containing protease inhibitor (10 µl mL⁻¹). The homogenate was centrifuged at 10,000 rpm for 10 min at 4° C [22]. Then, the supernatant was collected and used for the desorption study. The partitioning properties of insulin and insulin-loaded MIPs through rat intestinal tissue lysates were studied by using the 3M™ Empore™-vacuum manifold system (3M Bioanalytical Technologies, St. Paul, Minnesota, USA). We attempted to increase the transport of insulin through the MIP compared with the NIP by using the static Empore disc technique. Because the interfacial transfers through the filter plate that can be blocked by two immiscible phases is created at the surface of a sinter across the unstirred liquid. Stagnant diffusion can occur between both sides of the filter, which could contribute to the resistance of mass transfer. Thus, the effect of the tissue lysate on the insulin transfer from the MIP and NIP nanoparticles was determined by equilibration with insulin in PBS at 37°C for 2 h before the experiment. A solution containing insulin (100 µg mL⁻¹) in PBS (pH 7.4) containing polymer nanoparticles were then placed in an Empore disk with PBS (pH 7.4) as eluent. In the control experiment, 500 µl of the tissue lysate obtained from the rat small intestine as mentioned above was added in the disk which biomacromolecule transfer and desorption at appropriate time interval for 24 h. The amount of insulin in the solution which was taken from the receptor phase of desorption and assayed by inductively coupled plasma optical emission spectrometry (ICP-OES; Optima 4300 DV; Perkin Elmer Instruments, Waltham, MA, USA) after dilution with phosphate buffer (pH 7.4). The samples were analyzed at a wavelength of 296 nm. The insulin concentration in the receptor phase

was determined by comparison with the appropriate calibration curve. Each experiment was done independently in triplicate.

2.7. Experimental animals and induction of type I diabetes

The experiments were carried out on male Wistar rats (8 weeks old) weighing approximately 200-250 g at the beginning of the experiment. The animals were housed at the Southern Laboratory Animal Facility, Faculty of Science, Prince of Songkla University, under standard conditions of temperature (23 ± 2 °C) and humidity ($50\pm 10\%$), with alternating 12-hour periods of light and darkness. The experimental protocols were approved by the Animal Ethical Committee of Prince of Songkla University (Ref. 36/2014). The animals were allowed free access to a standard diet (dry pellet) and water *ad libitum* before the induction of type I diabetes (T1D) by a single intraperitoneal injection of streptozotocin (STZ) at a dose of 35 mg/kg body weight dissolved in citrate buffer (pH 4.5). Seventy-two hours after the STZ injection, type I diabetes (T1D) was confirmed by measuring the blood glucose concentration with a glucose meter (Accu-Chek[®] Performa) and test strips (Roche Diagnostics GmbH, Mannheim, Germany). Only rats with blood glucose levels above 250 mg/dL were considered as T1D. Blood samples were collected from the tip of the tail vein. In all the experiments, the body weight of the animals was recorded.

2.8. Immunohistochemistry (IHC) and determination of insulin uptake

The MIP and NIP loaded with insulin (50 IU/kg) were given orally to the STZ-induced diabetic Wistar rats that had been fasted overnight. Three hours after the oral administration, the rats were sacrificed, and each intestinal segment was dissected and fixed in 10% formalin. The tissues were processed for paraffin blocking and subsequently sectioned (5 μ m) by using an 820 Spencer microtome (Leica). The paraffin was removed from the sectioned tissues by using xylene. The tissue sections were rehydrated in different grades of ethanol, incubated with 3% hydrogen peroxide to block the endogenous peroxidase, and then washed with 0.3% Triton X-100 in PBS (PBST). The de-paraffinized sections were permeabilized with 1% glycine in PBST and then blocked with 10% bovine serum albumin (BSA) for 1h at room temperature, followed by overnight incubation with guinea pig anti-insulin antibody (1:100

dilution) in a moist chamber at 4° C. The tissues were then rinsed with PBST, after which goat anti-guinea pig IgG conjugated with HRP (1:1000 dilution) was added for 1 h at room temperature. Next, the tissues were washed with PBST and stained with diaminobenzidine (DAB), followed by counterstaining with Mayer's hematoxylin. The resultant sections were then dehydrated in a series of graded ethanol solutions and cleared in xylene before being examined under a DP73 microscope equipped with the cellSens software (Olympus).

2.9. Fluorescence microscopy and in vivo absorption of polymer-FITC and insulin-Rh

The MIP-FITC was synthesized by using the method previously described [23], with minor modification. Briefly, the fluorescein isothiocyanate (FITC) solution was dissolved in anhydrous dimethyl sulfoxide (1 mg/ml). Then, 500 µl of the FITC solution was added to 10 ml of polymer suspension in PBS (1 mg/ml). The reaction mixture was kept in darkness for 8 h. The unconjugated FITC was then removed by washing the resultant precipitate and centrifuged at 10,000 rpm for 10 min until no fluorescence appeared. Similarly, the control polymer NIP nanoparticles were used to prepare the NIP-FITC. Insulin-Rh was prepared by applying the method reported in the literature [24]. Initially, rhodamine 6G (Rh) was dissolved in ethanol (1 mg/ml) and slowly added to an insulin suspension in PBS (7 mg/ml); the solution was then stirred overnight. Next, the synthesized insulin-Rh was washed thoroughly and centrifuged at 10,000 rpm for 10 min until no fluorescence appeared in the supernatant.

2.10. Immunofluorescence studies

The synthesized MIP-FITC and NIP-FITC loaded with insulin-Rh (1 mg/ml, 1 ml) were given orally to overnight-fasted diabetic Wistar rats. The rats were sacrificed 3 h after the oral administration and then were dissected to collect the intestinal segments, which were immediately washed with cold PBS. The isolated intestinal segments were embedded in OCT compound and frozen at -20° C. The frozen tissues were cut into 5-µm-thick sections with the use of a CM1850 cryostat (Leica) and then placed on 2% coated slides. The slides were post-fixed with cold acetone for 10 min, followed by washing with cold PBS. The nuclei of the cells were then stained with

4',6-diamidino-2-phenylindole dihydrochloride (DAPI). The excess DAPI staining solution was removed by rinsing with PBS thrice. The cover slips were mounted on slides and photographed under a DP73 fluorescence microscope (Olympus) to examine the absorption and distribution of FITC-labeled polymer nanoparticles and insulin-Rh in the different intestinal segments.

2.11. Image analysis

The fluorescence intensity of the images was measured in digital units (D.U.). The mean fluorescence intensity was obtained as the total pixel intensity divided by the total pixels in the region of interest (D.U./pixels), using the ImageJ software developed by the National Institutes of Health (NIH). The intestinal absorption of MIP-FITC and insulin-Rh was measured by determining the mean fluorescence intensity on micrographs of four samples per animal (n=4) per group. The images were threshold; 16 villi from four samples per animal (n=4) per group were analyzed [25]. Statistical analysis was carried out by applying two-way analysis of variance (ANOVA), followed by Tukey's post hoc test. A p-value <0.05 was considered statistically significant.

2.12. Ultrastructural immunochemistry of intestinal segments

The insulin transport through the polymer nanoparticles across the intestinal epithelium was investigated by immunogold staining with TEM [26]. In the present work, the animals were prepared according to the same protocol as in the IHC study previously described. The use of phase contrast images obtained from the immunofluorescence study and immunogold staining, as well as the TEM examination of the tissues, allowed a quantitative assessment of the spatial features of the objects, with high discrimination capability. The MIP and NIP loaded with insulin (50 IU/kg) were given orally to overnight-fasted diabetic Wistar rats. Three hours after the oral administration, the rats were sacrificed, and the intestinal segments were collected and washed in PBS (pH 7.4). The tissue samples were cut into sections (0.1-0.5 mm³), fixed in 2.5% glutaraldehyde for 12 h, and then washed with PBS thrice. The specimens were post-fixed in 1% osmium tetroxide for 2 h and then washed thrice with distilled water. Next, the samples were stained with 2% uranyl acetate for

20 min and dehydrated in different grades of ethanol. Propylene oxide and epoxy resin were infiltrated into the samples and embedded by polymerization at 70 °C for 12 h to prepare the blocks for TEM.

Thin sections (50-70 nm) of tissue in epoxy resin were mounted onto nickel grids for use in immunogold labeling. The samples were incubated with citrate buffer (pH 6) at 90 °C for 15 min and then rinsed with PBST. The grids were treated with a blocking solution (2% BSA) for 2 h before overnight incubation with guinea pig anti-insulin antibody (1:20 dilution) at 4° C. Then, goat anti-guinea pig IgG conjugated with HRP (1:50 dilution) was reacted for 2 h at room temperature, and the specimens were incubated with ABC reagent for 1 h. A solution of gold nanoparticles with biotin (1:20 dilution) was applied on the surface of the tissue samples, which were then washed with distilled water. The sections were counterstained with uranyl acetate and lead citrate before being studied under a JEM 2100F transmission electron microscope (JEOL Inc., Tokyo, Japan).

2.13. Microscopic examination of the MIP-loaded insulin in diabetic rats

STZ-induced diabetic male Wistar rats weighing approximately 180–200 g were acclimatized to cages with wire mesh lids. The animals were randomly divided into two groups of five rats each. The first group was orally given MIP nanoparticles loaded with insulin (100 mg/kg) daily for 14 days. The other group, which was considered as a control group, did not receive any treatment. The rats were allowed to a normal diet and water *ad libitum*, and changes in their body weight were carefully observed. After the animals were sacrificed, their internal organs were dissected and fixed in 10% formalin to prepare paraffin blocks, which were cut into 5-µm sections by using a microtome. The sectioned tissues were then stained with hematoxylin and eosin (H&E) by applying standard procedures [27]. All slides were analyzed by using a DP73 microscope equipped with the cellSens software (Olympus).

3. Results and discussion

3.1. Characterization of the MIP

The surface morphology and AFM were used to observe the imprinted cavities on the surface of the particles after the polymerization procedure. The TEM observations of insulin associated with the MIP (Figure 1A) showed well-distributed, discrete particle, rather than that for the NIP which showed more particles aggregates within the polymer matrix after the polymerization (see Figure 1B). Upon the synthesis of MIP, some of the unreacted areas of the functional monomers were found to be the same as those in the control polymer (NIP), as shown in TEM images (Figure 1B and D). The most satisfactory technique for elucidating the cavities imprinted by this approach was AFM which showed a rather high set of nanosized patterns, corresponding to the template (Figure 1E). The AFM image in Figure 1E shows the insulin template on the surface of a substrate. Because AFM is a localized analytical technique, it could provide an appropriate representation of the surface of the particles after the insulin template was washed off. Additionally, Figure 1F shows connected pores on the nanoparticles with the presence of significant differences on the particle surface, confirming the formation of a protein structure inside the polymer network.

Therefore, based on the analysis of the AFM images, the diameter of the three-dimensional structure of the nanosized porous particles of the MIP (Figure 1F, inset) was the insulin template onto the surface of a substrate lied approximately $2 \times 25 \times 25$ nm (height \times length \times width), as shown in the inset of Figure 1E. The image of morphological surface of MIP can be used to explain the interaction between the peptide chains as compared to the NIP (Figure 1G). The AFM images of NIP showed rather high set of nanosized scale material on the NIP. This is attributed to alter the polymer chain packing density according to the polymerization procedure with the omitting of the protein printed molecule that achieved under similar condition. AFM images (Figure 1F and G) show significant differences on the particle surface between the MIP and the NIP. Moreover, zeta potential of the insulin imprinted nanoparticles was found to be -32.3 ± 4.23 mV. This is attributed to specific control of the therapeutic protein which caused by the interaction between the insulin-imprinted nanoparticles MIP due to the particle surface made by the assembled sites from the appropriate monomeric system. The average particle size of the insulin-imprinted nanoparticles prepared by using the precipitation polymerization technique was found

to be 198.73 ± 3.05 nm, as determined by dynamic light scattering. These results provided insight into specific function of the peptide hormone achieved from the chemical functional precursor used in this study [15].

3.2. Evaluation of the recognition ability of the MIP

The recognition ability of the MIP for binding the protein template was examined by fluorescence spectroscopic analysis with the use of phosphate buffer (pH 7.4). Figure 2 (A, B) shows the relative intensity of fluorescence emission of insulin in the presence and absence of the MIP/NIP nanoparticles. The fluorescence intensity of insulin was enhanced upon the addition of MIP (see Figure 2A). In addition, the fluorescence spectroscopic analysis showed that the insulin concentration was dependent on the fluorescence intensity due to the particle surface made by the assembled sites from the appropriate monomeric system, which resulted in binding to the insulin. In comparison to the NIP, the amount of insulin adsorbed on the MIP at all the studied concentrations indicated that there had been an effective construction of the insulin binding sites within the imprinted polymers. When the relative fluorescence of the MIP with different concentrations of insulin was considered, a better linear relationship (Figure 2C) with the correlation coefficient ($R^2 = 0.9653$) compared with the NIP ($R^2 = 0.3196$) was found. This result indicated that the surface properties of the MIP, probably tyrosine residues are intrinsic fluorophores [28] that led to the dramatic difference between the MIP and the NIP. The results showed that higher binding affinity of MIP increased linearly fluorescence intensity as compared to the NIP that showed negligible change in fluorescence intensity with increasing of the insulin concentrations as high as 3 μ M. The selectivity upon adsorption process into the MIP binding sites is high in an aqueous medium (imprinting factor of MIP/NIP = 2.67) and high adsorption capacity which suggested that the binding within multiple point interaction. Concerning the data on the loading capacity and the loading efficiency of MIP was 55.75 mg of insulin per gram of nanoparticles and 82.13%, respectively [15]. The imprinted polymers, MIP showed higher interactions for the adsorption process towards the template than did the NIP in an aqueous solvent to the specific binding site.

3.3. Differential scanning calorimetry

To determine whether the thermal characteristics of the obtained polymer corroborate to the binding recognition and high selectivity of the imprinted cavities, we performed a thermal analysis using DSC, before and after template removal (Figure 3A). The DSC profile of insulin showed an endothermic peak at 103.8 °C (inset), which indicates the denaturation process of the protein [29]. All the polymers showed a depression in the phase temperature characteristics associated with the respective cross-linked polymer and slightly different molecular species within the polymer chain networks reduced approximately 325 °C. The MIP showed an endothermic peak at 334.5 °C which is related to the thermal decomposition, whereas the peak for the NIP shifted to a higher endothermic temperature (351.9°C) due to denser cross-linking in the polymer network [30]. Although the slight depression in the phase temperature characteristics of the MIP compared with the NIP, as well as the higher endothermic peak of the MIP-insulin (at 349 °C) compared with MIP alone (at 334.5 °C), indicating a little disturbance from the molecular bonding in a rigid glassy polymer. Therefore, this technique allowed the investigation of the energy formed by the interaction between the template and the MIP, compared with NIP by which structural facts and thermodynamic properties could not be strongly attributed to the increased resistance to thermal degradation.

3.4. Desorption experiments

Figure 3B shows the amount of diffused protein across the interfacial region within the pore that was impregnated with the MIP into the intestinal tissue lysate. The percentages of desorption for MIP with and without tissue lysate were found 45% and 25%, respectively, in PBS (pH 7.4) as eluent. The elution and the desorption of insulin from the MIP was less than that from its NIP where a considerable extent of insulin was transferred to almost 2.4 times more compared with the MIP into the receptor medium. This low desorption of the insulin was observed in the case of MIP that was incubated in the presence of tissue lysate and allowed for potential selective recognition compared to the NIP. The charged polymer and its bulk layer consisted of MIP binding sites rendered the incorporation of the desorptivity for MIP was lower,

which was agreeable to the previous report [31]. At pH 7.4 the MIP contained charged carboxylate anion as well as the insulin to be charged under this condition [32]. Previous observed different and surface topography influence of the MAA-HEAA polymers on imprinting the insulin in the polymer could be a consequence of the different chemical functionalizations of the molecular imprint sites that led to a differentiation of the molecular entities of the template biomacromolecules [15]. The presence of high free volumes in the polymeric network should give diffusion contribution of the polymer matrix. The particle size of MIP, which was about 200 nm; this could be corroborated by a previous study that used atrial natriuretic peptide [33]. In comparison to the NIP, the MIP which had produced free space of the region occupied onto the nanosized insulin-MIP. Such binding cavities, within free space of the molecular size region occupied onto the MIP led to imperative role with the impregnated tissue lysate that disturbed the insulin across into the intestinal epithelial cells. The observed surface morphologies occurred by a self-assembly process, provided insights into the specific function of insulin in the presence of MAA-co-HEAA in the MBAA-polymer for the selectivity by molecular-scale alteration of the insulin-imprinted cavities.

3.5. *Intestinal uptake of insulin-loaded MIP*

The bioactivity of the insulin loaded into the MIP was expected to vary with the physiologic conditions and required further examination. This result indicates that the anti-insulin antibody is highly specific and can be used to detect insulin. Immunostaining without incubation with the anti-insulin antibody served as a negative control (Figure 4A). Figure 4B shows the duodenum section stained with the anti-insulin antibody treated with the insulin loaded MIP for 3 h. As can be seen, the insulin-positive staining inside enterocytes which formed into layer of columnar epithelial cells as well as on the lacteal side of the villi (Figure 4B, inset). Positive staining of β -cells from normal (non-diabetic) rats was observed only in the insulin-producing pancreatic β -cells (Figure 4C). On the other hand, no immunoreactivity was found after oral administration of the insulin-loaded NIP (Figure 4D) due to the lack of insulin recognition that could not be detected by IHC study. In the present

study, the results showed that the difference of the uptake for insulin could be distinguished by the anti-insulin antibody treated with MIP and NIP.

3.6. The internalized insulin in vivo absorption

The MIP-loaded insulin showed a difference in IHC after 3 h of oral administration, as described above. Figure 5 (A and B) presents the fluorescence images of the intestinal segments after the oral administration of MIP-FITC and NIP-FITC loaded with insulin-Rh, respectively. As shown in Figure 5A, the fluorescent images of intestinal segments for MIP-FITC was generally distributed on the mucus layer with a greater amount on the lacteal side of the villi (white arrow) in all the sections. In the MIP, insulin-Rh was found mostly inside the enterocytes and on the lacteal side of the villi (yellow arrow). However, there was a decrease in the fluorescence of insulin-Rh (red fluorescence) in all sections for the NIP (Figure 5B). Upon oral administration with the insulin-loaded MIP resulted in a significantly higher fluorescence intensity of rhodamine-labeled insulin ($P < 0.0001$) compared with the NIP is almost 10 times. Moreover, the MIP increased the rate and extent of insulin-Rh fluorescence dissipation after 3 h of oral administration. It is noted that no significant difference between the fluorescence intensity (green fluorescence) of MIP-FITC and that for NIP-FITC was obtained. Insulin consists of two disulfide-linked chains of peptides A and B, and its stability is sensitive to the net charge on the peptide, therefore the intrinsic charge of the insulin loaded MIP at pH 7.4 enabling the high unbound insulin under the conditions of intestinal epithelial cells. In contrast, NIP was less efficient in transporting insulin into the intestinal epithelium whereas the MIP showed high selectivity. Therefore, the protein recognition based on molecular imprinting resulted in the creation of MIP with great affinity to selectively recognize the protein template during the re-binding event, which is agreeable to the previous literature [34]. It was noted that the MIP nanoparticles that had binding cavities for the specific structural features were appropriately formed by the chemical functionalities and that two of the key factors was to control the particle size and the selection of the solvent.

3.7. The absorption of insulin in the intestinal segments

The data obtained from electron microscopy showed the transport of insulin across the intestinal epithelium, showing that the insulin have infiltrated across the intestinal epithelial cells where the release of insulin took place (Figure 6). The amount of insulin molecules was larger when administered with the use of an MIP compared with an NIP. The higher nanoparticle-biotin absorption for the MIP ($P < 0.0001$) enabled the transport of insulin, eventually leading to intestinal absorption (see Figure S1). The NIP was less effective because of the absence of insulin recognition and led to no interaction; this finding is concomitant with the IHC results. For the MIP, a greater amount of insulin was found around the surfaces adorned with the microvilli of the enterocytes (Figure 6A), compared to the corresponding NIP (Figure 6C). Interestingly, the penetration of insulin into enterocytes was observed through the transcellular pathway (white arrows) as they were not present in the surface of the outermost epithelial cells (black arrows), despite it is a common route for most molecules and the nutrients across the GI (Figure 6B and D). The previous study on the diffusion of nanoparticles within rat intestinal tissues has been reported through Caco-2 cells or to use mouse reverted intestinal sac models with inhibitors [35], however the transport mechanism is slightly elucidated. Scheme 1 shows the illustration of the distribution into differential segments of intestine for MIP nanoparticles. Accordingly, at a higher pH of the GI tract, the MIP could transport more protein compared to free insulin or insulin-loaded NIP. The diffusion of insulin exclusively in GI epithelial cells was the mode of transport of the 200-nm nanoparticles [36]. The observed distribution into different segments of the intestine, confirmed that insulin was released, to successfully deliver insulin to the GI epithelial layer, but not at the site of administration. At the different intestinal sections, the binding cavities formed on MIP nanoparticles, capable the lipophilic domains of dye over the affected areas of sites with the interplay of the intestinal epithelial layer. We examined root mean square (RMS) roughness of MIP around 1.2 nm in an image analysis of AFM method which was found to be significant lower compared to NIP (see Figure S2). The finding indicated that the surface adhesion of the insulin on the extracellular mucous gel, and hence the protein-mucin uptake, which promoted the insulin penetration into the systemic circulation [37]. As a result, higher absorption of insulin occurred that reflected on the significant reduction of blood glucose level

when administered orally with the MIP nanoparticles than that of NIP [15]. MIP nanoparticle to pass from an aqueous phase to the membrane of the GI epithelial cells it must initially overcome its hydration energy that crossed biological barriers. So the distribution of the insulin-MIP when the system for the delivery of insulin was exposed to physiological conditions was unaffected by the extracellular matrix and its penetration into the intestinal cell membrane. We hypothesize that the uptake of protein structure which is not only the binding affinity in the conditions but also the mechanism on the epithelial adsorptive cells. The MIP could give the specific anchored polymer with the assembled sites from the insulin molecules that can provide the activity of insulin administered orally.

3.8. Nanotoxicity of the insulin-loaded MIP

We examined how the insulin-loaded MIP regulates activity within the several tissues to function properly, which the investigation was carried out in the STZ-induced diabetes. A little body weight gain of the treated animals was found which was similar to the control group for 14 days in the STZ-induced diabetic rat (Figure 7A). After treatment with a daily oral dose of MIP loaded with insulin (100 mg/kg), the intestinal tissues showed intact enterocytes, similarly to the control (see Figure 7B). For the results obtained, the insulin absorption into gastrointestinal epithelial cells enabled the observation of enterocytes, such that the development of the pancreatic β cell that suggested improvements in treatment of diabetes for MIP. There was no sign of necrosis and inflammation of the hepatocytes and the structure of the kidney still preserved without any changes in the renal corpuscles (see Figure 7B). No such sign of toxicity was found, concerning body weight change and clinical symptoms i.e. diarrhea, fever were found 14 days after the experiment.

4. Conclusions

In this work, we reported the capability of insulin mimicking nanomaterial within free space of the molecular size region for the transport of insulin across the intestinal epithelium in vivo. We anticipated that the biomimetic method according to the ability of such the binding sites on the nanosized scale of material within an

intestinal fluid. The two important findings in this work are valuable in the field of systemic absorption of bioactive compound. Firstly, the finding suggested that self-assembly of the protein template by molecular imprinting approach, which created an innovative mimicking of the structure of therapeutic protein for GI transport *in vivo*. The MIP incubated within the extracellular mucous seemed to have a markedly reduced insulin release due to complementary of the functional groups, leading to the lipophilic domains within affected areas across the GI epithelial cells to be probed. The second finding is the parenteral-switching-oral delivery of insulin as demonstrated in this study that highlighted a biorecognition property of this peptide delivery is of important for efficient insulin function in the streptozocin-induced diabetic rats with less toxicity.

Acknowledgements

We thank the National Research University Project of Thailand, Office of the Higher Education Commission (code no. PHA 540545c), for its financial support; the Drug Delivery System Excellence Center at PSU; the Nanotechnology Center (NANOTEC), Ministry of Science and Technology, Thailand, through its Center of Excellence Network program; Graduate Studies at PSU; and the Faculty of Pharmaceutical Sciences, for their laboratory facilities.

References

- [1] D.R. Owens, B. Zinman, G. Bolli, Alternative routes of insulin delivery, *Diabetic Med.* 20(11) (2003) 886-898.
- [2] S.K. Kim, S. Lee, S. Jin, H.T. Moon, O.C. Jeon, D.Y. Lee, Y. Byun, Diabetes correction in pancreatectomized canines by orally absorbable insulin-deoxycholate complex, *Mol. Pharm.* 7(3) (2010) 708-717.
- [3] J.H. Hamman, G.M. Enslin, A.F. Kotzé, Oral delivery of peptide drugs, *Bio Drugs* 19(3) (2005) 165-177.

- [4] S.A. Zaidi, Latest trends in molecular imprinted polymer based drug delivery systems, *RSC Adv.* 6(91) (2016) 88807-88819.
- [5] N.J. Yang, M.J. Hinner, Getting across the cell membrane: an overview for small molecules, peptides, and proteins, site-specific protein labeling: *Methods Mol. Biol.* (2015) 29-53.
- [6] R.M. Samstein, K. Perica, F. Balderrama, M. Look, T.M. Fahmy, The use of deoxycholic acid to enhance the oral bioavailability of biodegradable nanoparticles, *Biomaterials* 29(6) (2008) 703-708.
- [7] A. Albanese, P.S. Tang, W.C. Chan, The effect of nanoparticle size, shape, and surface chemistry on biological systems, *Annu. Rev. Biomed. Eng.* 14 (2012) 1-16.
- [8] R. Schirhagl, U. Latif, D. Podlipna, H. Blumenstock, F.L. Dickert, Natural and biomimetic materials for the detection of insulin, *Anal. Chem.* 84(9) (2012) 3908-3913.
- [9] A.M. Bannunah, D. Vllasaliu, J. Lord, S. Stolnik, Mechanisms of nanoparticle internalization and transport across an intestinal epithelial cell model: effect of size and surface charge, *Mol. Pharm.* 11(12) (2014) 4363-4373.
- [10] W. Naklua, K. Mahesh, P. Aundorn, N. Tanmanee, K. Aenukulpong, S. Sutto, Y.Z. Chen, S. Chen, R. Suedee, An imprinted dopamine receptor for discovery of highly potent and selective D₃ analogues with neuroprotective effects, *Process Biochem.* 50(10) (2015) 1537-1556.
- [11] Y. Hoshino, H. Koide, T. Urakami, H. Kanazawa, T. Kodama, N. Oku, K.J. Shea, Recognition, neutralization, and clearance of target peptides in the bloodstream of living mice by molecularly imprinted polymer nanoparticles: a plastic antibody, *J. Am. Chem. Soc.* 132(19) (2010) 6644-6645.
- [12] L. Jaiswal, S. Rakkit, K. Pochin, P. Jaisamut, C. Tanthana, N. Tanmanee, T. Srichana, R. Suedee, A thalidomide templated molecularly imprinted polymer that promotes a biologically active chiral entity tagged in colon carcinoma cells and protein-related immune activation, *Process Biochem.* 50(12) (2015) 2035-2050.
- [13] L. Xu, Y.-A. Huang, Q.-J. Zhu, C. Ye, Chitosan in molecularly-imprinted polymers: current and future prospects, *Int. J. Mol. Sci.* 16(8) (2015) 18328-18347.

- [14] H. Zeng, Y. Wang, X. Liu, J. Kong, C. Nie, Preparation of molecular imprinted polymers using bi-functional monomer and bi-crosslinker for solid-phase extraction of rutin, *Talanta* 93 (2012) 172-181.
- [15] P. K. Paul, A. Treetong, R. Suedee, Biomimetic insulin-imprinted polymer nanoparticles as a potential oral drug delivery system, *Acta Pharm.* 67(2) (2017) 149-168.
- [16] B. He, Z. Jia, W. Du, C. Yu, Y. Fan, W. Dai, L. Yuan, H. Zhang, X. Wang, J. Wang, The transport pathways of polymer nanoparticles in MDCK epithelial cells, *Biomaterials* 34(17) (2013) 4309-4326.
- [17] B. He, P. Lin, Z. Jia, W. Du, W. Qu, L. Yuan, W. Dai, H. Zhang, X. Wang, J. Wang, The transport mechanisms of polymer nanoparticles in Caco-2 epithelial cells, *Biomaterials* 34(25) (2013) 6082-6098.
- [18] D. Kumar Malik, S. Baboota, A. Ahuja, S. Hasan, J. Ali, Recent advances in protein and peptide drug delivery systems, *Curr. Drug Deliv.* 4(2) (2007) 141-151.
- [19] T.-H. Yeh, L.-W. Hsu, M.T. Tseng, P.-L. Lee, K. Sonjae, Y.-C. Ho, H.-W. Sung, Mechanism and consequence of chitosan-mediated reversible epithelial tight junction opening, *Biomaterials* 32(26) (2011) 6164-6173.
- [20] M.-C. Chen, K. Sonaje, K.-J. Chen, H.-W. Sung, A review of the prospects for polymeric nanoparticle platforms in oral insulin delivery, *Biomaterials* 32(36) (2011) 9826-9838.
- [21] S. Sajeesh, K. Bouchemal, V. Marsaud, C. Vauthier, C.P. Sharma, Cyclodextrin complexed insulin encapsulated hydrogel microparticles: An oral delivery system for insulin, *J. Control. Release* 147(3) (2010) 377-384.
- [22] I. Castagliuolo, K. Karalis, L. Valenick, A. Pasha, S. Nikulasson, M. Wlk, C. Pothoulakis, Endogenous corticosteroids modulate *Clostridium difficile* toxin A-induced enteritis in rats, *Am. J. Physiol. Gastrointest. Liver Physiol.* 280(4) (2001) G539-G545.
- [23] Y.-H. Lin, C.-K. Chung, C.-T. Chen, H.-F. Liang, S.-C. Chen, H.-W. Sung, Preparation of nanoparticles composed of chitosan/poly- γ -glutamic acid and evaluation of their permeability through Caco-2 cells, *Biomacromolecules* 6(2) (2005) 1104-1112.

- [24] K. Sonaje, E.-Y. Chuang, K.-J. Lin, T.-C. Yen, F.-Y. Su, M.T. Tseng, H.-W. Sung, Opening of epithelial tight junctions and enhancement of paracellular permeation by chitosan: microscopic, ultrastructural, and computed-tomographic observations, *Molecular Pharm.* 9(5) (2012) 1271-1279.
- [25] M. Chang, E.B. Kistler, G.W. Schmid-Schönbein, Disruption of the mucosal barrier during gut ischemia allows entry of digestive enzymes into the intestinal wall, *Shock* 37(3) (2012) 297.
- [26] J.N. Skepper, J.M. Powell, Immunogold staining of epoxy resin sections for transmission electron microscopy (TEM), *Cold Spring Harb. Protoc.* 2008(6) (2008) pdb. prot5015.
- [27] E.-Y. Chuang, K.-J. Lin, F.-Y. Su, F.-L. Mi, B. Maiti, C.-T. Chen, S.-P. Wey, T.-C. Yen, J.-H. Juang, H.-W. Sung, Noninvasive imaging oral absorption of insulin delivered by nanoparticles and its stimulated glucose utilization in controlling postprandial hyperglycemia during OGTT in diabetic rats, *J. Control. Release.* 172(2) (2013) 513-522.
- [28] L.A. Munishkina, A.L. Fink, Fluorescence as a method to reveal structures and membrane-interactions of amyloidogenic proteins, *BBA Biomembranes* 1768(8) (2007) 1862-1885.
- [29] B. Sarmiento, A. Ribeiro, F. Veiga, D. Ferreira, Development and characterization of new insulin containing polysaccharide nanoparticles, *Colloids Surf. B* 53(2) (2006) 193-202.
- [30] M. Esfandyari-Manesh, B. Darvishi, F.A. Ishkuh, E. Shahmoradi, A. Mohammadi, M. Javanbakht, R. Dinarvand, F. Atyabi, Paclitaxel molecularly imprinted polymer-PEG-folate nanoparticles for targeting anticancer delivery: Characterization and cellular cytotoxicity, *Mat. Sci. Eng. C Mater. Biol. Appl.* 62 (2016) 626-633.
- [31] G.Z. Kyzas, S.G. Nanaki, A. Koltsakidou, M. Papageorgiou, M. Kechagia, D.N. Bikiaris, D.A. Lambropoulou, Effectively designed molecularly imprinted polymers for selective isolation of the antidiabetic drug metformin and its transformation product guany lurea from aqueous media, *Anal. Chim Acta* 866 (2015) 27-40.

- [32] X.-Q. Zhang, X. Xu, N. Bertrand, E. Pridgen, A. Swami, O.C. Farokhzad, Interactions of nanomaterials and biological systems: Implications to personalized nanomedicine, *Adv. Drug. Deliv. Rev.* 64(13) (2012) 1363-1384.
- [33] C. Wang, M. Howell, P. Raulji, Y. Davis, S. Mohapatra, Preparation and characterization of molecularly imprinted polymeric nanoparticles for atrial natriuretic peptide (ANP), *Adv. Funct. Mater.* 21(23) (2011) 4423-4429.
- [34] H. Sunayama, Y. Kitayama, T. Takeuchi, Regulation of protein-binding activities of molecularly imprinted polymers via post-imprinting modifications to exchange functional group within the imprinted cavity, *J. Mol. Recogn.* e2633 (2017) 1-6.
- [35] S. Simovic, Y. Song, T. Nann, T.A. Desai, Intestinal absorption of fluorescently labeled nanoparticles, *Nanomedicine* 11(5) (2015) 1169-1178.
- [36] H. Hillaireau, P. Couvreur, Nanocarriers' entry into the cell: relevance to drug delivery, *Cell. Mol. Life Sci.* 66(17) (2009) 2873-2896.
- [37] D.-L. Liu, J. Martin, N. Burnham, Optimal roughness for minimal adhesion, *Applied Phys. Lett.* 91(4) (2007) 043107.

Legends

Figure 1: Surface morphology of insulin-imprinted nanoparticles as obtained by SEM (A, MIP; B, NIP) and TEM (C, MIP; D, NIP). The AFM images show the topography and surface geometry of insulin (E), the MIP (F), and the NIP (G). The insets show the nanosize geometry of the insulin molecule (E) and imprinted cavity (F).

Figure 2: Fluorescence emission spectra of insulin with (A) and without (B) MIP/NIP nanoparticles ($\lambda_{\text{ex}}=280$ nm); (C) the relative fluorescence intensity (I/I_0) at 300 nm with different concentrations of insulin.

Figure 3: (A) DSC thermograms of the MIP, the NIP, the insulin- loaded MIP, and insulin alone (inset); (B) the desorption of insulin with and without intestinal tissue lysate.

Figure 4: The representative insulin-immunostained sections of pancreatic β cells: (A) negative control and (C) the positive staining of islet β cells indicated the specificity of the anti-insulin antibody. (B) A representative immunostained section of the duodenum after oral treatment with insulin-loaded MIPs for 3 h showed positive staining of the anti-insulin antibody in the enterocytes and on the lacteal side of the villi (inset; the arrows indicate the lacteal side of the villi. (D) The immunostained section of the duodenum with insulin-loaded NIPs showed no immunoreactivity of the anti-insulin antibody in the villi. IS; islets of Langerhans.

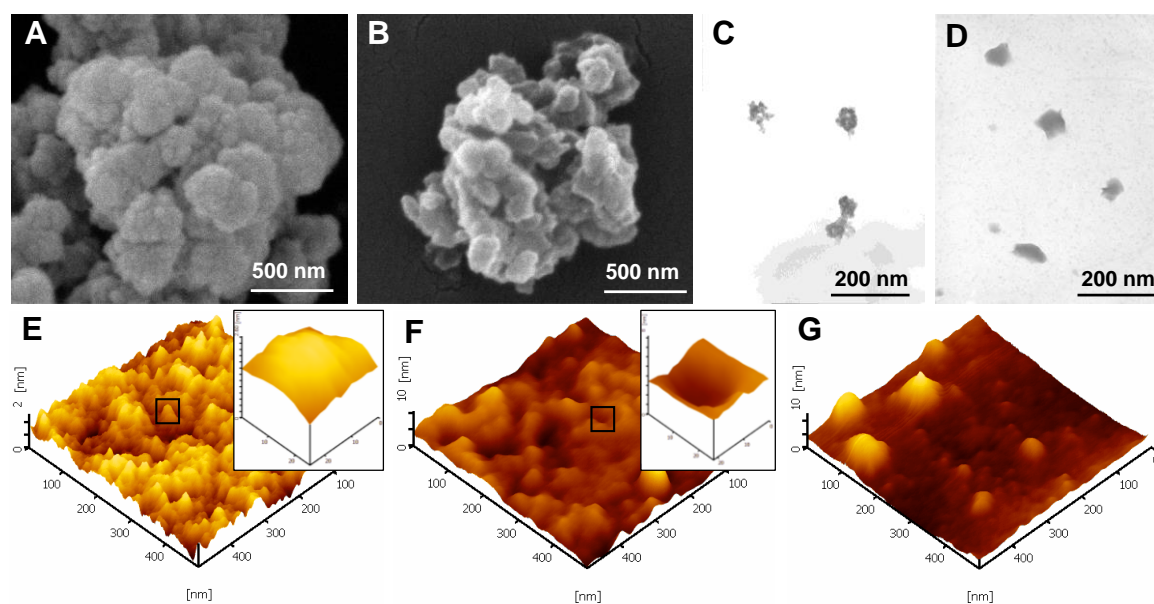
Figure 5: (A) Fluorescence images showing the transport of FITC-labeled MIP (green, MIP-FITC) and the absorption of Rh-labeled insulin (red, insulin-Rh) in rat small intestinal tissue segments (blue, nuclei) at 3 h after oral treatment with fluorescence-labeled MIPs and insulin. (B) The transport and absorption of insulin through NIP nanoparticles; the white arrows indicate the presence of FITC-labeled MIP/NIP at the villi, the yellow arrow indicates Rh-labeled insulin, which was abundantly distributed within the villi of the small intestines, and the white asterisks indicate the intestinal lumen. (C) The fluorescence intensity of polymer-FITC and (D) insulin-Rh for the MIP and

the NIP. The values are the means \pm SEM (n=4) per group. ***P< 0.0001 compared with NIP.

Figure 6: TEM micrographs of immunogold-stained intestinal segments 3 h after oral administration of the insulin-loaded MIP (A and B) and NIP (C and D). Insulin was investigated by immunolabeling with guinea pig anti-insulin antibody, followed by goat anti-guinea pig antibody conjugated with 60-nm biotin gold nanoparticles (black dots). The permeation of insulin occurred through the transcellular route (white arrows), and no insulin was observed on the surface of the paracellular space (black arrows). Scale bar, 2 μ m. Insets designate the 12000 x magnified views of tissue region.

Scheme 1: Schematic of the transport of insulin-loaded MIP nanoparticles across the intestinal epithelial cells through the oral route and of the insulin release by endocytosis and transcytosis through the enterocytes. The transport can be explained by the *in vitro* release of insulin through an Empore disc impregnated with MIP in the presence of intestinal tissue lysate in the receptor phase at pH 7.4.

Figure 7: (A) Changes in body weight over time and (B) representative H&E-stained histologic sections of the intestine, liver, and kidney before and after treatment with MIPs. The rats showed no significant morphologic changes after oral treatment with MIPs for 14 days. CV, central vein; RC, renal corpuscle (glomerulus and granular capsule). The asterisks indicate the duodenal lumen.

Figure(s)**Figure 1**

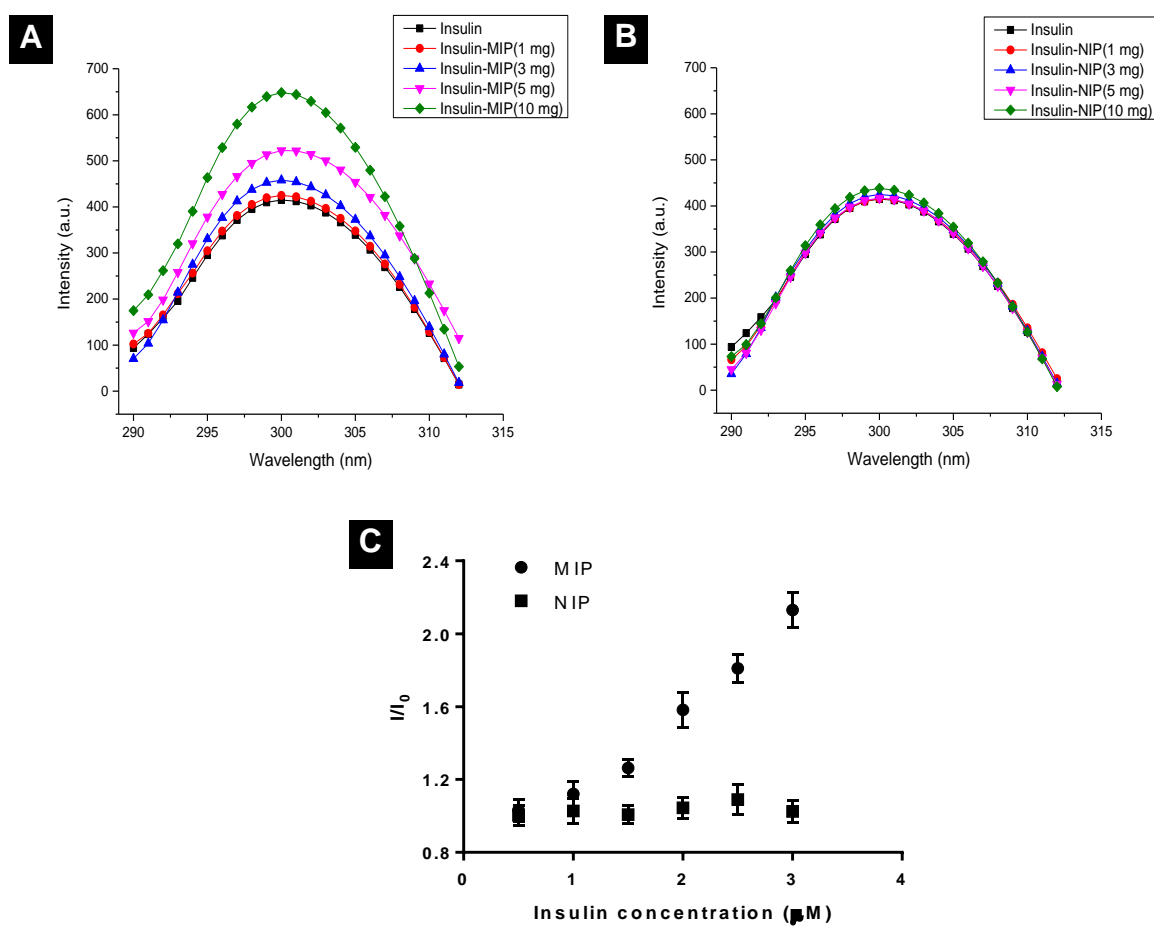


Figure 2

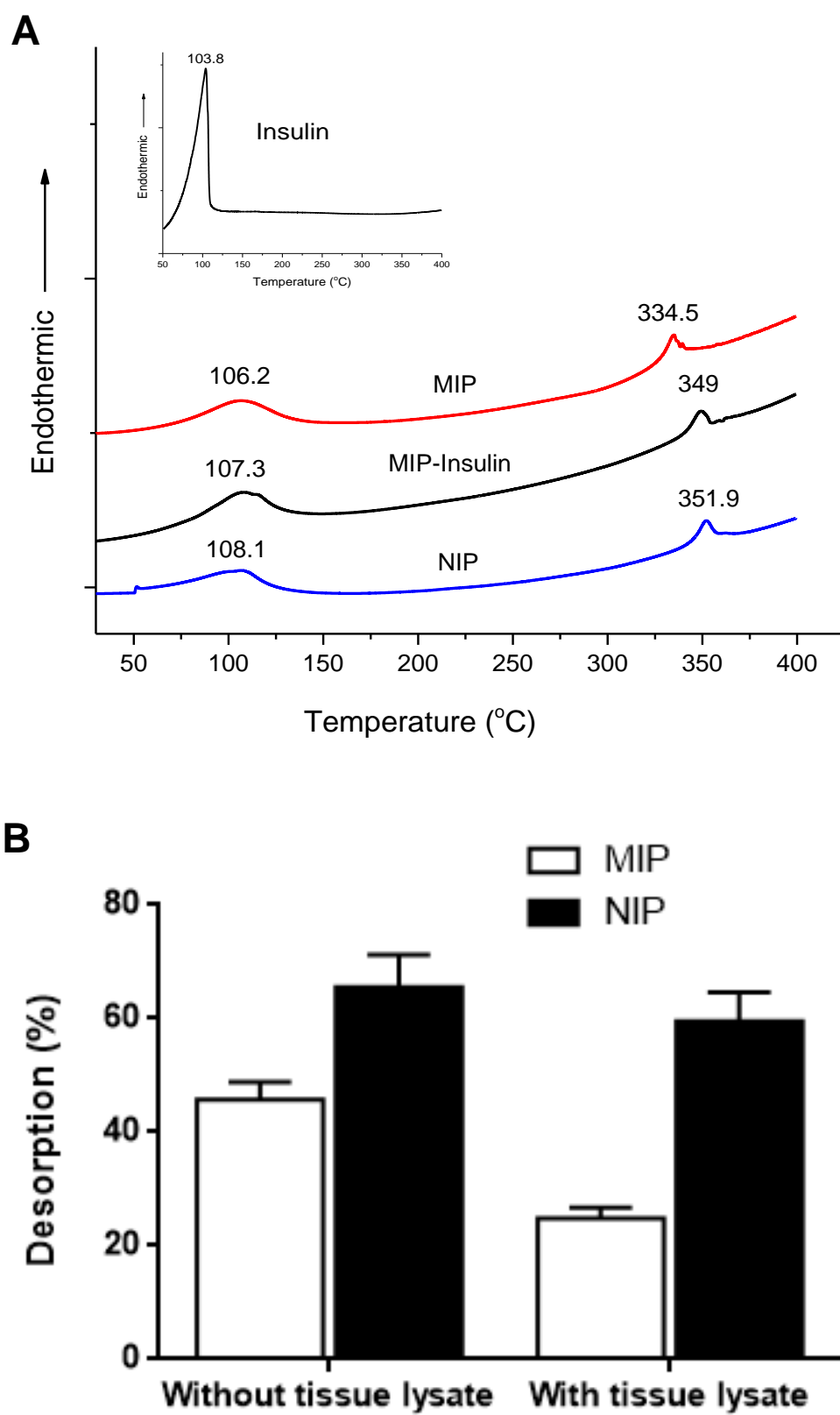


Figure 3

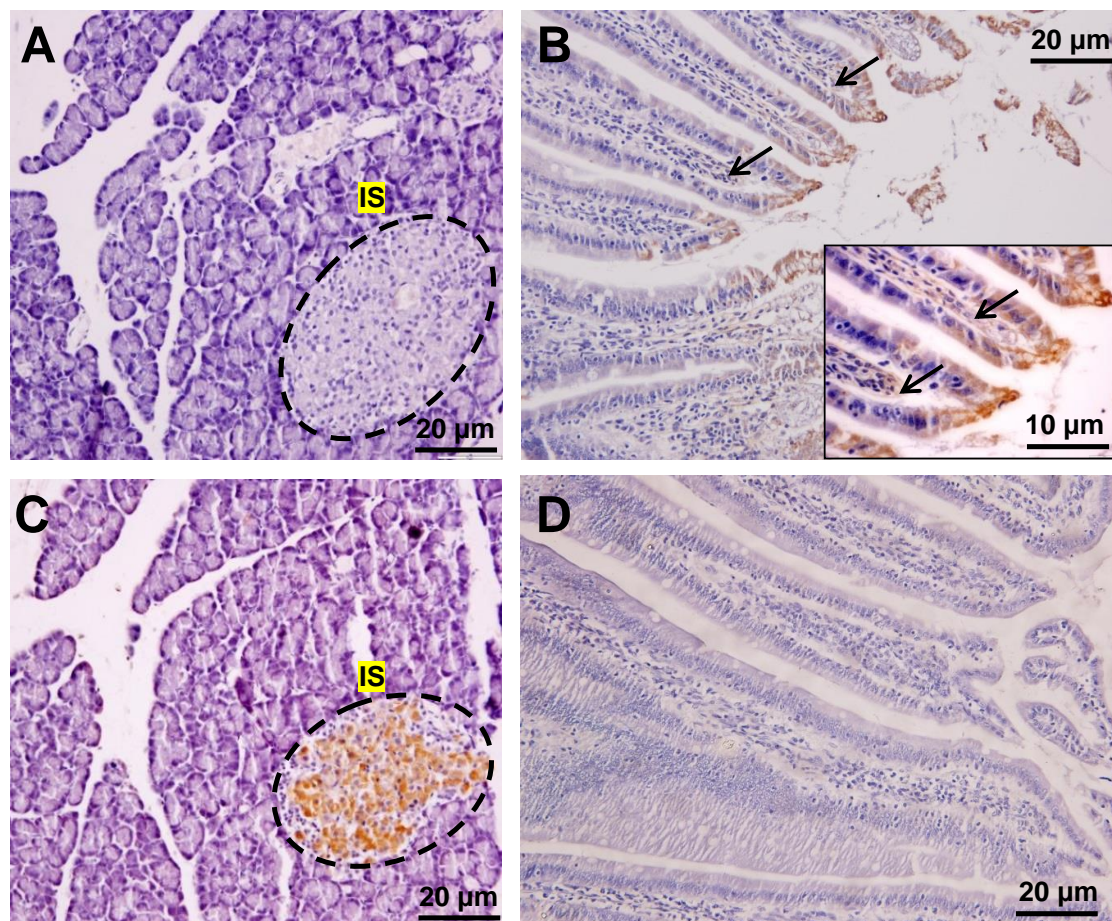


Figure 4

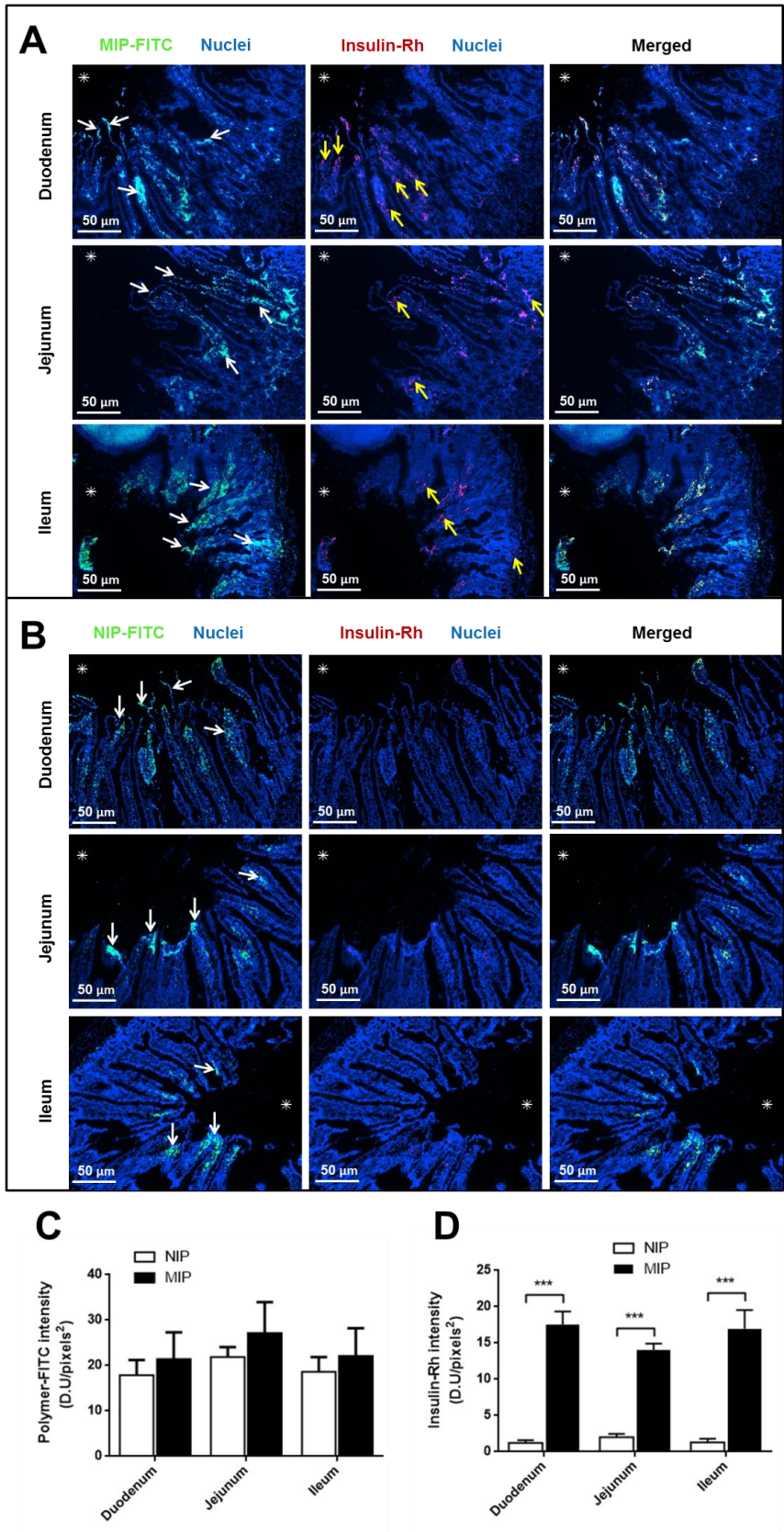


Figure 5

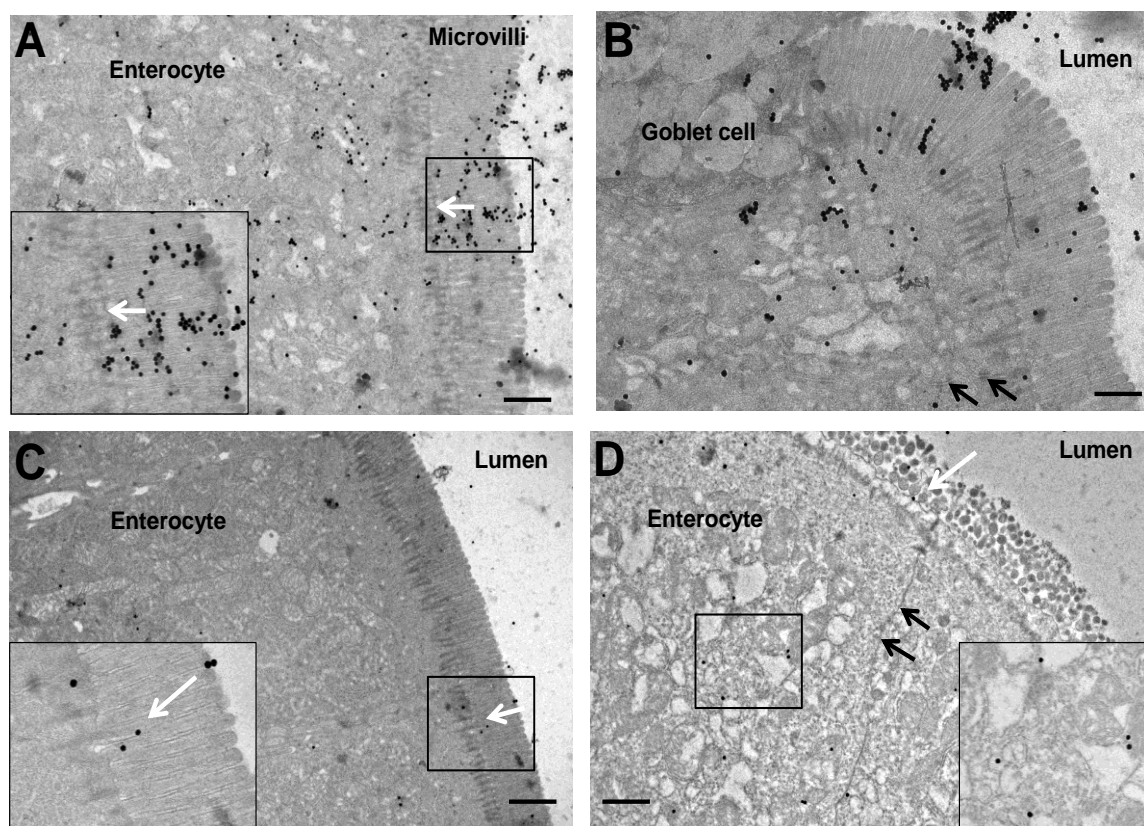
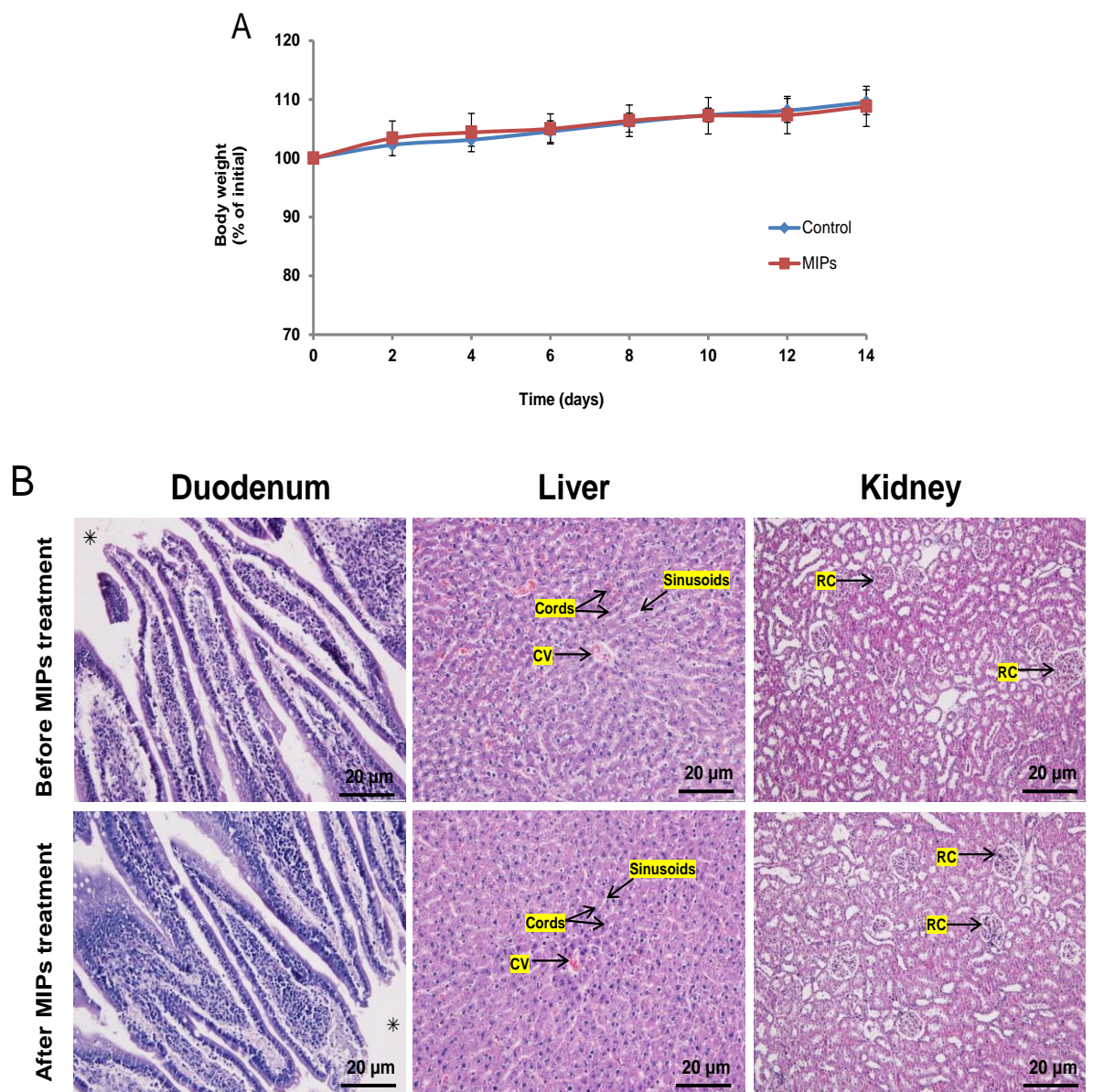
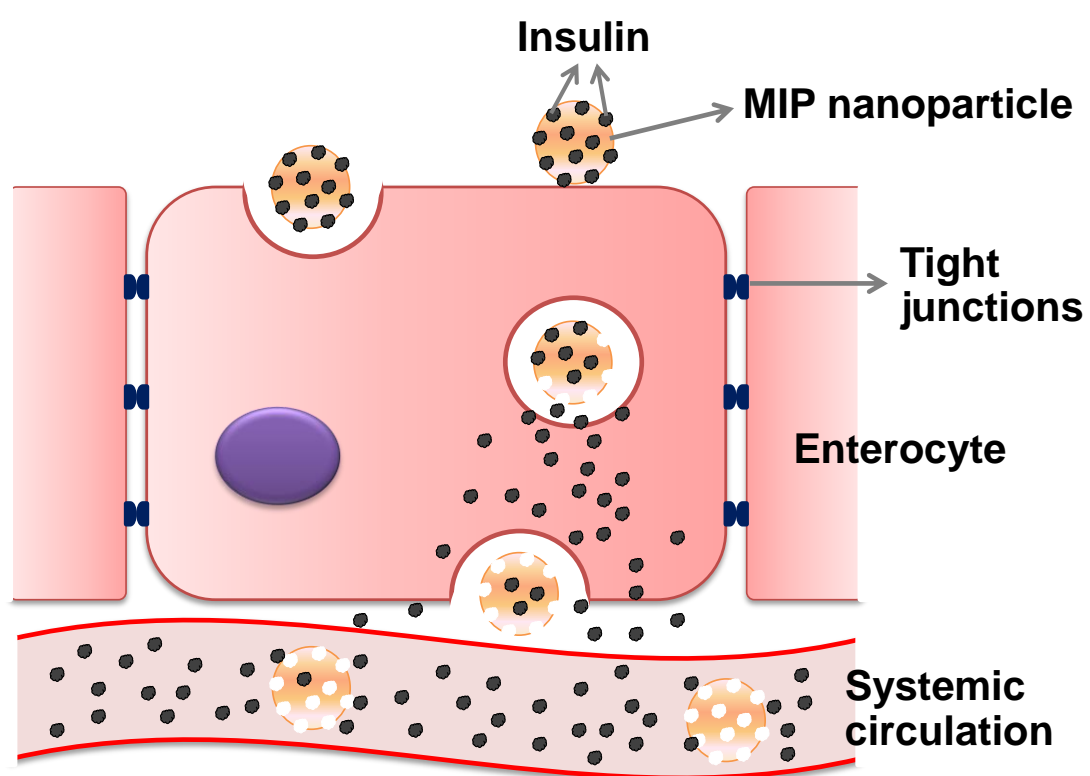


Figure 6

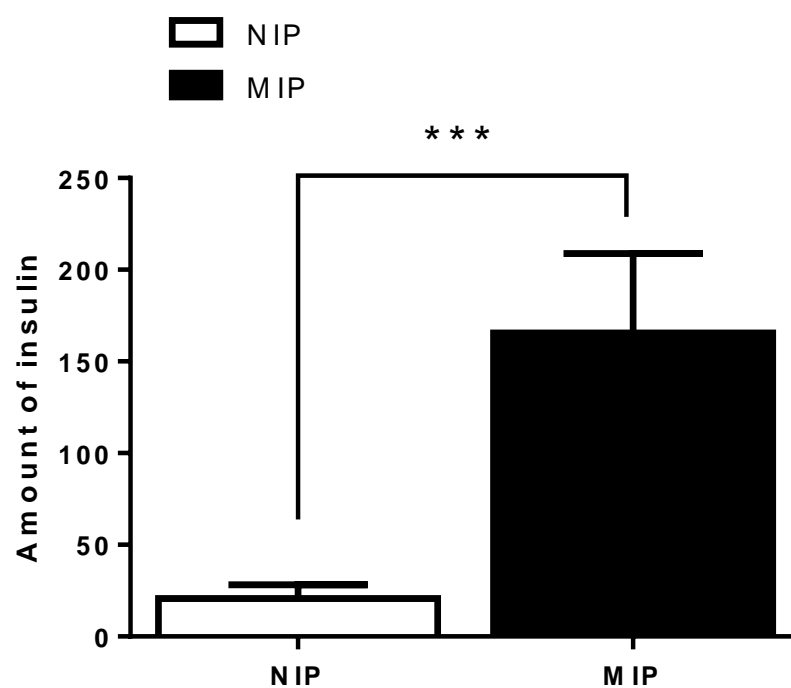




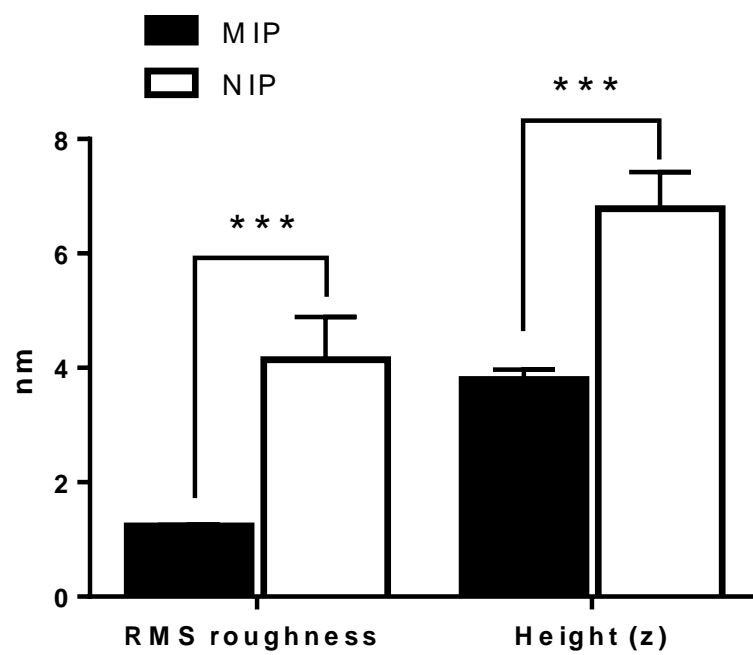
Scheme 1

Supplementary materials

Figure S1



The values are the means \pm SEM (n=4). ***P< 0.0001 compared with NIP.

Figure S2

The values are the means \pm SEM (n=3). ***P< 0.0001 compared with NIP.

Animal Ethic Approval



PRINCE OF SONGKLA UNIVERSITY

15 Karnjanawani Road, Hat Yai, Songkhla 90110, Thailand

Tel. (66-74) 286958 Fax (66-74) 286961

Website : www.psu.ac.th

MOE 0521.11/ 1019

Ref.36/2014

September 29 , 2014

This is to certify that the research project entitled "Preparation and characterization of biomimetic molecularly imprinted polymer for controlled release drug delivery system of anti-diabetic drugs" which was conducted by Assoc. Prof. Dr.Roongnapa Srichana, Faculty of Pharmaceutical Sciences, Prince of Songkla University, has been approved by The Animal Ethic Committee, Prince of Songkla University.

A handwritten signature in black ink, reading "Kitja Sawangjaroen". The signature is fluid and cursive, with a long horizontal stroke at the end.

Kitja Sawangjaroen, Ph.D.

Chairman,

The Animal Ethic Committee, Prince of Songkla University

VITAE

Name Mr. Pijush Kumar Paul

Student ID 5610730008

Educational Attainment

Degree	Name of Institution	Year of Graduation
B. Pharm	Gono Bishwabidyalay (University), Bangladesh	2008
M.Sc. (Pharmaceutical Technology)	The University of Asia Pacific, Bangladesh	2009

Scholarship Awards during Enrolment

1. Thesis grant, Education fee and salary
National Research University Project of Thailand, Office of the Higher
Education Commission (Code no. PHA 540545c).
2. Thesis grant
The Graduate School, Prince of Songkla University.
3. Conference Scholarship
Faculty of Pharmaceutical Sciences, Prince of Songkla University.

Work – Position and Address

Lecturer, Department of Pharmacy, Gono Bishwabidyalay (University), Mirzanagar,
Savar, Dhaka-1344, Bangladesh.

List of Publication and Proceeding

Paul, P. K., Treetong, A., Suedee R., 2017. Biomimetic insulin-imprinted polymer nanoparticles as a potential oral drug delivery system. *Acta Pharmaceutica* 67: 149-168.

Paul, P. K., Nopparat, J., Nuanplub, M., Treetong, A., Suedee R., 2017. Improvement in insulin absorption into gastrointestinal epithelial cells by using molecularly imprinted polymer nanoparticles: Microscopic evaluation and ultrastructure. Accepted in *International Journal of Pharmaceutics*.

Proceedings

Oral presentation

Paul P. K., Suedee R. Molecularly imprinted polymer as a nanocarrier for protein drug delivery. Asian Graduate Congress on Pharmaceutical Technology, National University of Singapore, Singapore, July 10-13, 2016.

Paul P. K., Suedee R. The approach to synthesize the biomimetic insulin imprinted polymer nanoparticles via precipitation polymerization. Japan-Thailand joint meeting on functional nanomaterials 2016, Dusit Thani Bangkok and Thailand Science Park, Pathum Thani Thailand, May 26-28, 2016.

Paul P. K., Suedee R. Protein Imprinted Nanoparticles as Drug Delivery Vehicles. The 3rd Current Drug development (CDD 2014), Ao Nang Beach, Krabi, Thailand, May 1-3, 2014.

Poster presentation

Paul P. K., Suedee R. Molecularly imprinted polymer as a nanocarrier for protein drug delivery. Asian Graduate Congress on Pharmaceutical Technology, National University of Singapore, Singapore, July 10-13, 2016.

Award

Paul P. K., Suedee R. Best poster award, Molecularly imprinted polymer as a nanocarrier for protein drug delivery at Asian Graduate Congress on Pharmaceutical Technology, National University of Singapore, Singapore, July 10-13, 2016.